

SCH OF PHARMACY



89 0022977 7

“Chromium Carcinogenesis: Mechanisms and Biomonitoring”

Robert Owen James Shayer

A thesis submitted to the University of London for examination for the degree of
Doctor of Philosophy

April 2000

Centre for Toxicology,
London School of Pharmacy,
29-39 Brunswick Square,
London
WC1N 1AX



ProQuest Number: 10104265

All rights reserved

INFORMATION TO ALL USERS

The quality of this reproduction is dependent upon the quality of the copy submitted.

In the unlikely event that the author did not send a complete manuscript and there are missing pages, these will be noted. Also, if material had to be removed, a note will indicate the deletion.



ProQuest 10104265

Published by ProQuest LLC(2016). Copyright of the Dissertation is held by the Author.

All rights reserved.

This work is protected against unauthorized copying under Title 17, United States Code.
Microform Edition © ProQuest LLC.

ProQuest LLC
789 East Eisenhower Parkway
P.O. Box 1346
Ann Arbor, MI 48106-1346

“...any advance in wisdom requires a good dose of shamelessness.”

Hanif Kureishi (from “Intimacy”)

Abstract

Whilst chromium (Cr) compounds (particularly water soluble complexes) have long been recognised as carcinogens, much information is still missing about how these agents exert their mutagenic, carcinogenic, and deoxyribonucleic acid (DNA) damaging effects. The activation of Cr(VI) by intracellular reductants such as glutathione (GSH), ascorbic acid (AsA) and cysteine (Cys), among others, is crucial for the mediation of its DNA damaging effects. Studies into the interaction of Cr(VI) with isolated DNA in the presence of GSH were principally concerned with identifying the existence of a mutual mechanistic pathway for the mediation of more than one type of prevalent DNA lesion. The role of reactive oxygen species in the mediation of Cr(VI)-induced DNA damage was considered with particular emphasis on single strand breaks (SSB) and apurinic/apyrimidinic sites (AP-sites). The potential sites of interaction of damaging species with the DNA macromolecule were considered, and from these and other studies several conclusions were drawn. It is demonstrated that Cr-DNA adducts can be formed independently of the reaction pathways giving rise to SSB and AP-sites, and that Cr(V), and possibly Cr(IV) species, as well as hydrolysing Cr(III)/GSH complexes are responsible for the formation of Cr-DNA adducts. Evidence is also provided to support the hypothesis that DNA-phosphate groups are the binding site of Cr-DNA adducts.

A bacterial mutation assay was employed to investigate the mutagenic potential of different types of Cr(VI)-induced DNA damage and it was demonstrated that DNA lesions induced during the *in vitro* conversion of Cr(VI) by GSH can be fixed into mutations during replication and passed onto progeny cells. There is an apparent role for Cr-DNA adduct formation in this process and since Cr(III) species are involved in the mediation of this type of damage it is proposed that Cr(III) represents a species with the potential capacity to cause fixed mutations in cell lines.

A novel whole animal model, involving the application of magnetic resonance imaging (MRI), was developed to enable levels of Cr compounds to be monitored in the lung. The technique was shown to be sensitive enough to detect amounts of Cr(III) as low as 5 µg per whole lung. In addition, this method was able to monitor the conversion of Cr(VI) to Cr(III) *in situ* despite post-mortem conditions: an important finding since it not only demonstrates the powerful reductive capacity of the lung but allows the detection of Cr(VI) which has been shown to be the primary damaging species in Cr-induced carcinogenesis.

Acknowledgements

Many thanks to Andreas Kortenkamp for his guidance, support and (seemingly endless) patience during my time as a member of “the shiny club”.

I would also like to thank Mark Raffray and Paul Kinchesh for their encouragement and practical input with the MRI studies, and Chris Biggs for a keen eye and a firm hand with our “volunteer” subjects.

For financial support I am grateful to the Ford Motor Company.

Special thanks must go to all the boys and girls in toxicology, particularly Chris, Clive, Dan, Jo and Dave for providing those much needed distractions outside of working hours.

I am indebted to my parents for their support during the writing of this thesis, and to Ron Johnston whose “Drapers seminars” have proved invaluable.

Contents

Abstract	1
Acknowledgements	3
Contents	4
Abbreviations	7
List of figures	9
List of tables	12
Chapter 1	
Introduction	13
1.1 Perspective	13
1.1.1 Uses of Cr compounds.....	13
1.1.2 Exposure and epidemiology.....	15
1.1.3 Genotoxicity of Cr compounds.....	18
1.1.4 DNA lesions generated by Cr compounds.....	20
1.2 Mechanisms of Cr genotoxicity	23
1.2.1 Uptake-reduction model of Cr carcinogenesis.....	23
1.2.2 Intracellular reduction of Cr.....	25
1.2.3 Mechanisms of the mediation of DNA lesions formed during the reductive conversion of Cr(VI) <i>in vitro</i>	28
1.2.4 Potential damaging species generated during the reduction of Cr(VI).....	35
1.3 Cr biomonitoring	42
1.3.1 A rationale for the biomonitoring of exposed individuals.....	42
1.3.2 Problems in Cr biomonitoring.....	43
1.4 Scope of this thesis	44
1.4.1 Aims and objectives.....	44
1.4.2 Experimental approaches.....	45
Chapter 2	
Associations between Cr-induced DNA strand breaks and Cr-DNA adducts	47
2.1 Introduction	47
2.2 Materials	48
2.3 Method	49
2.3.1 Separation of unbound ⁵¹ Cr using <i>Microcon</i> filters.....	49
2.3.2 Separation of unbound ⁵¹ Cr using NENsorb columns.....	50
2.3.3 Separation of unbound ⁵¹ Cr using gel electrophoresis.....	51
2.3.4 Separation of unbound ⁵¹ Cr using the <i>Promega Wizard DNA clean-up system</i>	52
2.3.5 Quantification of the level of strand breaks in PM2 DNA using densitometry.....	53
2.4 Results	55
2.4.1 Separation of unbound ⁵¹ Cr using <i>Microcon</i> filters.....	55
2.4.2 Separation of unbound ⁵¹ Cr using NENsorb columns.....	57

2.4.3	Separation of unbound ⁵¹ Cr using gel electrophoresis	59
2.5	Discussion	70
Chapter 3		
<i>The formation of SSB and Cr-DNA adducts in isolated DNA during the reduction of Cr(VI) by GSH proceeds via distinct pathways</i>		
		71
3.1	Introduction	71
3.2	Method	72
3.3	Results	75
3.3.1	Influence of GSH on the induction of SSB and Cr-DNA adducts	75
3.3.2	Influence of catalase on SSB formation and Cr binding to DNA	76
3.3.3	Further investigations of the characteristics of Cr-DNA adduct formation	78
3.4	Discussion	81
Chapter 4		
<i>An investigation into the potentially pre-mutagenic lesion generated during the reduction of Cr(VI) by GSH</i>		
		90
4.1	Introduction	90
4.2	DNA damage, mutations, and the multistage model of carcinogenesis	90
4.3	Potentially mutagenic lesions generated during the reduction of Cr(VI) by GSH	92
4.4	Approaches for the study of pre-mutagenic lesions	94
4.5	An <i>in vitro</i> mutation assay to determine the pre-mutagenic lesion generated during the reduction of Cr(VI) by GSH	95
4.6	Materials	99
4.7	Method	99
4.7.1	Media and plates	99
4.7.2	Resuspension of <i>E. coli</i> JM105	101
4.7.3	Preparation of competent cells	101
4.7.4	Treatment and purification of plasmid	102
4.7.5	Transformation of competent cells	104
4.8	Results	105
4.9	Discussion	120
Chapter 5		
<i>Cr biomonitoring – a review</i>		
		123
5.1	Introduction	123
5.2	Monitoring internal exposure: Cr in body fluids	125
5.3	Effect monitoring: cytogenetic surveillance studies in lymphocytes	127
5.4	Monitoring early biological effects: DNA damage in lymphocytes	135
5.5	Cr levels in the lung	140
5.6	Lymphocytes and Cr uptake	142
5.7	Summary	144

Chapter 6**Magnetic resonance imaging (MRI) as a technique for
Cr biomonitoring**

Magnetic resonance imaging (MRI) as a technique for Cr biomonitoring	146
6.1 Nuclear magnetic resonance (NMR)	146
6.2 Principle of MRS and MRI	147
6.3 Reproducibility of magnetic resonance images	153
6.3.1 Magnetic field homogeneity.....	153
6.3.2 Water content of tissue.....	154
6.3.3 Influence of paramagnetic nuclei.....	155
6.4 Materials and methods	158
6.4.1 Materials.....	158
6.4.2 Experimental procedures.....	158
6.5 Results	163
6.5.1 <i>In vitro</i> modelling.....	163
6.5.2 <i>In vivo</i> modelling.....	166
6.5.3 Image analysis and the "region of interest".....	174
6.5.4 Quantification of the Cr(III) MRI signal.....	176
6.6 Discussion	180
 Chapter 7	
Summary	183
 References	189

Abbreviations

A	Adenine
AMV	Avian myeloblastosis virus
AP-sites	Apurinic/apyrimidinic sites
AsA	Ascorbic acid
ATP	Adenosine triphosphate
BER	Base excision repair
bp	Base pairs
BSA	Bovine serum albumin
C	Cytosine
CHO	Chinese hamster ovary (cells)
CPM	Counts per minute
Cr	Chromium
Cys	Cysteine
DBNBS	3,5-dibromo-4-nitrosobenzene
DMPO	5,5-dimethyl-1-pyrroline-N-oxide
DMSO	Dimethyl sulphoxide
DNA	Deoxyribonucleic acid
DPC	DNA-protein crosslinks
DPM	Disintegrations per minute
DTT	Dithiothreitol
EDTA	Ethylenediaminetetraacetic acid
EMF	Electromotive force
ESR	Electron spin resonance spectroscopy
G	Guanine
GS [•]	Thiyl radical
GSH	Reduced glutathione (γ -glutamyl-cysteinyl-glycine)
GSSG	Oxidised glutathione
HEPES	(4-[2-hydroxy-ethyl]-1-piperazineethane-sulphonic acid)
HPLC	High performance liquid chromatography
HPRT	Hypoxanthine guanine phosphoribosyl transferase
IPTG	Isopropylthio- β -D-galactoside
MIG	Metal inert gas (welding)
MMA	Manual metal arc (welding)
MRI	Magnetic resonance imaging
NADPH	Nicotinamide adenine dinucleotide phosphate (reduced)
NER	Nucleotide excision repair
NMR	Nuclear magnetic resonance

NMRI	Nuclear magnetic resonance imaging
NMRS	Nuclear magnetic resonance spectroscopy
4-NQO	4-Nitroquinoline-1-oxide
OH·	Hydroxyl radical
8-OHdg	8-Hydroxydeoxyguanosine
pH	= $-\log_{10}[\text{H}_3\text{O}^+]$
ROS	Reactive oxygen species
SCE	Sister chromatid exchanges
SSB	DNA single strand break
T	Thymine
TB	Tris-borate buffer
TE	Tris-EDTA buffer
TIG	Tungsten-inert gas (welding)
Tris	Tris-(hydroxymethyl) aminomethane
UHQ	Ultra high quality water
X-gal	5-bromo-4-chloro-3-indolyl- β -D-galactoside

List of figures

Figure 1.1 Diagrammatic representation of the uptake-reduction model of Cr(VI). p. 24

Figure 2.1 Typical photograph of DNA bands run on an agarose gel and stained with ethidium bromide. p. 54

Figure 2.2 Comparison of Cr-DNA adduct formation in presence (□) and absence (O) of GSH. p. 56

Figure 2.3 Comparison of Cr binding in presence and absence of GSH after isolation of plasmid with NENsorb Nucleic Acid Purification Resin. p. 57

Figure 2.4a Scattergram to illustrate influence of GSH concentration on Cr-DNA adduct formation. p. 60

Figure 2.4b Scattergram to illustrate influence of GSH concentration on SSB induction. p. 61

Figure 2.5a Influence of catalase on the formation of Cr-DNA adducts during the reductive conversion of Cr(VI) by GSH. p. 62

Figure 2.5b Influence of catalase on the formation of SSB during the reductive conversion of Cr(VI) by GSH. p. 63

Figure 2.6 Scattergram to show the influence of Cr concentration on the formation of Cr-DNA adducts. p. 64

Figure 2.7 Scattergram to show Cr-DNA adduct formation as a time dependent process. p. 64

Figure 2.8a Scattergram to illustrate the influence of “ageing” reaction mixtures on the generation of single strand breaks. p. 65

Figure 2.8b Scattergram to illustrate the influence of “ageing” reaction mixtures on Cr-DNA adduct formation. p. 66

Figure 2.9a Diagrammatic representation of an autoradiograph obtained after exposing agarose gels to Hyperfilm. p. 68

Figure 2.9b Diagrammatic representation of an autoradiograph obtained after exposing agarose gels to Hyperfilm. p. 69

Figure 3.1 Comparison of loss of absorbance vs. time for Chelex-treated and untreated phosphate buffer containing 100 μ M AsA. p. 73

Figure 3.2. Influence of GSH on the induction of SSB and Cr-DNA adducts in PM2 DNA. p. 76

Figure 3.3. Influence of catalase on the induction of SSB and Cr-DNA adducts in PM2 DNA. p. 77

Figure 3.4. Influence of [Cr] on Cr-DNA adduct formation in presence of GSH. p. 79

Figure 3.5. Influence of time on Cr-DNA adduct formation in presence of GSH. p. 79

Figure 3.6. Influence of "ageing" reaction mixtures before the addition of DNA on the formation of Cr-DNA adducts. p. 81

Figure 3.7 Schematic representation of the proposed mechanisms involved in Cr(VI)-mediated DNA damage. p. 89

Figure 4.1 Photograph of agarose gel run to determine integrity of pUC19 plasmid. p. 103

Figure 4.2 Distribution of mutation frequencies for six treatment groups (1-6) as a replicate series of three studies. p. 111

Figure 4.3 Boxplots showing treatment groups 1-6 for replicate studies A-C. p. 118

Figure 6.1 Orientation of nuclei during MRS. p. 149

Figure 6.2 "Birdcage" coil into which sample is placed. p. 152

Figure 6.3 Superconducting magnet. p. 152

Figure 6.4 Dissection of rat trachea. p. 161

Figure 6.5 Insertion of cannula into rat trachea. p. 161

Figure 6.6 Assembly of sample in coil. p. 162

Figure 6.7 Placement of coil in magnet. p. 162

Figure 6.8a MRI scan to show the conversion of Cr(VI) to Cr(III) in the presence of GSH. p. 164

Figure 6.8b Reduction of Cr(VI) to Cr(III) by GSH as a function of time. p. 165

Figure 6.9 MRI scan to show comparison between lungs perfused with phosphate buffer (A) and 0.5 mM Cr(III) (B). p. 167

Figure 6.10a MRI scan to illustrate changes in signal intensity with increasing dose of Cr(III). p. 170

Figure 6.10b Graph to show increase in signal intensity with increasing dose of Cr(III). p. 171

Figure 6.11a Graph to demonstrate conversion of Cr(VI) to Cr(III) in post-mortem rat lung after single installation of 100 μg Cr(VI). p. 173

Figure 6.11b Time course scans after single installation of 100 μg Cr(VI). p. 173

Figure 6.12 Comparison of signal intensity as determined by densitometry using a defined region of interest or the whole lung area. p. 175

Figure 6.13 Comparison of signal intensity after single dose of 30 μg Cr(III). p 179

List of tables

Table 4.1 Mutation Frequency in pUC19 Plasmid DNA after *in vitro* modification with Cr(VI)/GSH. p. 107

Table 4.2 Results from statistical analysis of mutation frequencies for replicate studies A-C. p. 119

Table 5.1 Urinary Cr levels among occupationally exposed and non-exposed individuals. p. 127

Table 5.2 Cytogenetic surveillance studies among Cr platers and ferroCr workers. p. 129

Table 5.3 Cytogenetic surveillance studies among stainless steel welders using the manual metal arc method. p. 131

Table 5.4 DNA damage in blood lymphocytes of Cr-exposed workers. p. 136

Table 5.5 Cr levels in the lungs of occupationally exposed and non-exposed individuals. p. 141

Table 6.1 Parameters used during MRI scans. p. 158

Table 6.2 Results from experiments designed to quantify inter-animal variation Cr(III) MRI signal. p. 178

CHAPTER 1

Introduction

Cr compounds (particularly water soluble forms) have long been recognised as carcinogenic to the lung upon inhalation, yet despite extensive research efforts, it is still unclear how they manifest their carcinogenic, mutagenic and DNA damaging effects. Exposure to Cr compounds is of concern in a variety of occupational environments, and many epidemiological studies have been carried out in an attempt to understand its effects. There is a particular need to clarify, at a molecular level, the cellular pathways leading to Cr carcinogenesis, since this will have important implications for the biomonitoring of exposed individuals and for risk assessments in occupational settings.

It is hoped that the present work will go some way towards furthering the development of techniques for the biomonitoring of exposed individuals.

1.1 Perspective

1.1.1 Uses of Cr Compounds

Cr is believed to be an essential dietary supplement in small quantities, playing a role in glucose and cholesterol metabolism (Mertz 1975), but has also been recognised as a respiratory carcinogen for many years. As a first series transition element it can exist in oxidation states ranging from -2 to +6, but it is only the 0, +3 and +6 states which really have any application in industry. The production of Cr pigments represents the largest use of this

element in the chemical industry, while other applications include the production of stainless steel and other alloys, and metal plating (IARC 1990).

Metallic Cr

Cr as a pure metal is used for a variety of reasons in the production of alloys. It may be used to confer oxidation and corrosion resistance (for example, in alloys based on nickel or cobalt), since in the elemental state, Cr is protected by a thin transparent coat of Cr_2O_3 which is extremely resistant to corrosion. Alternatively it may be used to control the microstructure of alloys (with aluminium or copper). Such materials have a range of uses in the engineering industry (cutting tools) and medicine (in surgical implants).

Cr (III) Compounds

Chromic acetate, chloride, hydroxide and nitrate are used as chrome plating reagents in the chemical industry, and in the production of textiles.

Chromic oxide is the most stable green pigment known and as such is used in applications requiring resistance to heat, light and chemical insult.

Cr (VI) Compounds

Chromates in a variety of forms (for example lead, barium, zinc etc.) are most commonly used in the production of pigments, with lead chromate in particular being used to generate the chrome-oranges and chrome-yellows so beloved by the automobile industry. Chromates may also be found in anticorrosion preparations and wood treatments.

1.1.2 Exposure and Epidemiology

The main routes of industrial exposure to Cr compounds are via inhalation, ingestion, and topical absorption. Inhalation of these compounds is the greatest risk in the chromate production, pigment manufacture, chrome plating and welding industries. There are two types of chrome plating techniques: the first is termed decorative plating where a thin layer of Cr is deposited over another metal coating such as nickel. The second technique, hard plating, produces a much thicker Cr coating on a metal base and is much more resistant to corrosion than decoratively plated material (IARC 1990). During the plating process, bubbles of oxygen and hydrogen generate Cr-trioxide mist by bursting through the surface of the liquid in the plating tanks. Decorative plating tends to result in lower chrome air levels than hard plating but many factors including year (e.g. volume of Cr work being carried out, implication of health and safety regulations), country and work conditions will influence this.

During the milling and packaging of chromate pigments, dusts and fumes are also produced, as is the case during welding, where substantial exposure to hexavalent Cr compounds can occur. The welding process generates particulate fumes that have chemical compositions that reflect the agents used. The greatest levels of Cr(VI) are produced by the manual metal arc welding technique, however improved methods and increased safety procedures have led to lower airborne Cr levels. Consequently, as a result of such high levels of exposure, Cr concentrations have been shown to be elevated in the blood, urine, lung tissue and lymph nodes of workers in these

occupations. Of particular concern are Cr levels in lung tissue where deposited particles of this metal can remain for long periods of time even when exposure has ceased (Cohen *et. al.* 1993). Such particles may be slowly taken up by cells, depending on certain physical properties of the compound in question i.e. oxidation state, solubility of initial salt (high solubility may facilitate absorption but may also increase rate of clearance) and the matrix in which the Cr enters the body (Gochfeld and Witmer 1991).

A great number of epidemiological studies have been performed on workers in chrome related industries (IARC 1990) and a clear link has been established between pulmonary exposure to Cr(VI) compounds and cancers of the airways. However, since workers are usually exposed to more than one form of Cr, the risk attributable to Cr(VI) alone is unknown. The type of cancer seen in subjects is dependent on the length of exposure and the nature of the Cr compound involved, with the most frequent type seen being squamous cell carcinoma. Rare sinusoidal cancers have also been reported in workers involved in the pigment producing industry (IARC 1990).

Despite exhaustive epidemiological investigation, a detailed relationship has still not been established between exposure and cancer risk. It is therefore of immediate concern that such a relationship is elucidated, thereby allowing the development of accurate and safe exposure levels to Cr compounds (Lees 1991).

Cr(VI) has been shown to cause sensitisation and is also believed to be responsible for non-genotoxic health effects such as respiratory distress, asthma and skin rashes (dermatitis). Immunological effects, as a result of sensitisation, have included increased granulocytes, elevated macrophages and a higher percentage of lymphocytes in bronchoalveolar lavage fluid from exposed animals. Cr compounds have also been implicated in gastrointestinal disorders such as stomach pain, duodenal ulcers and indigestion. Renal and hepatotoxic effects have also been reported as a result of exposure to Cr compounds (IARC 1990).

Cr is, perhaps unsurprisingly, also an environmental contaminant, but at much lower levels than is found in occupational settings. Sources of exposure include air, as a result of the combustion of fossil fuels (although this process is the source of many other toxic heavy metals, not just Cr), water, as a result of industrial discharges (fresh water having slightly elevated levels of Cr compared with sea water), and food (also the result of industrial discharges). Smokers and beer drinkers may also exhibit elevated levels of urinary Cr as a result of high levels of this metal in tobacco and yeast (IARC 1990).

1.1.3 Genotoxicity of Cr Compounds

The genotoxicity and subsequent carcinogenicity of Cr compounds is mediated by the formation of a variety of DNA lesions. Such lesions have been widely reported following the treatment of animals, cells or isolated DNA with Cr compounds, and include single strand breaks (SSB), DNA interstrand crosslinks (Hamilton and Wetterhahn, 1986), apurinic/apyrimidinic-sites (AP-sites) (Cantoni and Costa 1984), DNA-protein crosslinks (DPC) (Zhitkovitch *et. al.* 1996), and Cr-DNA adducts in *in vivo* and *in vitro* systems (Tsapakos and Wetterhahn 1983, Standeven and Wetterhahn 1991).

The various forms of genotoxic damage induced by Cr compounds have been well documented. Genetic effects have been observed in a variety of bacterial and mammalian cultured systems and include chromosomal aberrations, sister chromatid exchanges (SCEs), gene mutations and DNA lesions. Cr(VI) and Cr(III) species vary in their genotoxic potential as a consequence of their different abilities to penetrate cell membranes. Whereas Cr(VI) complexes, which possess a tetrahedral conformation, readily cross cell membranes and are subsequently reduced by intracellular constituents to Cr(III), such octahedral Cr(III) complexes are relatively impermeable to the plasma membrane. This results in intracellular “trapping” of Cr(III) and the establishment of a concentration gradient across the cell wall. It has been reported in some cases that Cr(III) may be taken up into the cell by phagocytosis but this is not believed to be a major component of Cr uptake (Jennette 1979).

SCEs and chromosomal aberrations are induced in mammalian cells upon exposure to Cr(VI) compounds *in vitro*, and elevated levels of both kinds of genotoxicity have been observed in white blood cells of workers exposed to Cr(VI) in electroplating factories (Bianchi and Levis 1985, IARC 1990).

Bianchi and Levis (1985) have also demonstrated that Cr(VI) compounds are mutagenic in bacterial, yeast and mammalian systems, as have Sugden *et al.* (1990), who demonstrated the complete, and partial oxygen dependence of mutations induced by potassium chromate in Salmonella typhimurium TA102 and TA2638 respectively. Opinion is divided, however, over the specific mutations induced in mammalian genes by Cr(VI) compounds. Yang *et al.* (1992) demonstrated a predominance of mutations in A-T -rich gene sequences of hprt (hypoxanthine guanine phosphoribosyl transferase) mutant Chinese Hamster Ovary cells, whilst Chen and Thilly (1994) showed three prominent hot spots at G:C base pairs in exon 3 of the hprt gene in human lymphoblasts.

Cr (III) compounds were shown not to be genotoxic in the majority of tests. Chromosome aberrations were only seen when using concentrations of Cr two to three orders of magnitude higher than Cr(VI), and SCEs have only been demonstrated in cells with active phagocytosis. However, some Cr(III) complexes have been shown to be mutagenic in the Ames test with the strains S. typhimurium TA98, TA100 and TA92 when complexed to certain ligands to facilitate their penetration into cells i.e. 2, 2'-bipyridyl (bipy) or 1,10-phenanthroline (Bianchi and Levis, 1985, 1987; IARC 1990).

Interestingly, the ability of Cr(III) complexes to form DNA lesions such as Cr-DNA-adducts or DPC *in vitro* has been demonstrated (Tsapakos and Wetterhahn 1983) and low concentrations of Cr(III) bound to DNA have been shown to increase DNA polymerase activity and decrease DNA replication fidelity (Snow 1994).

1.1.4 DNA Lesions Generated by Cr Compounds

Single Strand Breaks (SSB)

Hamilton and Wetterhahn (1986) demonstrated the generation of persistent SSB in the red blood cells of chick embryos treated with Cr(VI), but were unable to show SSB in chick embryo liver or rat lung, liver or kidney. *In vitro* studies involving the treatment of cultured cells with Cr(VI) showed extensive breakage of DNA, a finding which contradicts the same studies *in vivo*. This can be explained by the fact that efficient repair mechanisms are present *in vivo* such that SSB are repaired very quickly (Cupo and Wetterhahn 1984, Snyder 1988). Strand breakage was observed in normal human fibroblasts and in excision deficient *Xeroderma pigmentosum* cells after treatment with potassium chromate, indicating that the breaks were not induced by the repair mechanism (Cupo and Wetterhahn 1984). SSB induced in human diploid fibroblasts and in cultured chick embryo hepatocytes exposed to non toxic levels of Cr(VI) were shown to be reversible, since they were no longer observed two hours after the metal was removed from the medium (Cupo and Wetterhahn 1984). Incubation of human diploid fibroblasts with Cr(VI) in the presence of catalase inhibited the formation of SSB, whilst the presence of potassium iodide and mannitol (both OH[·] scavengers) had no effect.

Treatment of cells with Cr(VI) and GSH led to an increase in the numbers of SSB (Snyder 1988).

Cr-DNA adducts

Cr-DNA adducts were detected in chick embryo hepatocytes after *in vivo* treatment with Cr(VI). These adducts have been proposed to mediate the formation of interstrand cross-links and protein/amino acid cross-links in such cells. No Cr adducts or cross-links were seen in chick erythrocytes following the same treatment (Hamilton and Wetterhahn 1986). Extensive Cr-DNA binding was observed after treatment of cultured mammalian cells with chromate after two hours (Sanilkow *et. al.* 1992, Zhikovitch *et. al.* 1995). The observation that bound Cr was extracted by the chelator ethylenediaminetetraacetic acid (EDTA) suggests that Cr binds to DNA as Cr(III) since other oxidation states of Cr, i.e. (VI), (V) or (IV) cannot be chelated by EDTA (Sanilkow *et. al.* 1992). Up to 50% of the Cr(III) bound to DNA of chinese hamster ovary cells (CHO cells) was found to be cross linked to free amino acids or GSH, thereby increasing the stability of binding (Zhitkovitch *et. al.* 1995). The majority of Cr-DNA adducts observed in treated CHO cells were located in the nuclear matrix subfraction of the chromatin, in which a number of essential nuclear processes, including replication and transformation, take place. These adducts were very persistent, being seen up to 48 hours after Cr treatment (Xu *et. al.* 1994).

In vivo treatment of chick embryos with Cr(VI) led to the formation of protein cross-links in hepatocytes but not erythrocytes (Hamilton and Wetterhahn

1986). Cultured chick embryo hepatocytes exposed to sodium chromate for two hours presented persistent DNA-protein cross-links, detectable even 40 hours after chromate was removed from the system. In contrast, DNA interstrand cross-links and SSB were completely repaired after 12 and 3 hours respectively (Cupo and Wetterhahn 1984). Pre-treatment of Chinese hamster V-79 cells with ascorbic acid (AsA) led to an increase in the level of protein cross-links detected after Cr(VI) treatment (Sugiyama *et. al.* 1991). Actin has been proposed as one of the proteins involved in cross-linking with DNA in CHO cells; no histone proteins were apparently involved. The protein cross-links were dissociated by EDTA, suggesting that the binding is mediated by Cr(III).

Alkaline Labile Sites

Evidence for the formation of alkaline labile sites was obtained from alkaline elution studies using cultured mammalian cells exposed to chromate. Christie *et. al.* (1984) and Cantoni and Costa (1984) observed that DNA from treated cells eluted with increasing rates at alkaline pH. The profile of the resulting elution curves differed markedly from those usually found with agents known to cause what Cantoni and Costa refer to as "frank" single strand breaks. This elution pattern was attributed to the formation of "alkaline labile sites", a type of lesion which, under the given conditions of alkaline elution, ultimately gives rise to single strand breaks. The alkaline labile sites observed could have been the result of an AP-site, (loss of a base from DNA) or a phosphotriester adduct. Both types of lesion are known to cause an increase in the lability of the phosphodiester linkages in the DNA sugar-phosphate

“backbone”, thereby making them vulnerable to alkaline hydrolysis. The formation of AP-sites has been shown to be potentially mutagenic (Loeb and Preston, 1986).

1.2 Mechanisms of Cr Genotoxicity

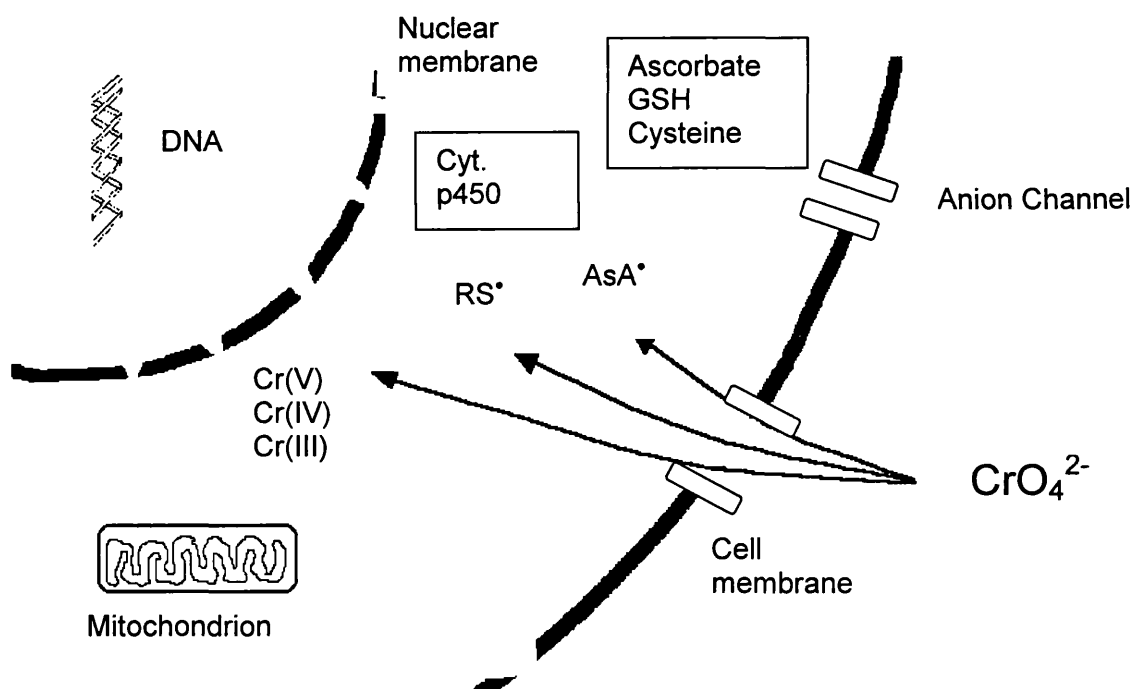
Extensive studies of the mechanisms of Cr genotoxicity over the last fifteen years have failed to elucidate the precise mode of action of these compounds and their role in carcinogenesis (for reviews see Standeven and Wetterhahn 1991, Cohen *et. al.* 1993). It is of vital importance that such mechanisms are understood at a molecular level, thereby allowing the development of physiologically based risk assessments to describe the relationship between external exposure to the carcinogen, dose at target tissue, and levels of DNA damage. Such assessments would allow the establishment of tolerable exposure levels in the workplace.

1.2.1 Uptake-Reduction Model of Cr Carcinogenesis

The uptake-reduction model of Cr as proposed by Jennette (1979) is widely regarded as a general model to describe the processes leading to Cr genotoxicity (Figure 1.1). Hexavalent Cr [Cr(VI)] complexes possess tetrahedral conformation and, as such, readily enter the cell via non-specific ion-channels in the same way as other tetrahedral anions (SO_4^{2-} , PO_4^{3-}). Once inside the cell, these ions are readily reduced by a number of intracellular constituents including glutathione (GSH), ascorbic acid (AsA), cysteine (Cys), and the cytochrome p450-mixed function oxidase system (cyt. p450), to the stable Cr(III) species. Trivalent Cr complexes are

octahedral and are therefore unable to pass back out of the cell, resulting in a concentration gradient of Cr(VI) across the cell membrane. Indeed, in studies where the uptake of Cr(VI) into Chinese hamster V-79 cells was investigated, Sehlmeier *et. al.* (1990) demonstrated that Cr accumulates in a concentration dependent manner, achieving up to 30 times the external concentration of 0.1 mmol/l. Such levels correspond to intranuclear levels of 6 mmol/l after 3 hours (Sehlmeier *et. al.* 1990).

Figure 1.1 Diagrammatic representation of the uptake-reduction model of Cr(VI)



It is widely believed that this reduction process is essential for the mediation of Cr genotoxicity since *in vitro* studies have shown that Cr(VI) is unreactive towards DNA, and that DNA lesions are only seen in the presence of Cr(VI) reducing agents (Bianchi and Levis 1985, Tsapakos and Wetterhahn 1983).

This would suggest that either Cr(III), or a reactive intermediate generated during the reduction process, is responsible for mediating Cr(VI) genotoxicity.

Whilst the intracellular reduction of Cr(VI) would appear to be responsible for the generation of DNA lesions, extracellular conversion of such species can be considered a detoxification process, since it results in the generation of Cr(III) which is unable to enter the cell. Significant levels of AsA have been demonstrated in the alveolar lining fluid of the rat and the guinea pig, and high levels of GSH exist in the epithelial lining fluid of the human lower respiratory tract (Suzuki and Fukuda 1990, Cohen *et. al.* 1993).

To further understand the mediation of Cr(VI) genotoxicity there is a need to determine the nature of the damaging species, its site of action on the DNA molecule and the type(s) of lesion thus formed, and the mutagenic potential of such lesions.

1.2.2 Intracellular Reduction of Cr

Having entered the cell, Cr(VI) compounds may undergo reduction at a variety of sites. The cytoplasm, mitochondria, endoplasmic reticulum and nucleus all possess enzymatic and non-enzymatic factors able to reduce Cr(VI) to Cr(III) (Connett and Wetterhahn 1983). At physiological pH (7.4) only the thiols Cys and GSH, and AsA react at significant rates to contribute to the intracellular reduction of Cr(VI) (Connett and Wetterhahn 1985).

Enzymatic systems which may play a role in the reduction process include the cytochrome p450 mixed function oxidase system, electron transport

complexes of the mitochondrial membrane, GSH reductase, aldehyde oxidase, and DT-diaphorase (Connett and Wetterhahn 1983, Standeven and Wetterhahn 1991a). Intact mitochondria contribute most to the reduction process, converting Cr(VI) to Cr(V) which inhibits respiration and the generation of adenosine triphosphate (ATP). This impairment of oxygen metabolism may influence oxygen concentration in other regions of the cell and play a role in the formation of reactive species (Cohen *et. al.* 1993).

Due to their high intracellular concentrations and ability to reduce Cr(VI) at physiological pH, the low molecular weight thiols (Cys and GSH) and AsA are believed to be the main contributors to the reduction of Cr(VI) and the subsequent generation of active species and DNA lesions (Connett and Wetterhahn 1983, Kortenkamp *et. al.* 1989, Suzuki 1990, Cohen *et. al.* 1993).

Whilst there are several intracellular systems with the potential to reduce Cr(VI) and therefore mediate Cr-induced carcinogenicity, this study aims to concentrate on the role of GSH in this process.

Intracellular levels of GSH can achieve millimolar concentrations in most cells; cytoplasmic levels in rat lung have been shown to be around 2 mM (Suzuki 1990), and in chick embryo hepatocytes and erythrocytes, 6 mM and 2 mM respectively (Misra *et. al.* 1994). GSH is generally regarded as playing a protective role in cell metabolism e.g. scavenging active species during oxidative stress, however, the involvement of GSH in the reductive conversion of Cr(VI) may contribute to the mediation of Cr carcinogenicity.

That GSH plays a vital role in the reduction of Cr(VI) *in vivo* is supported by a number of observations. A positive correlation between levels of SSB and GSH in chick embryos treated with Cr(VI) was demonstrated by Hamilton and Wetterhahn (1986) whereby depleting the levels of intracellular GSH by treating with buthionine sulfoximine led to fewer SSB. Conversely, increasing GSH levels by pretreatment with n-acetylcysteine resulted in increased DNA damage. In a study carried out by Standeven and Wetterhahn (1991), rats that had been treated with Cr(VI) were shown to excrete the metal in bile as Cr(III). When the animals were pre-treated to reduce GSH levels, Cr was excreted exclusively as Cr(VI), suggesting that depletion of GSH prevented normal hepatic reduction of Cr. Treatment of cells with Cr(VI) would, therefore, be expected to deplete levels of GSH, however this has not been demonstrated in other studies (Standeven and Wetterhahn 1991a, Misra *et al.*, 1994). Such observations could be explained were GSH not to play a major role in the *in vivo* intracellular reduction of Cr(VI) but it is more likely that the changes in GSH levels may have been too small to be detected, or that the cells may have rapidly increased biosynthesis to compensate GSH depletion.

During the reduction of Cr(VI) by GSH, a number of reactive intermediates are generated including Cr(V) (O'Brien *et al.* 1985), glutathione thiyl radicals (Aiyar *et al.* 1991), and active oxygen species (Jones *et al.* 1991). Due to the complex redox chemistry of Cr in aqueous media, one or more of these species may be responsible for the formation of potentially mutagenic lesions such as SSB and DNA interstrand crosslinks (Hamilton and Wetterhahn

1986), AP-sites (Casadevall and Kortenkamp 1995), Cr-DNA adducts (Borges *et. al.* 1991) and DNA-protein/amino acid crosslinks (Zhitkovitch *et. al.* 1995).

1.2.3 Mechanisms of the Mediation of DNA Lesions Formed During the Reductive Conversion of Cr(VI) *in vitro*

Single Strand Breaks (SSB)

The induction of SSB in isolated DNA during the reduction of Cr(VI) by a variety of intracellular constituents has been widely reported. As a result of studies involving the induction of SSB in plasmid DNA and a 110 base pair (bp) DNA fragment during the reduction of Cr(VI) by hydrogen peroxide, it has been proposed that hydroxyl radicals were the cleaving species (Kawanishi *et. al.* 1986, Aiyar *et. al.* 1989). However, the relevance of this observation to an *in vivo* system has been questioned in light of the extremely high concentrations of hydrogen peroxide employed. Further evidence to weaken the argument for the role of hydroxyl radicals in Cr-induced carcinogenesis *in vivo* comes from studies by Standeven and Wetterhahn (1991) where the formation of another type of DNA lesion, modified base adducts e.g. 8-hydroxydeoxyguanosine (8-OHdG), was investigated. Such lesions are characteristic of the type of damage caused by hydroxyl radicals. However, when the liver and kidneys of rats which had received a single intraperitoneal dose of sodium dichromate (up to 40 mg/kg), were analysed, no modified bases were detected, suggesting that hydroxyl radicals are not generated during the reductive conversion of Cr(VI).

The role of GSH in the generation of SSB during the reduction of Cr(VI) has been the cause of some controversy. Kortenkamp *et. al.* have demonstrated SSB in isolated PM2 DNA using this system (Kortenkamp *et. al.* 1989, Kortenkamp and O'Brien 1994) but Wetterhahn and co-workers have failed to observe such lesions (Aiyar *et. al.* 1989, Borges *et. al.* 1991). Reactive oxygen species, generated during the reaction by contaminant traces of metal, were proposed as the source of SSB (Borges *et. al.* 1991). However, the levels of SSB remained unchanged even after traces of catalytic metals were removed from the reaction solutions (Kortenkamp and O'Brien, 1994). It seems that the conflicting observations arose as a result of very different experimental systems. Whereas the Kortenkamp group employed physiologically relevant conditions (5 mM GSH, <0.3 mM Cr(VI)) and approximately 3 hours incubation time, Wetterhahn and co-workers selected much higher concentrations of reagents (1.8 mM Cr[VI], 18 mM GSH) and a shorter incubation period of only 30 minutes. The discrepancy can be explained thus: at concentrations exceeding 15 mM, GSH acts as a very efficient scavenger of any potentially damaging species i.e. those generated during the reduction of Cr(VI) and therefore likely to induce SSB. Consequently solutions containing GSH at high concentrations lose their ability to induce SSB. It remains a fact however, that a species generated during the reduction of Cr(VI) by GSH has been shown to induce SSB, and that this process can be inhibited by catalase and by the exclusion of oxygen (Casadevall and Kortenkamp, 1995), thereby indicating a role for molecular oxygen. Interestingly, the lesion was not prevented by the presence of glucose, a potent hydroxyl radical scavenger (Kortenkamp *et. al.* 1990,

Kortenkamp and O'Brien 1994).

While it is clear that Cr(VI)/GSH systems are capable of inducing SSB in DNA, the relevance of such lesions *in vivo* is unclear due to efficient repair mechanisms operating within the cell. The mutagenic, and subsequent carcinogenic, potential of this type of DNA damage is discussed later.

AP-sites

The formation of DNA AP-sites results from the cleavage of the N-glycosidic bond that connects the deoxyribose sugar with the purine or pyrimidine base. This base is then released leaving the phosphodiester backbone intact but susceptible to alkaline hydrolysis.

Depurination and depyrimidation occur at significant rates under physiological conditions (Lindahl and Anderson 1972), with the rate of base release increasing with low pH and higher temperature. Purines are released more readily than pyrimidines (Loeb and Preston 1986, Povirk and Steighner 1989). The rate of AP-site formation can also be influenced by chemical modification, for example, reaction with electrophilic mutagens to form base-adducts can decrease the stability of the N-glycosidic bond (Drinkwater *et. al.* 1980, Gamper *et. al.* 1980, Loeb and Preston 1986, Prakash and Gibson 1992). Using AP-endonucleases in combination with electrophoresis techniques, Drinkwater *et. al.* (1980) demonstrated the formation of AP-sites upon treatment of isolated SV40 DNA with a variety of electrophilic compounds, ranging from simple alkylating agents, such as methyl

methanesulfonate and N-methyl-N-nitrosurea, to alkylating agents like benzo(a)pyrene-diol-epoxide, and aromatic amines such as N-acetoxy-2-acetylaminofluorene.

Cr-DNA Adducts

The ability of Cr(III) complexes to bind to isolated DNA and to cell nuclei has been demonstrated, and is known to be strongly influenced by the nature of the ligands involved (Tsapakos and Wetterhahn 1983, Kortenkamp *et. al.* 1992, Hneihen *et. al.* 1993). High levels of Cr binding were observed in isolated calf thymus DNA and in salmon sperm nuclei with aquo-Cr(III) complexes, but this was shown to be greatly reduced when Cr(III) was complexed with amino acid ligands or tridentate peptides (Hneihen *et. al.* 1993). Kortenkamp *et. al.* (1992) also demonstrated the influence of the type of ligand, and the charge of the complex, on DNA interactions. Their observation that cationic Cr(III) complexes induced DNA condensation, and the lack of evidence to support the proposal that cationic Cr(III) species are generated *in vivo*, led to their argument that such Cr(III) species do not provide a relevant model for Cr binding *in vivo*. It is therefore apparent that the reactivity of Cr(III) species *in vivo* is strongly influenced by the nature of the complexing ligands.

Cr(VI) appears to be unreactive towards isolated DNA or nuclei without the presence of a reducing agent, as demonstrated in a number of studies.

Several compounds have been shown to mediate the reductive conversion of Cr(VI), including thiols (GSH, Cys) (Aiyar *et. al.* 1989, Borges and

Wetterhahn 1989, Borges *et. al.* 1991), microsomes/NADPH (Tsapakos and Wetterhahn 1983) and AsA (Bridgewater *et. al.* 1994). The species involved in Cr-DNA adduct formation, and the site of interaction on the DNA molecule have been the source of much speculation. Borges and Wetterhahn, in the light of the rapid reduction of Cr(VI) *in vivo* have proposed that an intermediate generated during this reduction process (probably Cr[V]) may be responsible.

It has also been suggested that Cr binds to the phosphate backbone of DNA, and also to the bases. Tsapakos and Wetterhahn (1983) observed high levels of binding in G-rich polynucleotides, and this hypothesis was supported by findings that specific polymerase arrest profiles observed at bases preceding guanine residues in a double stranded pSV2neoTS plasmid DNA treated with chromate and AsA suggested base binding. Such specificity would not be expected if Cr-DNA adducts were formed at the phosphate backbone since this region of the DNA molecule could be considered to be homogenous (Bridgewater *et. al.* 1994). In contrast, Sanilkow *et. al.* (1992) did not observe base binding upon analysis of DNA from human osteosarcoma cells treated with ^{51}Cr by high performance liquid chromatography (HPLC). They concluded that Cr binds at the DNA phosphate backbone. Kortenkamp and O'Brien (1991) have also demonstrated, via ^{31}P NMR studies, the interaction of Cr with the phosphate group on ATP. Further studies to elucidate the nature of the binding species and the site of interaction were carried out in this laboratory, and the results are discussed later.

DNA-Protein/Amino Acid Crosslinks

That aqueous Cr(III) species can form DNA-protein crosslinks with bovine serum albumin (BSA), actin and histones in plasmid DNA has been demonstrated by Sanilkow *et. al.* (1992). The extent of crosslinking appears to be influenced by the proportion of GSH and histidine contained in the protein, in the order BSA>actin>histone. As with other types of DNA lesion, Cr(VI) does not induce DNA-protein crosslinks unless a reducing agent is present (Tsapakos and Wetterhahn 1983, Sanilkow *et. al.* 1992), and the levels of crosslinking also appear to be influenced by the nature of the reducing species involved. In studies where calf thymus DNA was treated with Cr(VI) and GSH or Cys for 30 min, the crosslinking of thiol to DNA via Cr(III) was observed to be ten times higher in the presence of GSH than with Cys (Borges and Wetterhahn 1989).

The crosslinking of amino-acids such as GSH, glutamic acid and histidine has been observed in CHO cells exposed to Cr(VI) (Zhitkovitch *et. al.* 1995). Up to 50% of the Cr present was involved in this type of binding and it is thought that such lesions may represent a significant type of DNA damage. DPC represent a type of lesion which is not readily repaired and may therefore influence the replication process (Costa 1991, Xu *et. al.* 1994).

It should be stressed that while all these lesions can be adequately described *in vitro*, these observations may have little or no relevance to an *in vivo* system. Repair mechanisms operating within the cell may prevent any of these lesions being "fixed" as mutations and even then, the mutational profile

of a cell may be dramatically altered during replication. To further understand the relevance of these types of DNA damage *in vivo* we need to establish their mutagenic potential in a cell. A mutation assay was employed to address these problems and the findings are discussed later.

1.2.4 Potentially Damaging Species Generated During the Reductive Conversion of Cr(VI)

It has been well established that a number of potentially damaging species are generated during the reduction of Cr(VI) to Cr(III) yet despite extensive research attempts, it is still unclear which intermediates are responsible for specific lesions, or indeed if a relationship exists between different types of lesion. *In vitro* studies have shown that Cr(VI) is unreactive towards isolated DNA unless a reducing agent is present (Tsapakos and Wetterhahn 1983). Similarly, Cr(III) complexes have been shown to be relatively inert, despite their ability to react slowly with isolated DNA leading to the formation of Cr-DNA adducts and DNA-protein/amino acid crosslinks (Tsapakos and Wetterhahn 1983, Sanilkow *et. al.* 1992). It seems likely, therefore, that the induction of lesions such as SSB and AP-sites should be mediated by a reactive species generated during the conversion of Cr(VI) (Kortenkamp *et. al.* 1989, Sanilkow *et. al.* 1992). However, the redox reactions of Cr(VI) and GSH (as well as other reducing agents) are complex, and identification of potentially damaging intermediates is difficult (O'Brien and Wang 1992, Stearns *et. al.* 1995). In addition, the formation of intermediates *in vitro* is highly influenced by the experimental conditions of the study e.g. buffer system used, pH, concentrations of the reactants. *In vivo*, the contribution of the different species to the mediation of Cr genotoxicity will depend on the amounts of unreduced Cr(VI) and/or intermediates that are able to penetrate the nuclear membrane and interact with genetic material. Some well-established intermediates and their potential to damage DNA are discussed.

Cr Species

Cr (V)

Cr (V) has been shown to be generated during the reduction of Cr(VI) by GSH. Such species contain a single unpaired electron and can therefore be detected using electron spin resonance spectroscopy (O'Brien *et. al.* 1985). After treatment of chick embryos with sodium dichromate *in vivo*, the formation of two transient Cr(V) complexes was observed in the red blood cells, while a single, more stable, species was observed in the liver (Liebross and Wetterhahn 1992). Similarly, a Cr(V) complex was observed upon incubation of cultured Chinese hamster V-79 cells with sodium chromate (200 μ M) for two hours. Pre-treatment of the cells with AsA resulted in a dramatic decrease in the amount of Cr(V) formed (Sugiyama *et. al.* 1991). Conversely, depletion of cellular GSH with buthionine sulfoximine led to a 170% increase in detectable Cr(V) when GSH depletion exceeded 85% (Sugiyama and Tsuzuki 1994).

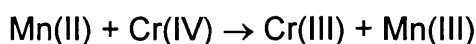
In vitro, Cr(V) complexes are formed during the reduction of Cr(VI) by a variety of thiols (e.g. GSH, Cys, dithiothreitol). The magnitude and half life of the Cr(V) signal, as detected by electron spin resonance spectroscopy (ESR), is dependent on the nature of the thiol involved and the buffer system employed (O'Brien *et. al.* 1985, Goodgame and Joy 1986, Aiyar *et. al.* 1989, Borges *et. al.* 1991).

The Cr(V) species was extremely persistent when GSH was present as the reductant whilst use of GSH led to very short lived Cr(V) species. This is

demonstrated in studies by Kitagawa *et. al.* (1988), where the half lives of Cr(V) in reaction mixtures of 10 mM Cr(VI)/30 mM GSH or GSH at pH 7.0 were shown to be 23-30 minutes and 3 minutes respectively. The stability of Cr(V) species in solution may therefore be of importance in the mediation of Cr toxicity.

Cr (IV)

Cr (IV) complexes are silent to ESR spectroscopy but have been detected by magnetic susceptibility measurements during the reduction of Cr(VI) at acid pH. Indeed Cr(IV) has been shown to be more predominant than Cr(V) under these conditions (Bose *et. al.* 1992). More recently, Stearns *et. al.* (1995) monitored the formation of Cr(IV) indirectly by using Mn(II) as a probe in solutions containing Cr(VI) and AsA. Mn reacts with Cr as follows;



thus the decrease in the intensity of the Mn(II) ESR signal was taken to represent an increase in Cr(IV). Consequently Cr(IV) was seen to increase with rising AsA levels. Similar studies have monitored the generation of Cr(IV) during the reduction of Cr(VI) by GSH at neutral pH. A decrease in the Mn(II) ESR signal was also observed under these conditions suggesting the generation of Cr(IV) (da Cruz Fresco *et. al.* 1995). Since Cr(IV) species are highly reactive they may represent an important species in the mediation of Cr(VI)-induced carcinogenesis (Shi *et. al.* 1994).

Cr (III)

As the final product of the reduction process of Cr(VI), Cr (III) species have been widely believed to be inert towards DNA. However, certain complexes have been shown to bind to isolated DNA and cell nuclei (Tsapakos and Wetterhahn 1983, Hneihen *et. al.* 1993, Kortenkamp and O' Brien 1991), and can crosslink proteins such as BSA, actin or histones to plasmid DNA *in vitro* (Sanilkow *et. al.* 1992). Studies to elucidate the precise role of Cr(III) complexes in the mediation of Cr-induced mutagenesis were carried out and the results are discussed later.

Cr (II)

The role of such species in the mediation of DNA damage is unclear since, under physiological conditions they are readily oxidised to Cr(III). However, because of their reactivity towards oxygen, they could be involved in the formation of other species capable of damaging DNA (Sugden *et. al.* 1992).

Reactive Oxygen Species

Reactive species such as hydroxyl radicals (OH) can be monitored indirectly using ESR spectroscopy in combination with spin-traps which form more stable radicals. Alternatively, DNA can be screened for "signature" forms of damage such as modified bases e.g. 8-hydroxydeoxyguanosine (8-OHdG) which are indicative of attack by active oxygen species.

Several authors have proposed a role for such species in the generation of DNA lesions during the reduction of chromate (Kawanashi *et. al.* 1986, Aiyar

et. al. 1989, Kortenkamp *et. al.* 1989, Shi *et. al.* 1994). The formation of OH[·] during the reduction of chromate by hydrogen peroxide (H₂O₂) has been reported in the presence of the spin-trap 5,5-dimethyl-1-pyrroline-N-oxide (DMPO) (Kawanishi *et. al.* 1986). This has been confirmed by Aiyar *et. al.* (1989) who also demonstrated the formation of 8-OHdG when calf thymus DNA was included in the reaction mixture. Reaction of Cr(VI) with GSH did not lead to the generation of OH[·] radicals unless H₂O₂ was added to the incubation (Aiyar *et. al.* 1989). Similarly, Shi *et. al.* (1994) only saw generation of OH[·] radicals in Cr(VI)/AsA/H₂O₂ systems. It is generally believed that such radicals are generated via a pseudo-Fenton reaction involving H₂O₂ and an intermediate oxidation state of Cr. The presence of a reducing agent would ensure a continuous supply of catalytic metal ions. Despite such conclusive findings, the relevance of these mechanisms is unclear when considering an *in vivo* system since the concentrations of H₂O₂ employed in these studies were in the millimolar range (1-18 mM), which greatly exceed expected intracellular levels of 10⁻⁷-10⁻⁹ M (Standeven and Wetterhahn 1991a).

Further suspicion about the involvement of OH[·] radicals comes from spin-trapping studies carried out by Jones *et. al.* (1991). Using the spin-traps 3,5-dibromo-4-nitrosobenzene (DBNBS) and dimethyl sulfoxide (DMSO) they detected the formation of the DBNBS-CH₃ radical in the presence of the Cr(V)-GSH complex, Na₄Cr(GSH)₂(GSSG).8H₂O. A strongly oxidising species was able to cleave the C-S bond of DMSO to form CH₃, which was

then trapped by DBNBS. It was originally believed that the strongly oxidising species were OH[·] radicals and a mechanism involving thiyl radicals and Fenton chemistry was proposed. However generation of OH[·] radicals during the reduction of chromate by GSH was later disproved by competition kinetics studies (Kortenkamp and O'Brien 1994). It was concluded that some other highly oxidising species capable of cleaving CH₃[·] from DMSO was involved.

In vivo treatment of rats with sodium chromate showed no significant increase in 8-OHdG in the liver or kidney (Standeven and Wetterhahn 1991a). However, increased levels of modified bases were seen in the red blood cells of chick embryos treated with sodium chromate, but not in liver cells. Accordingly, it has been proposed that the high levels of haemoglobin present in erythrocytes may have induced the formation of OH[·] radicals (Misra *et. al.* 1994). Furthermore the results of studies of the mutational spectra of the hprt gene of cultured cells do not agree with the idea of OH[·] radical involvement (Yang *et. al.* 1992, Chen and Thilly 1994). The mutational spectrum generated by Cr(VI) differed markedly from that induced by hydrogen peroxide, molecular oxygen, iron(II) or copper(I)/(II), all thought to be dependent on OH[·] radicals or activated oxygen species. Whether or not reactive oxygen species are generated *in vivo* and whether or not the 8-OHdG assay is sensitive enough to detect potentially very low levels of such species remains to be clarified.

Thiyl Radicals

Thiyl radicals are formed *in vitro* during the conversion of chromate by GSH via a one-electron reduction step (O'Brien and Wang 1992), as detected by ESR/spin-trap studies (Aiyar *et. al.* 1989). Although unlikely to cause direct DNA damage, $GS\dot{\cdot}$ can participate in a series of radical reactions which may ultimately lead to the generation of reactive species such as superoxide, hydrogen peroxide, or $OH\dot{\cdot}$ radicals. Also, during this one-electron reduction, Cr(V) species are generated which are likely to be free of ligands and subsequently highly reactive. Thus the generation of thiyl radicals may be considered a significant pathway in the production of DNA-damaging species.

Whilst much work has been carried out to elucidate the mode of action of chromate at a molecular level, little is known about the implications of these types of damage in an intact organism i.e. which lesions represent potentially mutagenic and carcinogenic changes. A simple *in vitro* model may enable us to correlate dose/damage responses but tells us nothing about effects *in vivo*. The complex nature of the multi-stage model of carcinogenesis, whereby the mutational profile of cells may be dramatically altered by repair mechanisms and other subsequent genetic changes would suggest that the whole picture is considerably more complicated. It is only through a comprehensive understanding of the mechanisms by which Cr(VI) compounds exert their carcinogenic potential that we can hope to develop methods for the biomonitoring of exposed individuals which are predictive of cancer risks.

1.3 Cr Biomonitoring

1.3.1 A Rationale for Monitoring Exposed Individuals

Biomonitoring (that is, investigations of the biological processes pertinent to a particular target organ or physiological process) of individuals exposed to Cr compounds should provide clues about the ongoing processes of Cr toxicity and provide a clearer overall picture of potential carcinogenic changes. With many of the potentially hazardous workplaces identified, the major concern is to develop and adopt preventative measures to avoid Cr exposures which lead to excess cancer risks. It is therefore necessary to define safe levels of exposure on a sound toxicological basis, and to devise methods for the biomonitoring of exposed individuals which are predictive of cancer risks.

1.3.2 Problems in Cr Biomonitoring

Methods of surveillance previously employed have included relatively non-invasive techniques such as the determination of Cr in body fluids (urine, plasma, blood) or the investigation of DNA damage in easily accessible, nucleated or “surrogate” tissue e.g. lymphocytes. In studies where body fluids were analysed for Cr, the determination of an *internalised dose* gave a good indication that exposure had taken place but gave no information about potential cancer risks. Similarly, monitoring the *early biological effects* of Cr exposure in lymphocytes (e.g. Chromosome aberrations, sister chromatid exchanges and gene mutations) gave an indication of the *biologically effective dose* of Cr i.e. the amount of ingested compound which began to show biological effects. However, any correlation between these observations and processes taking place in the target organ (the lung) rely on the assumption that the cells under investigation (lymphocytes) accurately reflect changes occurring in other tissues.

In studies where the lymphocytes of exposed workers were investigated for early biological effects, the results were somewhat inconclusive (Popp et. al. 1991, Gao et. al. 1994, Zhitkovitch et. al. 1996), a surprising observation considering the enormous genotoxic potential of Cr(VI). However, this may be explained by the relatively small differences in Cr concentration between the lymphocytes of exposed and control groups. The toxicokinetics of inhaled Cr(VI) and the dynamics of lymphocyte traffic further complicate matters. After ingestion, only a small fraction of the total inhaled dose is distributed

in the body, while the bulk remains in the lung for very long periods of time. Given that the daily recirculation of lymphocytes from the lungs back to the blood is negligible compared to recirculation from such organs as the spleen, it seems more likely that circulating lymphocytes (those under investigation for biological effects) are exposed to Cr from the blood and therefore do not reflect processes occurring in the lung. This would explain the similarities in lymphocyte Cr concentration seen in exposed and control subjects. These findings, taken on their own, would suggest that lymphocytes do not represent an appropriate model for the biomonitoring of exposed individuals. However, it should be stated that in all these studies, workers were exposed to Cr levels below $50 \mu\text{g}/\text{m}^3$, the current exposure limit in many industrialised countries. At higher exposure levels, lymphocytes may well provide a useful model for the effect monitoring of Cr exposure.

1.4 Scope of this Thesis

1.4.1 Aims and Objectives

The aims of this study are, initially, to further characterise the binding of Cr to DNA in the presence of GSH. Under physiological conditions the rate of Cr-DNA adduct formation, and influence of Cr and GSH concentrations on binding will be investigated. Information gained from these studies will enable a clearer picture of the reactive species involved in the mediation of Cr-induced DNA damage to be formed, and subsequently, will allow the elucidation of potential common

mechanistic pathways in these processes. It is also hoped that clues will be uncovered as to the site(s) of action of Cr species at the DNA molecule. Having described a model for the role of different species in Cr-induced DNA damage, and the various pathways involved, the influence of specific types of damage will be investigated to determine their mutagenic potential. Demonstrating that one or more forms of Cr-induced DNA damage may be passed on to progeny cells as a heritable change will allow a clearer picture to be developed of how Cr mediates its carcinogenic effects.

Since Cr-induced carcinogenesis is primarily of concern in industry, it is proposed to develop a monitoring technique involving MRI which will allow the determination of amounts of Cr compounds in the lungs of exposed individuals. Information obtained by using this technique may then hopefully be considered in conjunction with data from previous biomonitoring studies and a comprehensive model of Cr toxicokinetics developed.

1.4.2 Experimental Approaches

If mutual mechanistic pathways in the formation of Cr-induced DNA damage are to be elucidated then it is crucial that the different types of damage which are being monitored are investigated in the same sample. To this end it is proposed to employ an electrophoresis method utilising ^{51}Cr as a marker to allow detection of Cr-DNA binding while in the same sample, strand breakage can be assessed by

staining the gels with ethidium bromide and performing densitometry.

Modulation of reaction conditions (pre-incubation of reagents, inclusion of catalase) will also give further information about the reactive species involved and may provide clues as to the site of action on the DNA macromolecule.

A bacterial mutation assay is proposed to monitor the effects *in situ* of different types of DNA damage which, again, can be predetermined by modifying the reaction conditions. Briefly, plasmid DNA is exposed to damaging agents which is then incorporated into host bacteria which may then exhibit phenotypic changes as a result of mutagenic changes.

The paramagnetic properties of Cr(III) enable its detection by MRI and it is proposed that a whole animal model is developed to explore the deposition of Cr compounds in the lung. The sensitivity of this technique will be assessed and it is hoped that the *in situ* conversion of Cr(VI) to Cr(III) can be demonstrated since Cr(VI) has been shown to be the primary damaging species in Cr-mediated carcinogenesis.

CHAPTER 2

Associations Between Cr-Induced DNA Strand Breaks and Cr-DNA Adducts.

2.1 Introduction

The question which arises from what is already known about the role of Cr(VI) in oxidative DNA damage, and which is pertinent to biomonitoring, is whether or not one type of lesion can be taken as a predictor of other types of damage and, if a relationship exists, whether this will enable us to develop approaches for the biological screening of exposed individuals. A clear relationship has already been demonstrated between the formation of SSB and AP-sites during the reduction of Cr(VI) by GSH (Casadevall and Kortenkamp 1995), and this finding led us to investigate the possible association between SSB and other types of DNA damage; namely the generation of Cr-DNA adducts. It should be stressed that whilst several authors have attempted to clarify the mechanism(s) of Cr-induced DNA damage, and in particular the formation of Cr-DNA adducts (Borges *et. al.* 1991, Aiyar *et. al.* 1991) data are still lacking about the characteristic binding of this metal to DNA, for example how binding is influenced by GSH concentration, or the time course required for Cr-DNA adduct formation to saturate. Other considerations include the influence of active oxygen species in this system, or the role of intermediates in the mediation of this type of damage. It is hoped that such investigations will help to clarify the mechanisms involved in Cr-induced DNA damage. This chapter describes the development of an

assay to monitor the incidence of two different types of DNA damage within the same sample. Initially, an experimental model was adopted which had previously been shown to be appropriate in this laboratory for the investigation of Cr-induced DNA damage (da Cruz Fresco 1995). However, further technical problems to be considered included the isolation of the DNA-Cr complex after treatment of the plasmid, and the determination of Cr-DNA adduct formation without the introduction of further damage to the sample which may then mask subsequent visualisation of SSB. Whilst every effort was made to ensure the success of these experiments, many technical difficulties were encountered which led to the ultimate choice of experimental technique adopted. It should be pointed out, therefore, that this Chapter represents a lot of the method development work which was carried out before a successful model was determined; the fruits of which are described in Chapter 3.

2.2 Materials

PM2 DNA (8 µg/ml) was obtained from Boehringer Mannheim (Lewes, East Sussex, UK), ⁵¹Cr as sodium chromate (37 MBq/4.4 µg Cr) was from Amersham (Amersham, UK), and potassium chromate was purchased from BDH Ltd. (Poole, Dorset, UK). Microcon filtration units were from Amicon (Amicon, USA), "Ready Cap" solid scintillation matrices were provided by Beckman (High Wycombe, UK). Glutathione, ethidium bromide, and catalase came from Sigma (Poole, Dorset, UK) and "Wizard" DNA clean-up kits were supplied by

Promega (Southampton, UK). Agarose was purchased from Bio-Rad (Hemel Hempstead, UK) whilst Hyper-film was from Amersham (Amersham, UK) and NENsorb resin was supplied by DuPont (Stevenage, Herts, UK) Soluscint A was from National Diagnostics (Kimberly Research, UK).

2.3 Method

2.3.1 Separation of Unbound ^{51}Cr Using Microcon 30 Filters

PM2 DNA (160 ng) in a final volume of 100 μl was incubated with 0.5 mM Cr(VI) as potassium chromate, containing ^{51}Cr sodium chromate (37 MBq/4.4 μg Cr) and GSH (5 mM) in phosphate buffer (0.1 M, pH 6.8) for 12 h at room temperature (around 20 $^{\circ}\text{C}$). The reaction was terminated by filtration with Microcon 30 filters, and the DNA isolated by a series of “washing” steps. Briefly, after the initial filtration to terminate the reaction, the DNA concentrate was resuspended in 500 μl of phosphate buffer and centrifuged through Microcon 30 filters at 7,500 rpm for 8 min. This step was repeated a number of times to ensure the removal of any unbound Cr from the DNA. After washing, the samples were resuspended in 100 μl of buffer and transferred to solid scintillation matrices. Any bound Cr was measured by counting the samples using the tritium channel on a Beckman LS6000IC scintillation counter.

2.3.2 Separation of Unbound ^{51}Cr Using NENsorb Columns

NENsorb columns were prepared by packing plastic tubes with approximately 200 mg of NENsorb resin and “primed” by flushing with “reagent A” (0.1 M Tris-HCl, 10 mM Triethylamine, 1 mM dipotassium or disodium EDTA, pH 7.7). Samples (containing 160 ng PM₂ DNA and 0.5 mM Cr[VI] spiked with ^{51}Cr as above, in the presence or absence of 5 mM GSH in a final volume of 20 μl phosphate buffer) were made up to a volume of 200 μl with “reagent A” and then loaded onto the columns. The columns were then washed with 3 ml of reagent A, followed by 3 ml of UHQ water. Finally, the DNA was eluted from the column by rinsing with “reagent B” (50 % methanol in UHQ water) and the samples dried before scintillation counting. To determine the volume of “reagent B” required to fully elute the DNA from the NENsorb columns, a sample was processed and the effluent collected in 200 μl fractions. In order to establish the volume of buffer required to fully elute the plasmid, the fractions were then run on an electrophoresis gel (0.8 % agarose, 1 h, 2.2 V/cm) and stained with ethidium bromide. The presence of methanol in these samples did result in the loss of some plasmid during the loading of the electrophoresis gel. However, by visualising the eluted DNA bands, it was determined that the bulk of the DNA had been eluted after 400 μl of “reagent B”, whilst remaining traces had been completely washed off the column after 1200 μl . Consequently, it was felt that 400 μl of “reagent B” was sufficient for our purposes to elute the plasmid. Of this 400 μl , aliquots of 20 μl were taken for scintillation counting (to

determine Cr-DNA binding), and gel electrophoresis (determination of single strand break formation).

2.3.3 Separation of Unbound ^{51}Cr Using Gel Electrophoresis

PM2 DNA (160 ng in a final volume of 20 μl) was incubated at room temperature in the presence of GSH (0 - 20 mM) and potassium chromate (0 - 1.5 mM, containing an equal volume of ^{51}Cr as sodium chromate, 37 MBq/4.4 μg Cr), in phosphate buffer. To a number of samples, catalase (10 $\mu\text{g}/\text{ml}$) was added. Control samples contained potassium chromate and GSH, but no DNA, or potassium chromate and DNA, but no GSH. In some experiments catalase was inactivated by denaturing the enzyme at 65 $^{\circ}\text{C}$ for 10 min. In order to evaluate the role of intermediates generated during the reduction of Cr(VI) by GSH, a series of "aged" reaction mixtures was prepared by pre-incubating GSH (5 mM) and labelled potassium chromate (0.5 mM) in phosphate buffer for 0-5 h. DNA was then added and the samples post-incubated overnight.

Gel electrophoresis was performed on the samples immediately after incubation (0.8 % agarose in TPE buffer, 1 h, 2.2 V/cm). The gels were stained with ethidium bromide and photographed under UV light for subsequent analysis to determine SSB levels (as described). DNA bands were excised from the gel under UV light and solubilised in 0.5 ml H_2O_2 (30 % w/w) plus 0.5 ml perchloric acid (70 %). To the solubilised gel slices, 5 ml of ethanol was added to prevent

subsequent precipitation of the agarose followed by 10 ml of liquid scintillant (Soluscint A). Cr binding was then determined by scintillation counting as described.

Where appropriate, electrophoresis gels were wrapped in "Saran" plastic film and exposed to *Hyper* film overnight. Autoradiographs were developed according to the manufacturers instructions.

2.3.4 Separation of Unbound ⁵¹Cr Using the Promega Wizard DNA Clean-up System

Alternatively, PM2 DNA (320 ng in a final volume of 40 µl) was incubated at room temperature in the presence of GSH (0-20 mM) and potassium chromate (0-1.5 mM) containing an equal volume of ⁵¹Cr as sodium chromate (37 MBq/4.4 µg Cr) in HEPES (4-[2-hydroxy-ethyl]-1-piperazineethane-sulphonic acid) buffer (15 mM, with NaCl 0.15 M, pH 7.0) for 18 h. To a number of samples, catalase (10 µg/ml) was added. Control samples contained potassium chromate and GSH, but no DNA, or potassium chromate and DNA but no GSH. In some experiments catalase was inactivated by denaturing the enzyme at 65 °C for 10 min. Samples were split into aliquots of 20 µl and prepared for the determination of the level of Cr-DNA adducts and SSB. In order to evaluate the role of intermediates generated during the reduction of Cr(VI) by GSH, a series of "aged" reaction mixtures was prepared by pre-incubating GSH (5 mM) and labelled potassium chromate (0.5 mM) in HEPES buffer for 0-5 h. DNA was then and the samples post-incubated overnight.

In order to separate unbound Cr from the reaction mixtures, samples were processed using the Promega *Wizard DNA Clean-up System* according to the manufacturer's instructions. Briefly, samples were suspended in *Wizard purification resin* (6M guanidine thiocyanate) and loaded onto *Wizard minicolumns*. Any unbound Cr was rinsed off the column by washing twice with 2 ml 80 % isopropanol. Finally, the Cr-DNA complex was eluted with UHQ water at 65 °C. In order to estimate the extent of recovery of the plasmid, aliquots of DNA which were not subject to purification were run on agarose gels. The intensity of the resulting bands was then compared with those of purified samples. By this technique, recovery of the plasmid was estimated to be close to 100 %.

2.3.5 Quantification of the Level of Strand Breaks in PM2 DNA

PM2 DNA was loaded onto agarose gels and electrophoresed as described. The gels were then stained with ethidium bromide and photographed under UV light (265 nm). An example of a typical photograph is shown (Figure 2.1). The relative intensity of the two DNA bands, corresponding to the supercoiled and open circular forms, was analysed by scanning a digitalised image of a gel using PC-image Plus 1.54 software. Subsequently the peaks were integrated using the program Fig. P. The example shown (lane 3) gives areas under curves of 1147 for form II (open circular) and 1005 for form I (supercoiled) in arbitrary units. If we assume the incidence of SSB along the DNA molecule to follow a Poisson distribution, then

the fraction f_s of unbroken (supercoiled) DNA molecules can then be determined using the formula;

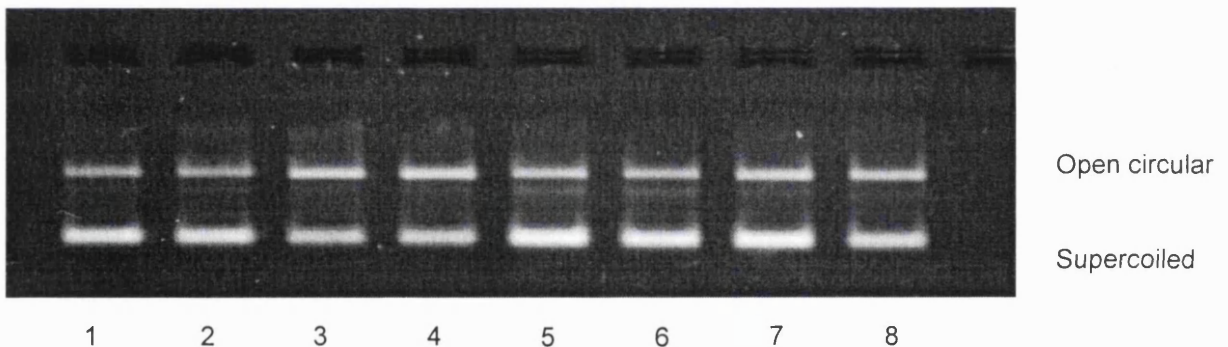
$$f_s = \text{form I} / (0.8 \text{ form II} + \text{form I})$$

$$\text{i.e. } f_s = 1005 / (0.8 \times 1147 + 1005)$$

$$= 0.52$$

The correction factor of 0.8 was used to account for the higher fluorescence of the open circular DNA (form II) when compared to intact supercoiled DNA (form I) (Kortenkamp *et. al.* 1989).

Figure 2.1 Photograph of DNA bands run on agarose gel and stained with ethidium bromide. Also shown is the accompanying densitometry profile from which the ratio of Open Circular to Supercoiled DNA is determined.



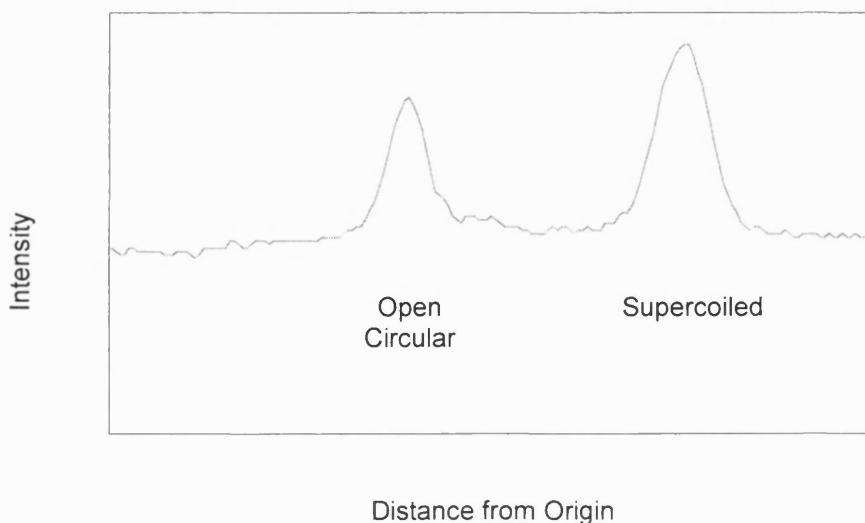
Key to gel lanes;

1 and 2 - 160 ng PM2 DNA + 0.5 mM Cr(VI)

3 and 4 - 160 ng PM2 DNA + 0.5 mM Cr(VI) + 5 mM GSH

5 and 6 - 160 ng PM2 DNA + 0.5 mM Cr(VI) + 5 mM GSH + 10 $\mu\text{g/ml}$ catalase

7 and 8 - 160 ng PM2 DNA + 0.5 mM Cr(VI) + 5 mM GSH + 10 $\mu\text{g/ml}$ denatured catalase



2.4 Results

2.4.1 Separation of Unbound ^{51}Cr Using Microcon 30 Filters

Initially our investigations were concerned with the exploration of the generation of more than one type of lesion in the same sample to determine whether a relationship exists which might provide evidence for a common mechanistic pathway. A connection between SSB and AP-sites was established previously (Casadevall and Kortenkamp, 1995) and therefore it was felt necessary to establish whether, under conditions where high levels of SSB were generated, Cr-adduct formation was also occurring.

In order to monitor levels of Cr-DNA adduct formation a radioisotope of Cr (^{51}Cr) was employed, bound levels of which could then be determined by scintillation counting. The problem presented by such an approach is the removal of any unbound ^{51}Cr from the reaction mixture thereby allowing an accurate determination of ^{51}Cr -DNA adduct formation to be made. Initial attempts to separate unbound ^{51}Cr involved the use of Microcon 30 filters. A series of "washing steps" were carried out in order to terminate the reaction and isolate the Cr-DNA complex. Figure 2.2 shows the results of a preliminary study designed to establish the number of "washing steps" required to completely remove any unbound ^{51}Cr from the plasmid (note that radioactivity is expressed as CPM rather than DPM since, for the purposes of these studies qualitative measurements were sufficient. CPM cannot be considered to be quantitative since the reduction in

number of counts per sample as a result of quenching is not taken into account).

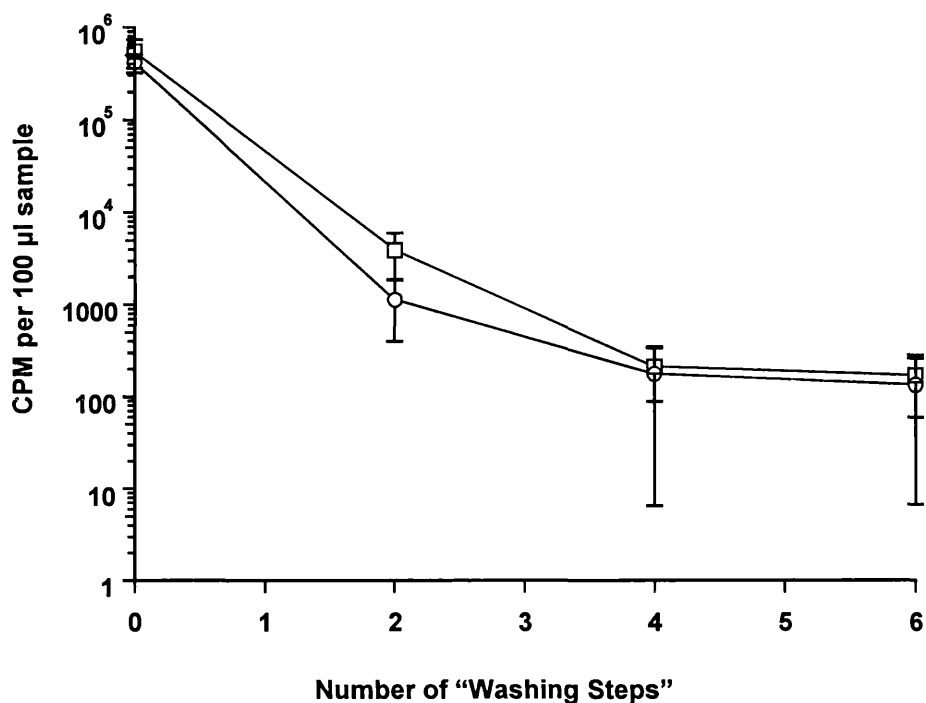


Figure 2.2. Comparison of Cr-DNA adduct formation in presence (□) and absence (○) of GSH determined by scintillation counting of isolated plasmid. Samples contain 0.5 mM Cr(VI) with or without 5 mM GSH in phosphate buffer. $n=4$, values are mean \pm SD ($n-1$).

While the level of radioactivity in reaction mixtures was around 4.0×10^5 CPM per 100 μ l for both treated (presence of GSH) and control samples, after rinsing the plasmid twice this level decreased by a factor of almost 100 to around 4.0×10^3 CPM. Third and fourth washing steps reduced the level of radioactivity to approximately 100 CPM in both control samples and those containing GSH. From these data it would appear that two washing steps would be sufficient to remove the bulk of any residual Cr in subsequent experiments. However, whilst there was an apparent difference in levels of radioactivity (and therefore Cr-DNA binding) between samples

containing GSH and control after two rinses, this distinction became less clear with further purification of the plasmid. When considering such similarity between sample sets and the fact that levels of radioactivity in all samples remained noticeably high at around 100 CPM per 100 μl after four purification steps it was felt that the separation of ^{51}Cr from the plasmid was incomplete (possibly a result of ^{51}Cr complexing/chelating with the filter). It was decided that other techniques for the purification of the plasmid which did not involve Microcon filters should be explored.

2.4.2 Separation of Unbound ^{51}Cr Using NENsorb Columns

Our primary concern at this stage was to determine an efficient means of separating any unbound ^{51}Cr from the reaction mixture whilst causing as little damage to the plasmid as possible.

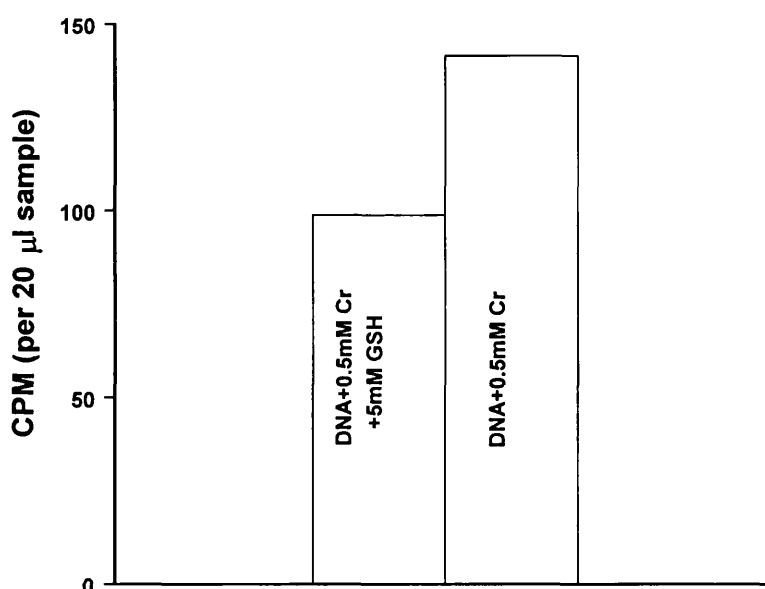


Figure 2.3 Comparison of Cr binding (determined by scintillation counting) in presence and absence of GSH after isolation of plasmid with NENsorb Nucleic Acid Purification Resin. Values are from a single determination.

To this end, a nucleic acid purification resin (NENsorb) was employed. A direct comparison of control samples and those containing GSH was carried out to determine the efficiency of the NENsorb technique for separating unbound Cr. Figure 2.3 shows the results from such a comparison. Samples containing GSH, in which it would be expected to observe greater levels of binding (and therefore higher levels of radioactivity) showed CPM of around 100 per 20 μ l. Such a low count not only represents very low potential binding of Cr to DNA (possibly due to the ratio of ^{51}Cr in the reaction mixture), but is evidently far lower than the level of radioactivity detected in our control sample (approximately 150 CPM per 20 μ l aliquot). In addition, when aliquots were analysed for levels of single strand break induction, the presence of residual methanol in the samples resulted in the loss of DNA from the gel wells by diffusion and made the determination of such damage impossible. While such contamination could feasibly have been overcome by filtration of the samples with Microcon 30 units, the contradictory results provided by scintillation counting, and disappointing findings from previous use of such filters prompted us to adopt another approach for the purification of the plasmid. It was also felt that the ratio of ^{51}Cr in the reaction mixture should be increased in an attempt to distinguish real findings from apparently high background counts in controls (see section 2.4.1).

2.4.3 Separation of Unbound ⁵¹Cr Using Gel Electrophoresis

Inconclusive findings using the Microcon 30 and NENsorb methods of plasmid purification prompted us to adopt a technique involving gel electrophoresis. Theoretically, during the electrophoresis of samples, not only will the open circular and supercoiled forms of the plasmid migrate at different rates along the gel, but, if a voltage is maintained across the gel for a sufficient period of time, any unbound ⁵¹Cr will separate completely from the Cr-DNA complexes formed as a result of the reductive conversion of Cr(VI) by GSH. Densitometry can then be performed on the gel to determine SSB formation, and the DNA recovered by excision for the estimation of Cr binding. Such an approach, whilst being quick and convenient also has the advantage of allowing the investigation of more than one type of DNA damage in the same sample.

Initial studies focused on the influence of GSH concentration on Cr-DNA adduct formation and SSB induction at a fixed concentration of 0.5 mM Cr(VI). Levels of radioactivity in control samples were estimated to be approximately 550 CPM per 160 ng DNA and rose proportionally to around 2500 CPM with GSH concentration (Figure 2.4a). While such findings suggest a relationship between Cr binding and the reduction of Cr(VI) by GSH, the levels of radioactivity in control samples seem very high. Conversely, levels of SSB were apparently at a maximum at the lowest concentration of GSH (0.4 – 0.5 SSB per 10,000 base pairs, values corrected for background

levels) and decreased to zero at 20 mM GSH compared to controls (Figure 2.4b). These findings support the hypothesis that a reactive peroxy-species may mediate SSB induction, and that distinct pathways exist in the formation of both lesions.

Figure 2.4a Scattergram to illustrate influence of GSH concentration on Cr-DNA adduct formation as determined by scintillation counting of treated plasmid. [Cr(VI)] = 0.5 mM. Each point represents a replicate.

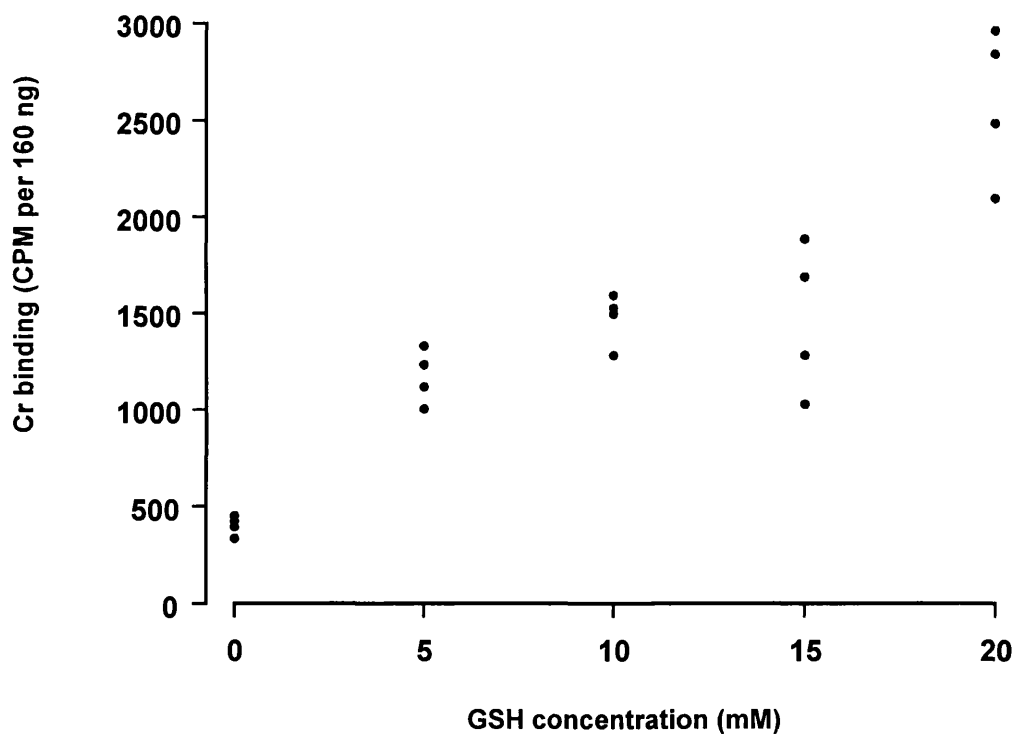
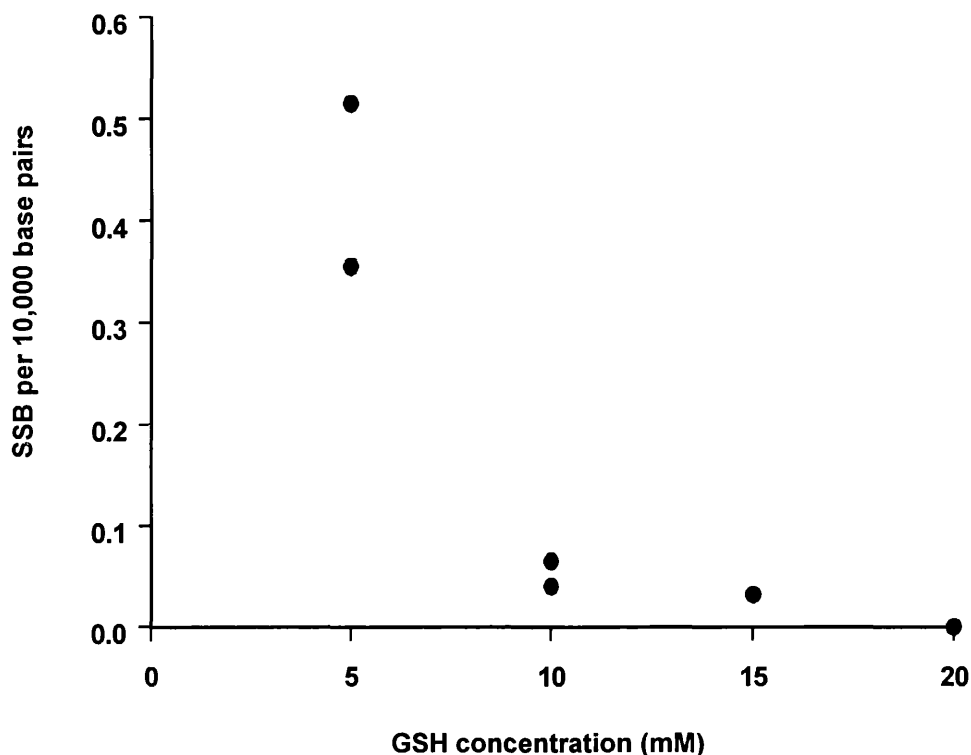


Figure 2.4b Scattergram to illustrate influence of GSH concentration on SSB induction. [Cr(VI)] = 0.5 mM. Each point represents a replicate.



In an attempt to confirm the role of a reactive oxygen species in the mediation of single strand breaks, and to further investigate the possibility of distinct pathways in the generation of SSB and Cr-DNA adducts, the influence of catalase during the reductive conversion of Cr(VI) was investigated. Figures 2.5a and 2.5b show the results from these studies. Catalase appeared to have little influence on the formation of Cr-DNA adducts with radioactivity levels being monitored at approximately 3000 CPM per 160 ng DNA in both treated (5 mM GSH, 0.5 mM Cr[VI]) and untreated samples (0.5 mM Cr[VI]). Again, counts of around 500 CPM were recorded for control samples suggesting incomplete separation of unbound ^{51}Cr . Denaturing of catalase by heating to 65°C for 10 min had no influence on Cr-DNA

adduct formation (data not shown). As observed at high concentrations of GSH, the presence of catalase in the reaction mixture had the apparent effect of “shutting off” SSB induction with treated samples demonstrating approximately 0.35 breaks per 10,000 base pairs (corrected for background), compared to 0.1 breaks per 10,000 base pairs in the presence of catalase.

Figure 2.5a Influence of catalase on the formation of Cr-DNA adducts during the reductive conversion of Cr(VI) (0.5 mM) by GSH (5 mM) as determined by scintillation counting of the treated plasmid. $n=6$, values are mean \pm SD ($n-1$).

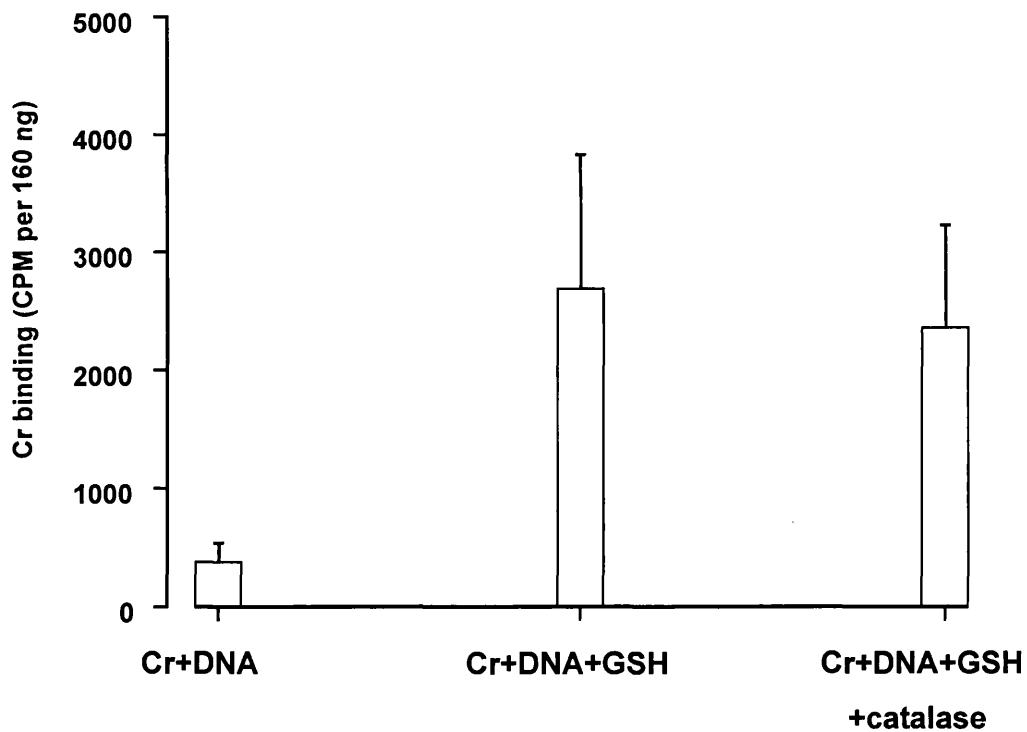
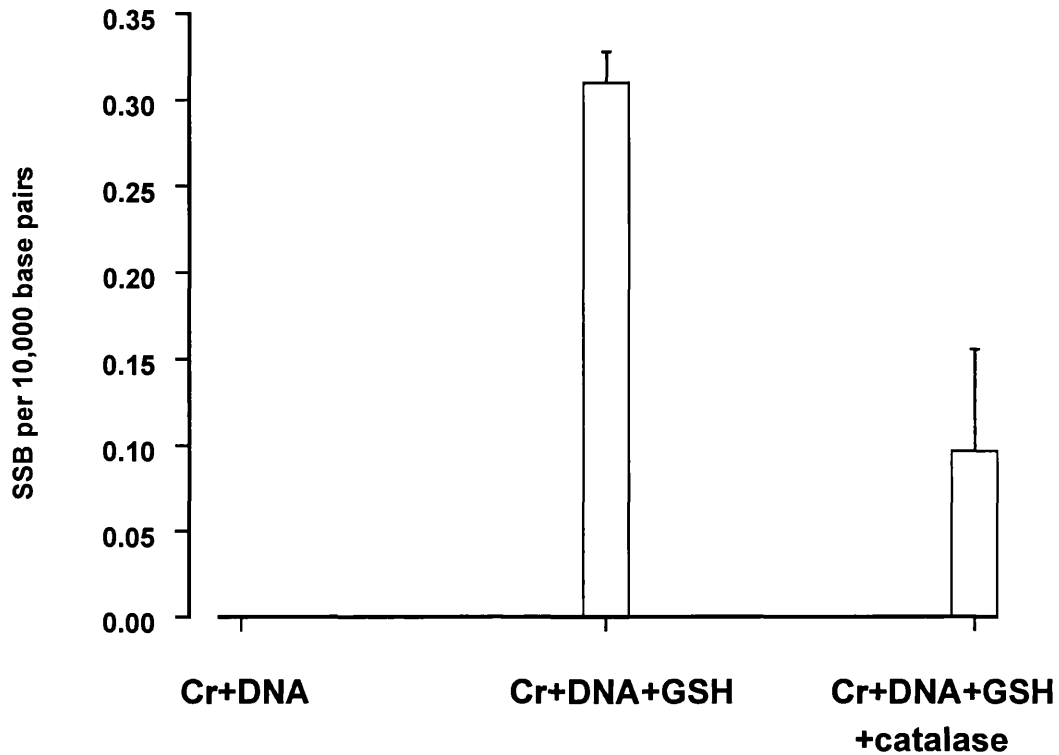


Figure 2.5b Influence of catalase on the formation of SSB during the reductive conversion of Cr(VI) (0.5 mM) by GSH (5 mM). $n=6$, values are mean \pm SD ($n-1$).



These findings would certainly suggest the presence of more than one pathway in the mediation of SSB and Cr-DNA adducts, and support the hypothesis for the role of an active oxygen species in the generation of SSB (and therefore AP-sites). However, the inconsistent results obtained from previous studies, and the very high background counts being measured for control samples both suggest fundamental problems with the technique of separation being employed. Indeed, subsequent experiments addressing the influence of Cr(VI) concentration on Cr binding, and investigations into Cr-DNA adduct formation as a time dependent process also generated data which were very difficult to replicate with noticeably high counts for control samples (Figures 2.6 and 2.7).

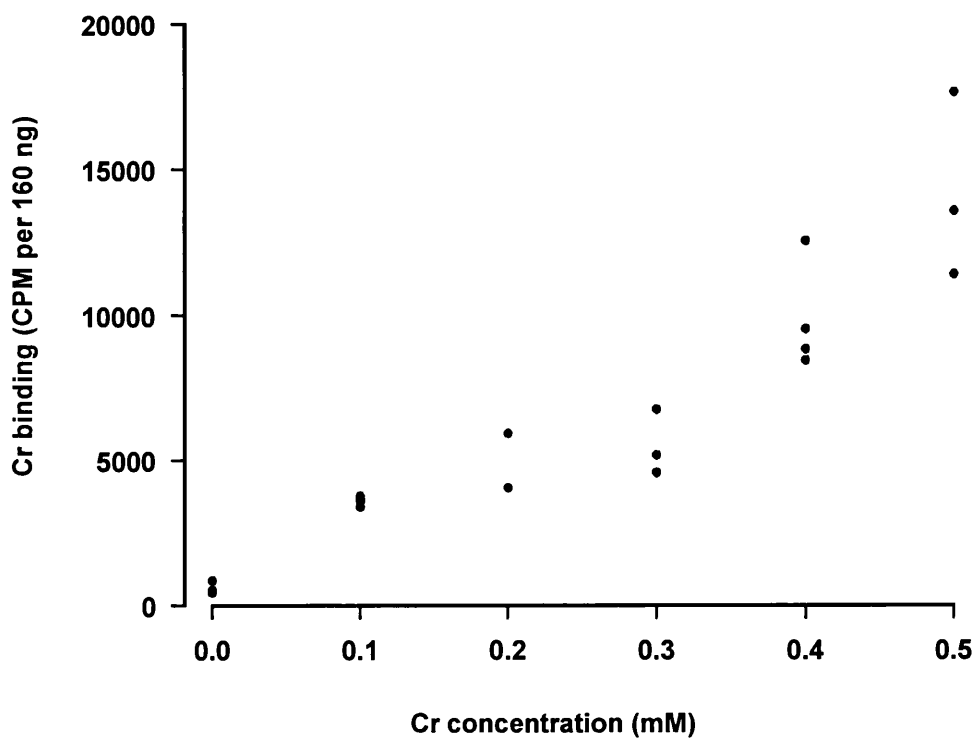


Figure 2.6 Scattergram to show the influence of Cr concentration on the formation of Cr-DNA adducts. Mean control value = 590 CPM per 160 ng DNA. Each point represents a replicate.

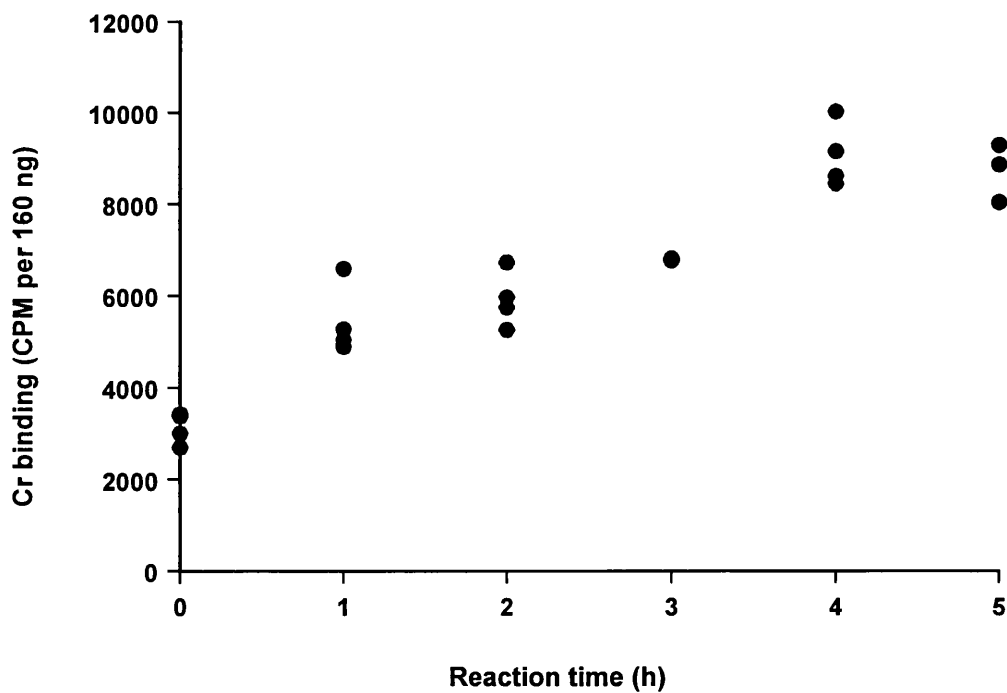


Figure 2.7 Scattergram to show Cr-DNA adduct formation as a time dependent process. Mean control value = 3125 CPM per 160 ng DNA. Each point represents a replicate.

In an attempt to probe the role of intermediates generated during the reduction of Cr(VI) by GSH, a series of “aged” reaction mixtures was prepared by pre-incubating GSH (5 mM) with labelled Cr(VI) (0.5 mM) in phosphate buffer for up to 5 hours. DNA was then added and the samples post-incubated overnight. While the number of strand breaks induced in the plasmid decreased with increasing “ageing” of reaction mixtures (Figure 2.8a) levels of Cr-DNA adducts remained constant irrespective of the pre-incubation time of GSH and Cr(VI) (Figure 2.8b). These findings would again support the theory that distinct pathways are involved in the generation of these adducts and would suggest a role for a Cr(III) species in the mediation of Cr binding. However, as with all previous studies, replication of data was inconsistent, leading us to question the integrity of the chosen experimental technique.

Figure 2.8a Scattergram to illustrate the influence of “ageing” reaction mixtures on the generation of single strand breaks. [GSH]=5 mM, [Cr(VI)]=0.5 mM. Each point represents a replicate.

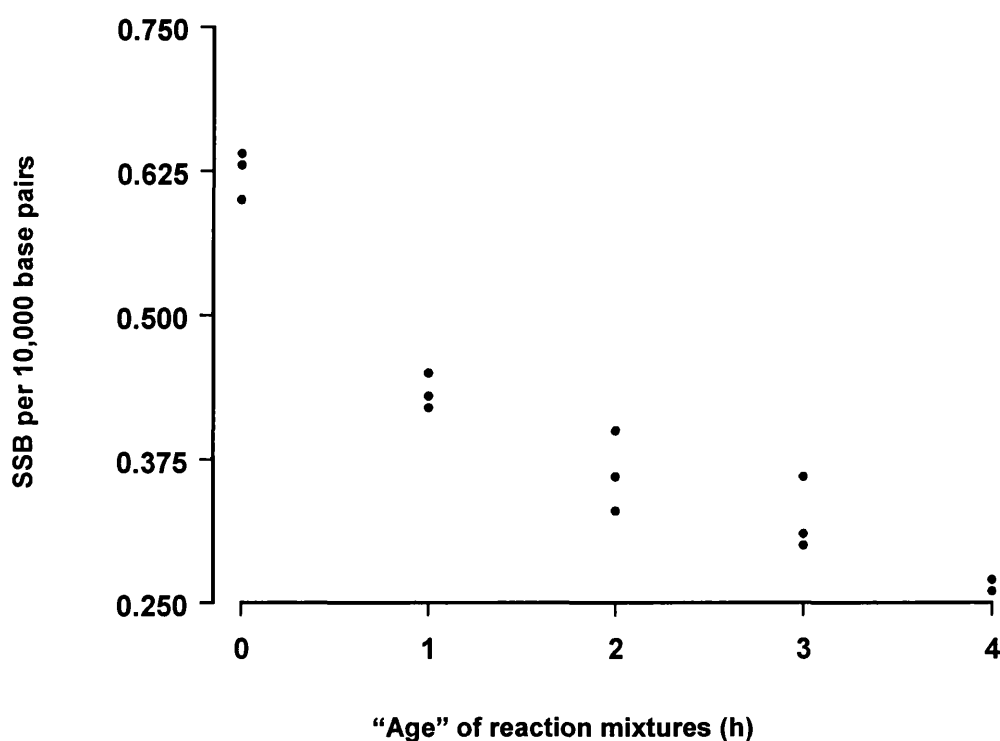
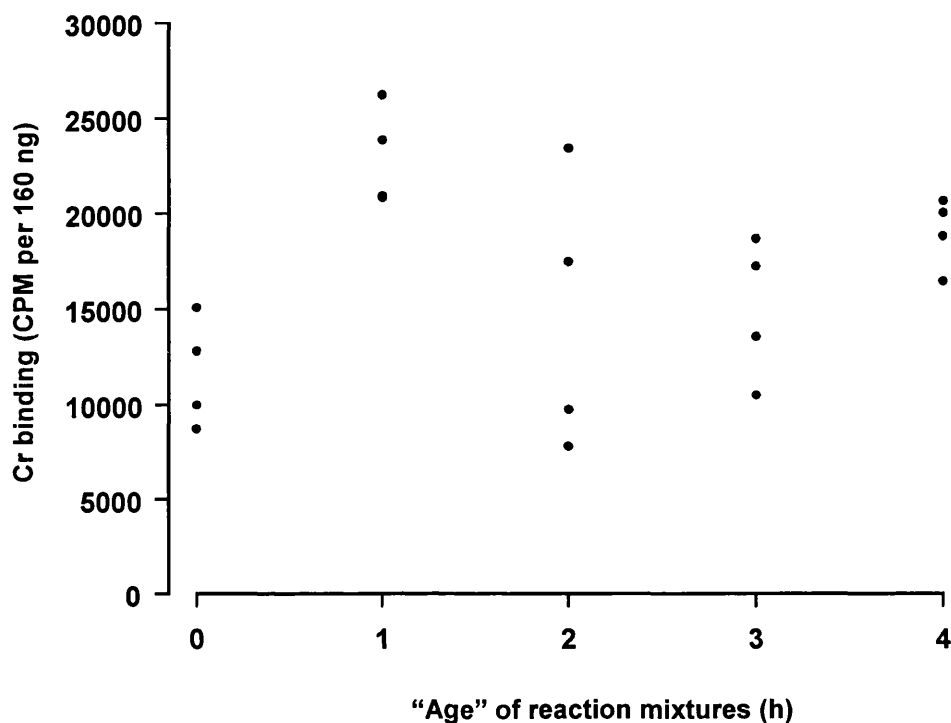


Figure 2.8b Scattergram to illustrate the influence of "ageing" reaction mixtures on Cr-DNA adduct formation. [GSH]=5 mM, [Cr(VI)]=0.5 mM. Each point represents a replicate.



The discrepancies in the observed data prompted a closer investigation of the movement of the unbound ^{51}Cr within the gel. Samples were prepared comprising control (spiked Cr with PM2 DNA), treated (spiked Cr and PM2 DNA in the presence of 5 mM GSH) and reference (spiked Cr and GSH) reaction mixtures in phosphate buffer and run on an agarose gel. After electrophoresing the samples, the gel was exposed to autoradiograph film overnight and the resultant image developed according to the manufacturer's instructions. The use of radioactive markers to trace the migration of the samples along the gel revealed not only strong bands of activity in lanes containing DNA and Cr in the presence and absence of GSH,

but also a distinct “fogging”, indicative of radioactive Cr, moving at the same rate as the plasmid in lanes containing only Cr and GSH (Figure 2.9a).

This finding immediately raised doubt about all our previous data; evidently a Cr complex was being formed in the reaction mixture independently of the plasmid, which was migrating along an agarose gel at the same rate as the DNA. This complex would therefore have been present in the excised agarose slices used to determine Cr-DNA binding. Consequently, this artefactual radioactivity would have masked any real effect due to legitimate Cr-DNA adduct formation and would also explain the high background counts obtained for control samples. The exact nature of the complex involved was not determined but it was felt that phosphate might play a crucial role in its formation. For this reason, duplicate samples were prepared in HEPES buffer and run on a second gel (0.8 % in TBE buffer). The gel was then exposed to Hyperfilm overnight. Figure 2.9b shows a diagrammatic representation of the resulting autoradiograph. The absence of any residual radioactivity in the lanes containing only GSH and Cr confirmed our suggestion that a Cr/phosphate complex had been forming in previous samples.

Figure 2.9a Diagrammatic representation of an autoradiograph obtained after exposing agarose gels to Hyperfilm. The samples in lanes 1 and 2, although not containing any plasmid, produced a distinct "fogging" which travelled along the gel at the same rate as the plasmid in lanes 3-6. Samples contained 0.5 mM Cr in phosphate buffer.

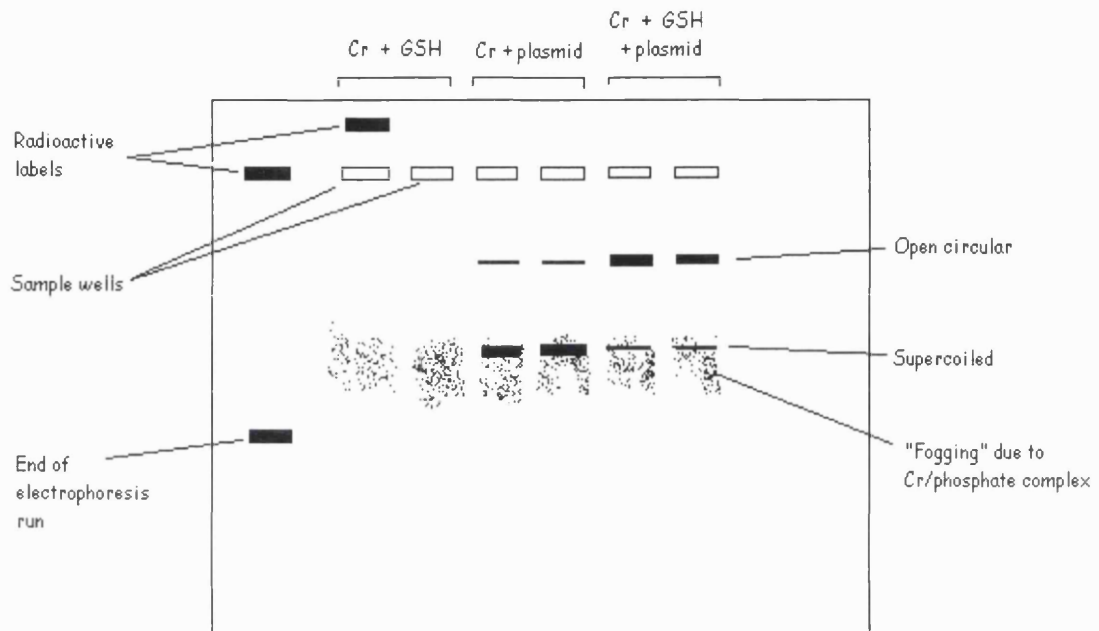
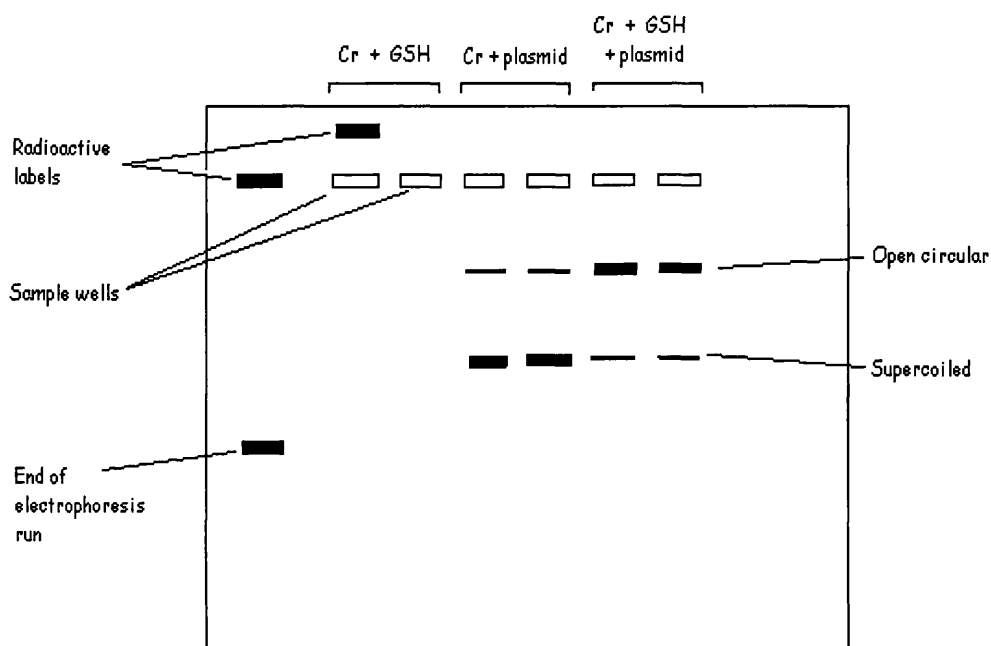


Figure 2.9b Diagrammatic representation of an autoradiograph obtained after exposing agarose gels to Hyperfilm. In this case the samples were prepared in HEPES and the gel was run in TBE buffer. Note the absence of "fogging" in all lanes.



2.5 Discussion

While HEPES, due to its lack of interaction with other inorganic reagents, now seemed the ideal buffer system to employ in these studies another complication was presented. Although phosphate was felt an unsuitable buffer due to the formation of Cr/phosphate complexes, it is ideal for the demonstration of single strand break induction at relatively low Cr concentrations. HEPES, on the other hand, while appearing to be ideal for the illustration of Cr-DNA adduct formation, requires much higher Cr concentrations before single strand breaks can be detected and it was felt that increasing the levels of Cr(VI) being used in these studies might compromise the physiological relevance of the experiments. It was decided to repeat our initial investigations into Cr-binding as a function of time, and “age” of reaction mixtures using a low Cr concentration (0.5 mM) in HEPES. The influence of GSH concentration and catalase on Cr-binding and strand break induction was also determined in HEPES but at the higher Cr concentration of 1.5 mM. Additionally, taking into account previous disappointing findings it was decided to employ a different method for the separation of unbound ^{51}Cr from reaction mixtures. To this end, samples were subsequently purified using the Promega *Wizard DNA Clean-up System* (see Chapter 3).

CHAPTER 3

The Formation of SSB and Cr-DNA Adducts in Isolated DNA During the Reduction of Cr(VI) by GSH Proceeds via Distinct Pathways

3.1 Introduction

Attempts to model the generation of Cr-DNA adducts *in vitro* clearly seem to have been hampered by selecting an inappropriate buffer system. Whilst phosphate buffer may provide a more physiologically relevant milieu (intracellular phosphate occurring at approximately 75 mEq/L), and is ideal for studies investigating the generation of SSB, Cr-DNA adduct formation under these conditions is low (and made extremely difficult due to the apparent formation of a high molecular weight Cr-phosphate complex). A system utilising HEPES as the buffering agent, however, can demonstrate both binding and strand breakage simultaneously, or binding with the absence of breaks at lower Cr(VI) concentrations. It is hoped that, by employing an albeit extreme, experimental model where both lesions are generated in the same sample, this study will demonstrate the existence of distinct mechanistic pathways for the formation of these two types of damage. Furthermore, it is hoped to characterise the modulation of Cr-DNA adduct formation more fully by utilising experimental conditions where Cr-DNA adducts are the only apparent lesion.

Preliminary studies using the Promega Wizard DNA Clean-up System to remove any unbound Cr from the reaction mixture have shown the

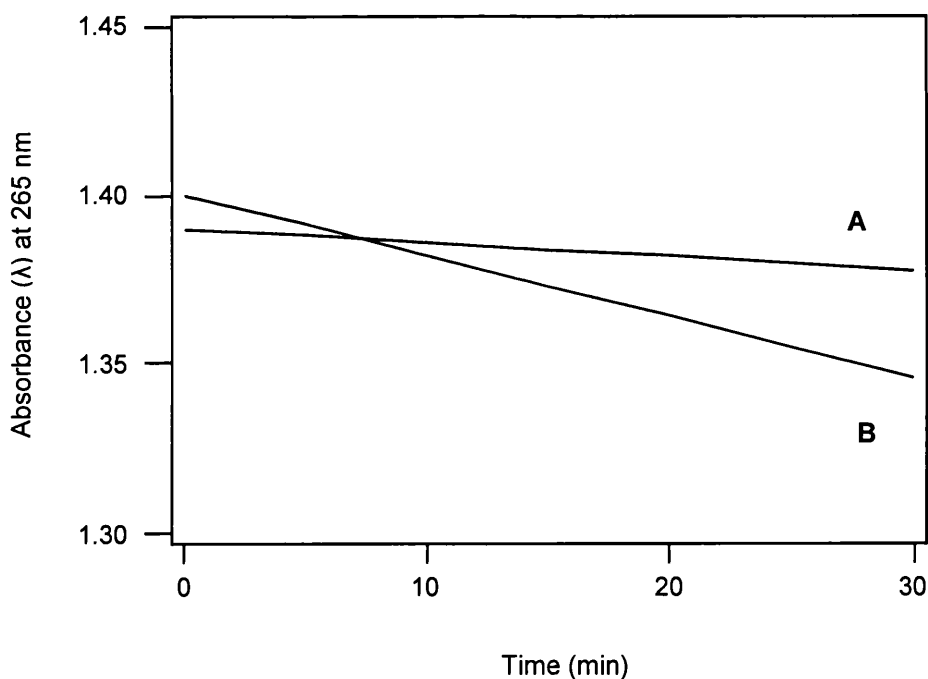
technique to be very convenient, reproducible and reliable, hence their selection for this modified protocol.

3.2 Method

PM2 DNA (320 ng in a final volume of 40 μ l) was incubated at room temperature in the presence of GSH (0 - 20 mM) and potassium chromate (0 - 1.5 mM, containing an equal volume of 51 Cr as sodium chromate, 37 MBq/4.4 μ g Cr), in HEPES buffer (15 mM, with NaCl 0.15 M, pH 7.0) for 18 h. To a number of samples, catalase (10 μ g/ml) was added. Control samples contained potassium chromate and GSH, but no DNA, or potassium chromate and DNA, but no GSH. In some experiments catalase was inactivated by denaturing the enzyme at 65 $^{\circ}$ C for 10 min. Samples were split into aliquots of 20 μ l and prepared for the determination of the level of Cr-DNA adducts and SSB. In order to evaluate the role of intermediates generated during the reduction of Cr(VI) by GSH, a series of "aged" reaction mixtures was prepared by pre-incubating GSH (5 mM) and labelled potassium chromate (0.5 mM) in HEPES buffer for 0-5 h. DNA was then added and the samples post-incubated overnight. Great care was taken to remove contaminating metal ions from buffer solutions (such as iron and copper), which have the potential to catalyse the auto-oxidation of AsA at neutral pH, leading to the generation of SSB. Briefly, buffer solutions were treated overnight with Chelex 100 resin (Bio-Rad, Hemel Hempstead, UK) and the removal of catalytic metals assessed using the ascorbate method by Buettner (1988). Successful removal

of catalytic ions was assessed by determining the loss of absorbance of AsA (at 265 nm) as a result of auto-oxidation. If ascorbate was found to be stable (i.e. loss of absorbance <0.5%) for at least 30 min, metal contamination was regarded as minimal. Figure 3.1 shows typical absorbance readings over 30 min for Chelex-treated and untreated buffer solutions.

Figure 3.1 Comparison of loss of absorbance vs. time for Chelex-treated and untreated phosphate buffer containing 100 μM AsA.



A - Loss of absorbance in Chelex treated phosphate buffer (0.1 M, pH 6.8); [AsA] = 100 μM ; $\Delta\lambda \text{ min}^{-1} = 0.42 \times 10^{-3}$.

B - Loss of absorbance in untreated phosphate buffer (0.1 M, pH 6.8); [AsA] = 100 μM ; $\Delta\lambda \text{ min}^{-1} = 8.0 \times 10^{-3}$.

In order to separate unbound Cr from the reaction mixtures, samples were processed using the Promega *Wizard DNA Clean-up System* according to the manufacturer's instructions. Briefly, samples were suspended in *Wizard purification resin* (6 M guanidine thiocyanate) and loaded onto *Wizard minicolumns*. Any unbound Cr was rinsed off the column by washing twice with 2 ml 80% isopropanol. Finally, the Cr-DNA complex was eluted with UHQ water at 65 °C. Any traces of isopropanol remaining in the sample will adversely affect the subsequent electrophoresis. To remove any residual alcohol, the samples were loaded onto *Microcon 30* filter units, suspended in 500 µl TE buffer (10 mM Tris, pH 7.5; 1 mM EDTA) and centrifuged at 10,000 rpm for 12 min. The samples were recovered in a final volume of 40 µl. In order to estimate the extent of recovery of the plasmid, aliquots of DNA which were not subject to purification were run on agarose gels. The intensity of the resulting DNA bands was then compared with those of purified samples. By this technique, recovery of the plasmid was estimated to be close to 100 %.

Purified samples were run on agarose gels to determine SSB induction as described. Similarly, Cr-DNA adduct levels were determined by scintillation counting as before.

3.3 Results

3.3.1 Influence of GSH on the Induction of SSB and Cr-DNA Adducts

The influence of GSH on the formation of SSB and Cr-DNA adducts in PM_{2.5} DNA was studied. The two lesions were analysed using aliquots from the same mixture. In agreement with results communicated earlier (Kortenkamp *et. al.* 1989) the level of SSB was found to decrease with rising GSH concentrations. With 1.5 mM Cr(VI), maximum numbers of SSB were observed at 5 mM GSH. SSB were almost completely suppressed at GSH concentrations of 15 mM and higher (Figure 3.2). In contrast, the levels of Cr-DNA adducts increased with rising GSH concentration and reached an optimum at 15 mM GSH.

A second set of experiments, investigating the influence of GSH on Cr-DNA adduct formation, was performed at the lower Cr concentration of 0.5 mM, a level at which SSB formation was negligible and Cr-DNA adducts were the only apparent lesion. The same trend in Cr-DNA binding with increasing GSH was also observed at the lower Cr concentration. These findings indicate that the formation of the two DNA lesions is mediated via different reactive species which may arise from distinct reaction pathways.

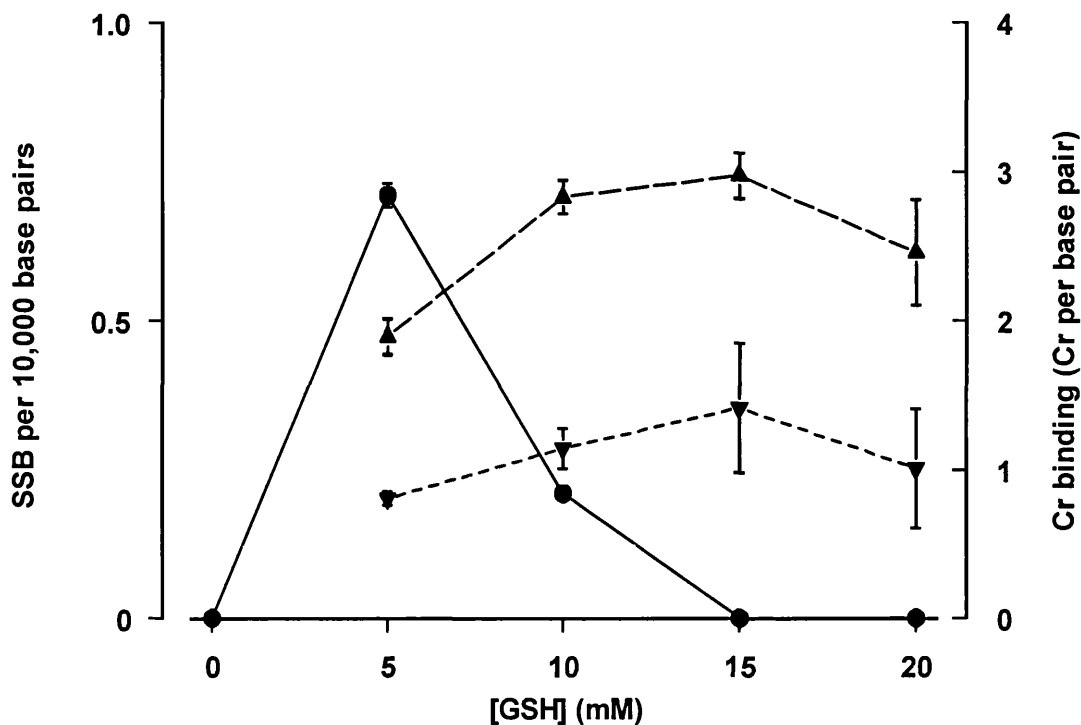


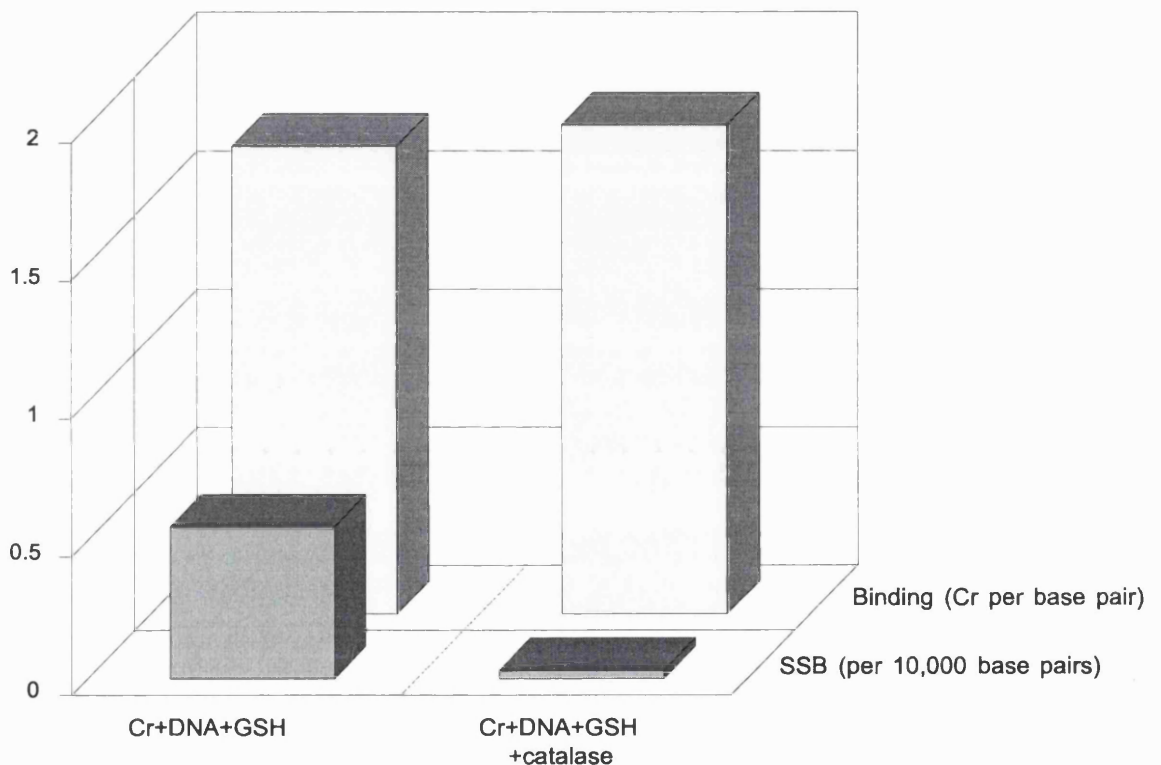
Figure 3.2. Influence of GSH on the induction of SSB and Cr-DNA adducts in PM2 DNA. \blacktriangle = Cr-DNA adducts, $[Cr] = 1.5 \text{ mM}$, \bullet = SSB, $[Cr] = 1.5 \text{ mM}$, $n = 6$, values are mean \pm SD ($n-1$). \blacktriangledown = Cr-DNA adducts, $[Cr] = 0.5 \text{ mM}$, $n = 4$, values are mean \pm 95% confidence intervals. The data shown here and in all other figures have been corrected for the number of Cr-DNA adducts in control samples containing no GSH.

3.3.2 Influence of Catalase on SSB Formation and Cr Binding to DNA

In order to probe further whether distinct reaction pathways are involved in the generation of SSB and Cr-DNA adducts by Cr(VI) and GSH, the influence of catalase on both lesions was studied. It has been shown previously that SSB arising from Cr(VI)/GSH systems can be inhibited by the administration of catalase (Kortenkamp *et al.* 1989, Casadeval and Kortenkamp 1995). Figure 3.3 shows that Cr binding to DNA was unaffected by addition of catalase in DNA treated with 1.5 mM Cr(VI) and 5 mM GSH. Aliquots taken from the same

samples and analysed for SSB revealed that this lesion was completely inhibited by catalase.

Figure 3.3. Influence of catalase on the induction of SSB and Cr-DNA adducts in PM2 DNA. [Cr] = 1.5 mM, [GSH] = 5 mM, values are mean, n = 2.



A further set of experiments was carried out to investigate the influence of catalase on adduct formation at the lower Cr(VI) concentration of 0.5 mM, again employing 5 mM GSH. Binding remained unchanged in the presence of catalase. Control reaction mixtures, containing no added catalase, showed binding levels of 0.91 ± 0.20 Cr per base pair, whilst samples co-incubated with catalase yielded 0.80 ± 0.16 Cr per base pair after 18 h of incubation (n = 4, means \pm 95 % confidence interval). These results further support the

hypothesis that SSB and Cr-DNA adducts are formed by species which arise from distinct reaction pathways.

3.3.3 Further Investigations of the Characteristics of Cr-DNA Adduct Formation

In order to gain insights into the nature of the species mediating Cr-DNA binding the characteristics of reaction conditions leading to the formation of these adducts was explored. To this end the influence of Cr(VI) concentration on the level of binding was studied.

In the presence of 5 mM GSH Cr-DNA binding increased with rising Cr(VI) concentration, and reached a plateau at 0.5 mM Cr(VI) of approximately 0.9 Cr per DNA base pair after 5 h of incubation (Figure 3.4). Time course studies revealed that the formation of Cr-DNA adducts is a relatively slow process, to a degree mirroring the sluggish reduction of Cr(VI) under these reaction conditions. Rate of Cr-DNA adduct formation was calculated to be 0.16 Cr/bp/h while the process was almost complete after a 5 h incubation (Figure 3.5).

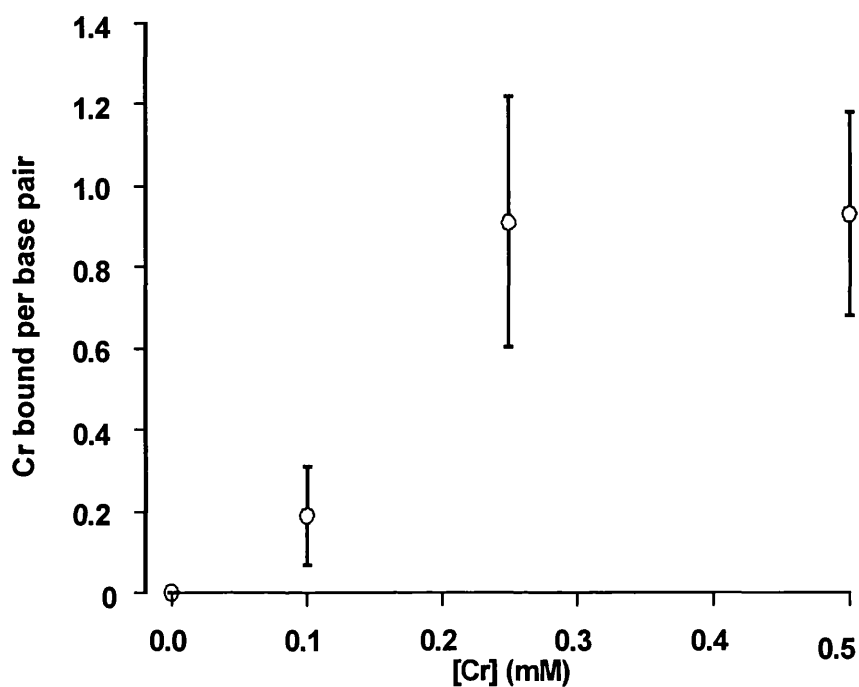


Figure 3.4. Influence of [Cr] on Cr-DNA adduct formation in presence of 5 mM GSH. Values are mean \pm 95% confidence interval, $n = 4$.

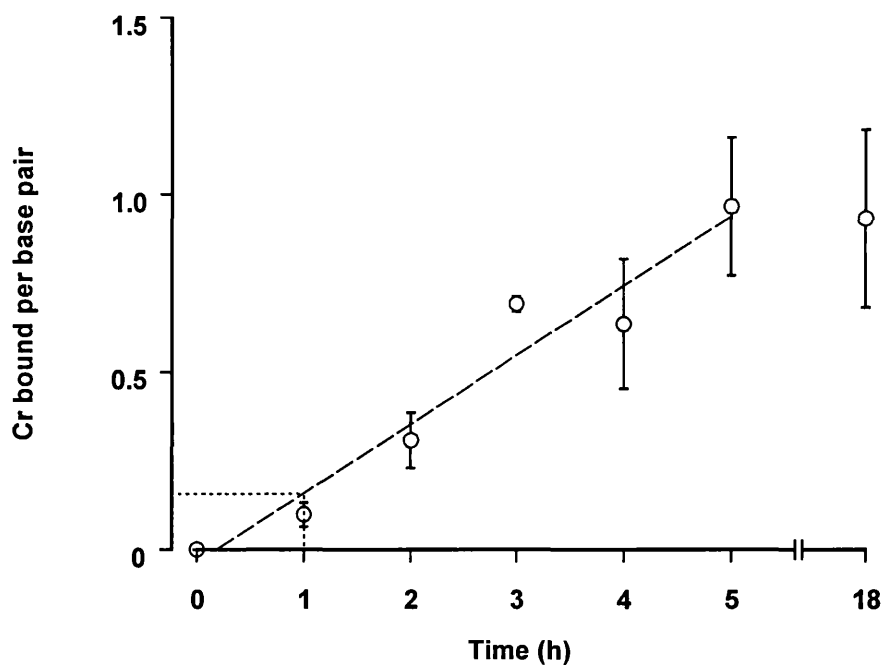


Figure 3.5. Influence of time on Cr-DNA adduct formation in presence of 5 mM GSH. Values are mean \pm 95% confidence interval, $n = 4$. Line was drawn from linear regression with the rate of Cr-DNA adduct formation being calculated as 0.16 Cr/bp/h.

Experiments with solutions of Cr(VI)/GSH which were “aged” for different periods of time were carried out. Reaction mixtures of 0.5 mM Cr(VI) and 5 mM GSH were pre-incubated for 1 - 5 h before the addition of DNA and a subsequent 18 h incubation. The longer such reaction mixtures were “aged” the fewer Cr-DNA adducts were seen with $T_{1/2}$ for Cr-DNA adduct formation being estimated to be 1.4 h (Figure 3.6). However, even after 5 h of pre-incubation, a time period sufficient to bring Cr(VI) reduction to completion (Kortenkamp *et. al.* 1989), the reaction mixtures did not lose their ability to induce Cr-DNA adducts. Interestingly, there was a slight increase in the level of adducts when the duration of “ageing” was extended beyond four hours. These results strongly suggest that species with a long half-life are involved in the formation of Cr-DNA adducts.

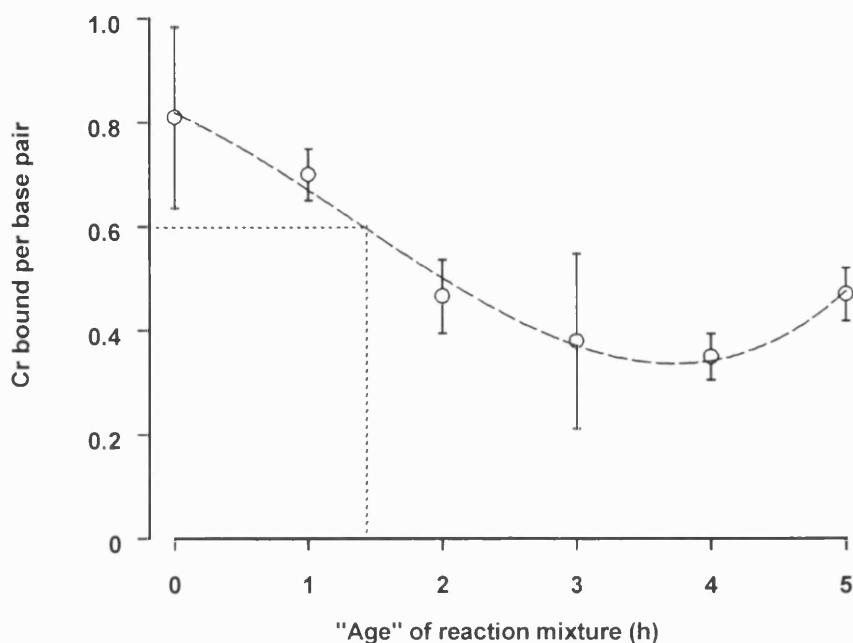


Figure 3.6. Influence of "ageing" reaction mixtures before the addition of DNA on the formation of Cr-DNA adducts. $[GSH] = 5 \text{ mM}$, $[Cr(VI)] = 0.5 \text{ mM}$, values are mean \pm 95% confidence interval, $n = 4$. Line drawn as cubic regression. $T_{1/2}$ was estimated to be approximately 1.4 h.

3.4 Discussion

The results of our studies on the influence of GSH on the induction of SSB and Cr-DNA adducts can be interpreted in terms of the effect of GSH concentration on the formation and interception of reactive species. At constant concentrations of Cr(VI) the rate of Cr(V) formation depends on the level of GSH. With high concentrations of GSH, large amounts of Cr(V) are generated very quickly, while at lower concentrations of GSH the formation of Cr(V) proceeds at a slower rate (Borges *et. al.* 1991). Assuming that Cr(V) is responsible for the formation of DNA lesions, the frequency of encounters of this

species with DNA is important. Because of the lower rate of Cr(V) formation, such encounters are relatively infrequent at low levels of GSH, but will rise with GSH concentration. It is likely that the number of critical "hits" with the target molecule, DNA, saturates above a critical concentration, so that the number of DNA lesions, plotted against rising concentrations of GSH, should level off or go through an optimum. Similar considerations apply to Cr(IV).

Qualitatively, these expectations are borne out by our experimental results (Fig 3.2). We observed an optimum number of SSB and a plateau for the level of Cr-DNA adducts in dependence of GSH. Importantly, however, the two curves were not congruent, as would be expected if the same species, Cr(V) or Cr(IV), were directly responsible for the induction of both lesions. GSH concentrations which almost completely suppressed the generation of SSB led to a large number of Cr-DNA adducts. It has been demonstrated that solutions with an excess of GSH over Cr(VI) contain large amounts of Cr(V) (Kortenkamp *et. al.* 1996, Borges *et. al.* 1991). It appears therefore that Cr(V) does not mediate the formation of SSB.

This conclusion is further substantiated by our observation that catalase completely suppressed the formation of SSB but left the level of Cr-DNA adducts unchanged. In previous papers, Kortenkamp *et. al.* (1996) and Casadeval and Kortenkamp (1995) have demonstrated that the species scavenged by catalase can be traced to molecular

oxygen, and that oxygen is required for the induction of SSB and AP-sites by Cr(VI)/GSH. Thus, in the absence of oxygen, Cr(V) appears to be unreactive towards DNA. Our findings correspond with observations of a strong enhancement of Cr(VI) mutagenicity by molecular oxygen in strains of *S. typhimurium* (Sugden *et. al.* 1990), and findings that SSB can be prevented in Cr(VI)-treated mammalian cells by the addition of catalase (Snyder 1988).

It appears therefore, that the mechanism proposed by Farrell and co-workers (1989) to explain the ability of $[\text{Cr}(\text{ehba})_2\text{O}]^-$ to cleave DNA is not apparent for Cr(V) species arising from Cr(VI)/GSH. The binding of such Cr(V) intermediates to DNA does not necessarily result in SSB. If this were the sole mechanism by which the two DNA lesions are formed in the Cr(VI)/GSH system, the curves in Figure 3.2 would be expected to be congruent. However, this does not rule out the possibility that hypervalent Cr species, when coming into contact with reactive oxygen species, may induce SSB or AP-sites with concomitant formation of Cr-DNA adducts attached to the site of reaction.

While there is no apparent direct involvement of Cr(V) species in the formation of SSB, Cr(V) is thought to be responsible for the induction of Cr-DNA adducts (Borges *et. al.* 1991). A role for Cr(III) in these processes has been ruled out (Stearns and Wetterhahn 1994, Borges *et. al.* 1991). However, in view of the kinetic inertness of Cr(III)

complexes (Larkworthy *et. al.* 1988) the incubation times of 30 min employed in previous studies may have been too short to observe any Cr(III)-mediated binding (Borges *et. al.* 1991, Aiyar *et. al.* 1991). In an attempt to probe a possible involvement of Cr(III) in causing Cr-DNA adducts we have assessed whether solutions of Cr(VI) and GSH, which have been allowed to react for several hours before addition of DNA, lose their ability to induce the lesion with increasing duration of pre-incubation.

The picture that emerged from these experiments was surprising (Figure 3.6). As would be expected assuming that an intermediate species, either Cr(V) or Cr(IV), is involved in mediating Cr binding, the level of Cr-DNA adducts initially decreased the longer the reaction mixtures were pre-incubated in the absence of DNA. However, the number of adducts did not reach zero when the pre-incubation period extended beyond three hours, but remained unchanged and even increased slightly after five hours of pre-incubation. As stated before, the reduction of Cr(VI) is complete within less than three hours under these experimental conditions. Indeed, Cr(V) ESR signals were not seen after more than 30 min in solutions containing 0.4 mM Cr(VI) and 5 mM GSH (Kortenkamp *et. al.* 1996), indicating that the concentration of Cr(V) species in such reaction mixtures is negligible. It is therefore impossible to explain the data in Figure 3.6 solely in terms of Cr(IV) or Cr(V) as the species mediating Cr-DNA binding, although these intermediate oxidation states may be involved. Our

findings suggest that Cr(III) complexes generated *in situ* also have a role in the formation of Cr-DNA adducts.

Although the structure of the Cr(III)/GSH complexes which are formed is far from clear, they are thought to carry an overall negative charge (Larkworthy *et. al.* 1988). For this reason they are unlikely to attack DNA with its negatively charged backbone. However, Cr(III)/GSH complexes slowly hydrolyse and this process is likely to yield species which can react with DNA (Larkworthy *et. al.* 1988). The relative bulkiness of the GSH ligands may contribute to the lability of these complexes and may explain why they are able to react with DNA. This idea is supported by observations of surprisingly high levels of Cr-DNA binding after treatment with the synthesised complex $K_2[Cr(L-GS)_2] \cdot 3H_2O$ (Hneihen *et. al.* 1993). Hydrolysis becomes more important the longer Cr(VI)/GSH reaction mixtures are allowed to age and this process may well explain the levelling off and slight upwards curvature seen in Figure 3.6. A summary of all these findings is presented in Figure 3.7.

These observations and hypotheses are in line with results communicated by Zhitkovitch *et. al.* (1996). Investigations of the mechanism by which Cr(VI) and ascorbate anions can form cross-links between tridentate amino acids (cysteine, glutamic acid, histidine) and DNA have led the authors to conclude that Cr(III)-amino acid complexes were the species responsible for adduct formation.

Furthermore, evidence was presented to suggest that the DNA phosphate groups are the primary binding sites for cross-links. It is conceivable that this is also the case with Cr(III) species produced during the reduction of Cr(VI) by GSH, and would explain the very low levels of binding to DNA seen in earlier studies using phosphate as the buffer system.

Due to the long incubation times used in these studies, we observed relatively high levels of Cr-DNA binding. Our data agree well with the level of Cr binding seen previously after shorter incubation times. In studies with calf thymus DNA, Borges and Wetterhahn (1989) obtained 10 Cr per 1000 base pairs after incubation with 1.8 mM Cr(VI) and 4.5 mM GSH for 30 min using Tris buffer. Similar studies using pBR322 DNA yielded 2-3 Cr per 1000 base pair after treatment with 0.48 mM Cr(VI) and 5 mM GSH for 30 min (Borges *et. al.* 1991). On the basis of our time course studies with 0.5 mM Cr(VI) and 5 mM GSH (Figure 3.4) we estimate that the number of Cr-DNA adducts after 30 min incubation time would be approximately 50 Cr per 1000 base pair. Given the differences in techniques and experimental systems this is in fairly good agreement with the data communicated by Borges *et. al.* (1991) and Borges and Wetterhahn (1989).

The concentrations of GSH which were chosen for these studies are in a physiologically and toxicologically relevant range. There is compartmentalisation of GSH inside cells, with cytosolic

concentrations estimated to lie in the range between 1 and 10 mM and intranuclear levels of around 20 mM (Bellomo *et. al.* 1992).

Taken together, these results enable the proposition of a unified model for the induction of oxidative damage (SSB and AP-sites) and cross-link type lesions by Cr(VI)/GSH. This model is intended to highlight areas which further require clarification and incorporates the following features;

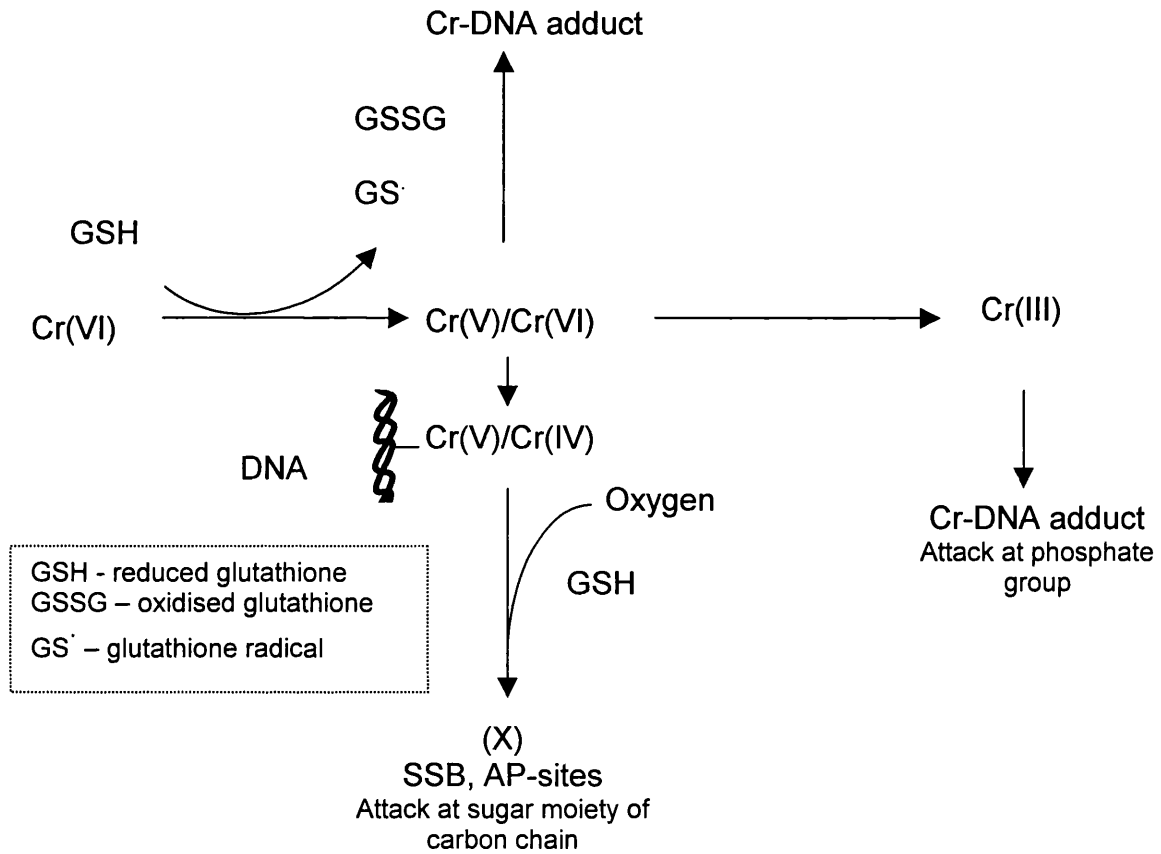
- Molecular oxygen is required for SSB and AP-sites to be formed (Casadeval and Kortenkamp 1995) but Cr(V) species, in the absence of oxygen, are unreactive (Kortenkamp *et. al.* 1996), as are Cr(III) complexes.
- SSB and AP-sites are formed with equal probability, indicating that the site of attack are carbon atoms of the DNA sugar moiety (Casadeval and Kortenkamp 1995).
- Hydroxyl radicals are unlikely to be the oxidising species leading to SSB and AP-sites (Kortenkamp *et. al.* 1996).
- Cr-DNA adducts can be formed independently of the reaction pathways giving rise to SSB and AP-sites.
- Cr(V), and possibly Cr(IV) species, as well as hydrolysing Cr(III)/GSH complexes are responsible for the formation of Cr-DNA adducts.
- DNA-phosphate groups are the binding site of Cr-DNA adducts.

As a starting point of these considerations (Fig. 3.6) it is envisaged

that a hypervalent Cr species (oxidation state IV or V) binds to DNA-phosphate groups, eventually yielding a 1:1 Cr-GSH DNA adduct. If the partly reduced metal centre encounters reactive oxygen species (arising, for example, from a reaction of molecular oxygen with GSH), highly oxidising intermediates may be produced leading to oxidations of carbon atoms of the DNA sugar moiety. This process is thought to give rise to either SSB or AP-sites, very likely leaving behind a Cr(III) residue attached to the site of reaction. Alternatively, highly oxidising species involving partly reduced Cr are formed free in solution and cause SSB or AP-sites only when diffusing to the surface of DNA. However, this process may not necessarily result in formation of Cr-DNA adducts. It is difficult to distinguish between an involvement of oxygen in the formation of reactive intermediates and a role for oxygen in the causation of DNA damage after initial oxidation of sugar carbon atoms. Both pathways may proceed independently.

At this point, ideas about the nature of the oxidising species arising from hypervalent Cr and reactive oxygen species are speculative. In view of the lack of evidence to support hydroxyl radicals (Kortenkamp *et. al.* 1996, Yang *et. al.* 1992, Chen and Thilly 1994, Kortenkamp and O' Brien 1994) we currently favour a possibility first suggested by Lefebvre and Pezerat (1992) for Cr(VI)/AsA systems, i.e. the involvement of Cr(V) superoxo- or peroxo- complexes. Research into the chemistry of such reactions is still in its infancy and requires more work however, a proposed summary of the interactions of Cr(VI) with DNA in the presence of GSH is presented in Figure 3.7.

Figure 3.7 Schematic representation of the proposed mechanisms involved in Cr(VI)-mediated DNA damage



In the absence of any interactions between Cr(V) or (IV) and oxygen, Cr-DNA adducts are likely to form. Even in the presence of oxygen, high levels of antioxidants such as GSH will favour this reaction pathway by both scavenging radicals and by promoting the formation of Cr(III). As they accumulate, slowly hydrolysing Cr(III)/GSH complexes are likely to contribute more and more to the formation of Cr-DNA adducts.

CHAPTER 4

An Investigation into the Potentially Pre-mutagenic Lesion Generated During the Reduction of Cr(VI) by GSH

4.1 Introduction

Although it is widely believed that the DNA lesions generated during the intracellular reduction of Cr(VI) are the cause of its genotoxicity, few attempts have been made to establish the fate of different types of damage after DNA repair, replication and transcription. It should be stressed that no one has ever attempted to monitor the mutagenic effects of such lesions *in situ* and despite the work of Costa *et. al.* (1990) it still remains unclear which of these types of damage are relevant to a cellular model. An improved understanding of such processes would greatly aid the biological monitoring of exposed individuals and it is therefore important to determine the mutagenic potential of the characteristic lesions generated during this process.

4.2 DNA Damage, Mutations and the Multi-Stage Model of Carcinogenesis

The interaction of a chemical carcinogen, such as Cr, with DNA will depend on many factors, including the influence of metabolic activation (e.g. modification of a xenobiotic via the cytochrome p450 mixed function oxidase system or, in the case of Cr, conversion by an intracellular reductant such as GSH) and the stage at which the cell is during its replication cycle (during replication the DNA is far more

accessible to chemical insult). As a result of such interactions, several types of DNA damage may result such as SSB, AP-sites, carcinogen-DNA adduct formation or DNA protein cross-links. Such damage may be efficiently repaired by the cell or may be passed on to the progeny cell line as a mutation. If the cell replicates whilst DNA damage is persistent, alterations in the genetic material may be produced in several ways. Mismatching of bases will lead to *point mutations* (these will usually be as a result of base substitution) whilst errors in the replication of damaged DNA, such as the insertion or deletion of bases may lead to *frame shift mutations*. Transpositions of large sections of DNA may also occur resulting in codon rearrangement.

A mutation may be defined as a heritable change in genetic material which causes alterations in the amino acid sequence of the resulting polypeptide gene product(s). Such changes will lead to characteristic alterations in the phenotype of the affected organism which is then recognised as a mutant. Therefore, for initial DNA damage to result in the generation of mutants, it must be “fixed” or imprinted during DNA replication before it can be expressed in subsequent generations.

DNA repair mechanisms can modulate the amount of damage initially introduced to the DNA of target cells. Damage may then either be recognised correctly and repaired or, under some circumstances, left unrepaired. During the replication of insufficiently repaired DNA, the rules of complementary base pairing can be disrupted and incorrect

bases can be incorporated. Such mutations are considered to be the *initiating* event in the complex process of transforming normal somatic cells into malignant tumour cells. Initiated cells may have a growth advantage over normal cells and, as a result, may proliferate faster. This clonal expansion of “initiated” cells is likely to be accompanied by further genetic changes involving gene amplifications, translocations or deletions of large parts of the genome. Eventually, further genetic (or *epigenetic*) changes may then transform such “dormant” tumour cells into malignant tumour cells.

4.3 Potentially Mutagenic Lesions Generated During the Reduction of Cr(VI) by Glutathione

Of particular interest in terms of mutagenesis are AP-sites. These lesions are believed to be one of the major types of damage to occur in the mammalian genome. Whilst the cell has evolved various DNA repair mechanisms for these lesions (see section 4.4, Lindahl 1982), their efficiency might not be complete and replication of AP-sites can lead to mutations. Unlike miscoding lesions, which have modified base-pairing properties and can be copied albeit with the insertion of incorrect nucleotides, AP-sites are non-coding and cannot be copied under normal conditions, i.e. they terminate DNA synthesis and would not, therefore, be expected to be “fixed” as mutations (Schaaper *et. al.* 1983). However, DNA synthesis was found to proceed past AP-sites *in vitro* with isolated DNA polymerases or *in vivo* under an error prone repair system (Loeb *et. al.* 1986). The first evidence for the mutagenic potential of AP-sites came from studies where the quantification of

misincorporated nucleotides was assessed during the *in vitro* replication of a depurinated (acid-heated) polynucleotide, poly(A-T) (Shearman and Loeb 1977). Infidelity of DNA synthesis *in vitro* using purified avian myeloblastosis virus (AMV) DNA polymerase was found to be proportional to the degree of depurination and was abolished by alkali treatment of the polynucleotide. Further evidence comes from studies using acid-heat denatured single stranded DNA. Kunkel *et. al.* (1981) demonstrated that during replication *in vitro*, E. coli DNA polymerase I was able to copy past AP-sites on single stranded $\phi X174 am^3$ phage DNA. The transfection of this DNA into E. coli SOS induced spheroblasts led to an increased mutagenicity of the phage (Kunkel *et. al.* 1981, Schaaper *et. al.* 1983, Schaaper and Loeb 1981). This increase in mutation frequencies was reversed when the depurinated phage was treated with alkali (Schaaper and Loeb 1981, Kunkel *et. al.* 1981) or with an AP-endonuclease (Schaaper *et. al.* 1983), both being treatments known to cleave DNA at AP-sites (Loeb *et. al.* 1986).

Whilst single strand breaks cannot be ruled out as potentially mutagenic lesions there is, as yet, no experimental model available which could be used to assess whether or not such damage is mutagenic. Furthermore, strand breaks induced by Cr(VI) *in vivo* are reported to be easily repaired (Cupo and Wetterhahn 1984). Similarly, little information is available about the potential mutagenicity of other DNA lesions such as Cr-DNA adduct formation. Again, this is due to

the lack of an experimental test system which could be employed for such investigations. The aim of this study is that, by employing specific experimental conditions to control the types of lesion being generated during the reduction of Cr(VI) by GSH, and by the application of a bacterial mutation assay the mutagenic potential of different types of DNA damage can be assessed.

4.4 Approaches for the Study of Pre-Mutagenic Lesions

The models generally used to determine the mutagenic potential of compounds rely on the identification of certain phenotypes which have arisen from characteristic mutational changes in specific genes (Levis and Bianchi 1982). The Ames assay, for example, utilises mutant phenotypes of *S. typhimurium* which can revert back to prototrophy as a result of a base substitution or a frame-shift mutation at a single base pair (Levis and Bianchi 1982, Standeven and Wetterhahn 1991b, Sugden *et. al.* 1990, IARC 1990). These tests have been useful in providing evidence for the ability of Cr(VI) compounds to generate point mutations (both base-pair substitution and frame-shift mutation) in *S. typhimurium* (Levis and Bianchi 1982, Cohen *et. al.* 1993) and have also been employed to demonstrate the oxygen dependence for the mutagenicity of Cr(VI) and Cr(III) compounds (Sugden *et. al.* 1990). However, this type of assay while allowing the quantification and characterisation of mutation, does not give any information about the type of lesion involved in Cr-mediated carcinogenesis.

Similarly, analysis of the damage induced in isolated DNA *in vitro* (Chapter 3) may allow characterisation of the type of lesion involved but does not provide any information about the fate of such types of damage after DNA repair, replication and transcription.

The ideal model then, for the study of potentially pre-mutagenic DNA lesions induced by Cr compounds would incorporate features of both test systems. Such models are called *in vitro* mutagenesis assays and, unlike cellular mutation assays, rely on the principle that mutations arise directly as a result of interaction between the test compound and isolated DNA. By employing this approach, a defined DNA lesion can be induced and its mutagenic effects studied *in vivo* after introduction of the modified DNA into bacteria (“transformation”).

4.5 An *In Vitro* Mutation Assay to Determine the Pre-Mutagenic Lesion Generated During the Reduction of Cr(VI) by GSH

A commonly used technique to study mutations arising from DNA damage is to modify plasmid DNA which carries two or more “marker genes” (or selectable genes). Plasmids are circular, double stranded DNA molecules which act as accessory genetic units in bacteria. They replicate independently from the bacterial genome but are dependent on host enzymes for replication and transcription. Once a cell has been transformed, plasmid molecules replicate and are passed on to the progeny during cell division. Plasmid molecules may be constructed to carry one or more marker genes. These are genes which code for a protein which provides the transformed bacteria with

a new phenotypically recognisable feature, for example, antibiotic resistance.

Such an approach facilitates the selection of transformed bacteria (by employing a selective growth medium). Utilising a second selectable marker gene allows the screening of mutants; if a second phenotypic characteristic is absent in transformed cells, this is an indication that the marker gene has been inactivated by a mutation.

This principle was employed by using a slight modification on a test system which had been previously used in this laboratory and which utilised the plasmid DNA pUC19.

pUC19 is 2686 base pairs in size and provides a histochemical selection system based on the plasmid borne *lacZ'* gene. This gene codes for the amino-terminal fragment of the enzyme β -galactosidase which is responsible for the conversion of lactose to glucose in the normal *E. coli* bacterium (Sambrook and Pollack, 1974). The expression of *lacZ'* can be induced by isopropylthio- β -D-galactoside (IPTG), a non-metabolisable *lac* operon inducer. The peptide encoded by the *lacZ'* gene is not sufficient to catalyse the conversion of lactose but can complement the host encoded fragment (lacking the *lacZ'* fragment) to produce the active enzyme. This enzyme activity can be assessed using the colourless substrate 5-bromo-4-chloro-3-indolyl- β -D-galactoside (X-gal) which is converted to an intensely

coloured blue compound (5-bromo-4-chlorindigo) by β -galactosidase (Wolf *et. al.* 1968).

pUC19 also carries the ampicillin resistance gene (amp^r) therefore, plating of transformed bacteria in medium containing ampicillin and X-gal will permit the selection of transformed clones, since not only will they possess ampicillin resistance, the colonies produced will be blue ($amp^r lacZ^+$). Clones harbouring non-functional $lacZ'$ genes (mutants) will lack β -galactosidase activity and will appear as white colonies ($amp^r lacZ^-$), indicating possible inactivation of the gene on pUC19 by *in vitro* modification.

The bacterial host chosen was *E. coli* JM105 (genotype: *thi, rpsL, endA, sbcB15, hsdR4, SupE, $\Delta(lac-proAB)/F'$ [*traD36, proAB⁺, LacI^q lacZ Δ M15]*). This strain carries a chromosomal deletion $\Delta(lac-proAB)$ which is partially complemented by an engineered F' episome, which carries $lacZ\Delta M15$ (the lac operon minus the $lacZ'$ fragment). Bacteria will produce an inactive marker β -galactosidase due to the $\Delta M15$ deletion. F' also carries $lacI^q$, a mutation that results in over-expression of the lac operon. In addition, *E. coli* JM105 is resistant to streptomycin.*

By exposing pUC19 to Cr(VI)/GSH systems, lesions will be formed randomly along the sequence of the plasmid (the assay is not gene-

directed). Mutations can, therefore, conceivably be formed at every position in the whole plasmid, including the *lacZ'* gene, and the *amp^r* gene which is used to ascertain successful transformation. The chosen selection method, however, can only detect non-lethal mutations which have inactivated the *lacZ'* gene. Bacteria harbouring plasmids which carry a mutation in the *amp^r* gene are unable to survive in the selection medium and cannot be scored. Whilst elevated mutation rates in the *amp^r* gene will result in slightly reduced transformation efficiencies, the assay system is unable to detect inactivations of both the *lacZ'* and the *amp^r* gene. It is therefore desirable to achieve as efficient transformation efficiencies as possible to negate any effect of this "double mutation".

From earlier work where DNA damage was induced in PM2 DNA (Chapter 3) we have been able to develop a model whereby we can modulate the type of damage being generated by changing the reactive environment. Experimental conditions were therefore chosen such that, in certain samples, both SSB and Cr-DNA adducts would be observed (5 mM GSH) yet in others, we would only see Cr binding (GSH >15 mM, presence of catalase). By comparing the mutation frequencies observed after transformation of bacteria with modified plasmid to those obtained with untreated DNA we aim to determine the mutagenic potential of the lesions concerned.

4.6 Materials

pUC19 plasmid DNA and E. Coli JM105 cells were obtained from Pharmacia Biotech (St. Albans, UK). IPTG (Isopropylthio- β -D-galactoside), N-N' dimethylformamide, X-Gal (5-bromo-4-chloro-3-indolyl- β -D-galactoside) and glycerol were from Sigma (Poole, Dorset, UK), as were the ampicillin and streptomycin. LB-medium (Luria-Bertani medium) capsules and Select agar were purchased from Bio101 inc. (USA), whilst SOC medium was provided by Gibco BRL (Paisley, UK). Filters were obtained from Whatman (Maidstone, Kent, UK).

4.7 Methods

4.7.1 Media and Plates

LB-media

LB-media was prepared according to the manufacturers instructions. Briefly, 25 pre-packed capsules were dissolved in 1 l of UHQ water and the solution autoclaved at 121 °C for 15 min.

M-9 Minimal Media Plates

15 g select agar was dissolved in 750 ml UHQ and the solution autoclaved. Upon cooling to 50 °C the following solutions were added in the following proportions;

“M-9 salts (5X)” (see preparation below)	200 ml
1 M MgSO ₄	2 ml
20 % glucose	20 ml
1 M CaCl ₂	0.1 ml
1 M thiamine-HCl	2 ml
UHQ water	to 250 ml

“M-9 salts” (5X) were prepared by dissolving the following salts in UHQ water to a final volume of 1 l. The solution was split into 200 ml aliquots and sterilised by autoclaving at 121 °C for 15 min.

Na ₂ HPO ₄ ·7H ₂ O	64 g
KH ₂ PO ₄	15 g
NaCl	25 g
NH ₄ Cl	5 g

LB-Plates for Blue/White Screening

Approximately 980 ml of LB-medium was prepared by dissolving 25 LB-medium capsules and 15 g select agar in UHQ water. After autoclaving, the solution was allowed to cool to approximately 50 °C and the following reagents were added;

X-Gal (50 mg/ml dissolved in N,N'-dimethylformamide)	800 µl
IPTG (0.2 M in UHQ)	2.5 ml
Ampicillin (in 8 ml UHQ)	100 mg

Streptomycin (in 2 ml UHQ)	25 mg
Sterile UHQ	to 1 l

The IPTG and antibiotic solutions were filter sterilised. X-Gal was added without sterilisation. The dissolution of the antibiotics may be facilitated by the addition of two or three drops of 1M NaOH to the UHQ.

The final medium was then poured out into 90 mm petri dishes in a laminar flow cabinet and allowed to set at room temperature. Upon setting, the plates were stored upside down at <5 °C.

4.7.2 Resuspension of E. coli JM105

The lyophilised culture was resuspended in 1 ml of LB-media and grown overnight at 37 °C before plating out onto M-9 minimal media containing 25 µl/ml streptomycin.

4.7.3 Preparation of Competent Cells

A primary culture was prepared by inoculating 10 ml of pre-warmed LB-medium with a single colony of E. coli JM105 and grown overnight at 37 °C with vigorous shaking (200 rpm). 500 ml of pre-warmed LB-medium was then inoculated with the primary culture and the cells grown at 37 °C/200 rpm until the absorbance of the medium at 600 nm reached a value between 0.45 and 0.55. This indicates that the cells have reached the logarithmic growth cycle which is essential for

the success of this procedure. Once logarithmic growth was achieved, the medium was rapidly chilled and left on ice for 1-2 h.

The cells were then transferred to two sterile centrifuge tubes (approx. 250 ml per tube, balanced by weighing) and spun at 2,500 rpm for 25 min at 4 °C. After centrifugation, the supernatant was discarded and the cells in each tube resuspended in approximately 250 ml ice cold trituration buffer (100 mM CaCl₂, 70 mM MgCl₂). These were then left on ice for a further 45 min. When thoroughly chilled, the resuspended cells were centrifuged again as before. Finally, the supernatant was discarded and the cells from each tube resuspended in approximately 3 ml ice cold trituration buffer. The cells were pooled, and 2 ml of 60% glycerol in UHQ water was added with gentle swirling to give a final concentration of 15% glycerol. 200 µl aliquots of the suspension were snap frozen on dry ice (or in liquid nitrogen) and stored at -80 °C until required.

4.7.4 Treatment and Purification of Plasmid

Plasmid pUC19 DNA (640 ng in a final volume of 20 µl; stock solution 128 µg/ml in 10 mM Tris, pH 7.5 and 1 mM EDTA) was incubated at room temperature in the presence of GSH (5 mM or 20 mM) and potassium chromate (1.5 mM) in HEPES buffer for 18 h. To a number of samples, catalase was added (10 µg/ml). Negative control samples contained pUC19 and GSH, and in some cases catalase was denatured by heating to 65 °C for 10 min. Positive controls were

prepared by incubating pUC19 in the presence of Fe(II)-EDTA/ H₂O₂ (25 uM/100 µM) at room temperature for 1 h.

After incubation, all samples were purified using the Promega *Wizard DNA Clean-up System* and Microcon 30 filter units (as described in Chapter 3). The plasmid was recovered in a final volume of 50 µl TE buffer (the final concentration of plasmid was assumed to be 12 ng/µl to take into account any loss of DNA during purification steps). A 20 µl aliquot of this solution was taken and gel electrophoresis performed to verify the integrity of the plasmid (Figure 4.1; for method see Chapter 2). The remaining sample was diluted 1:4 in TE buffer and 2 µl (equivalent to 6 ng of plasmid) used to transform the competent cells.

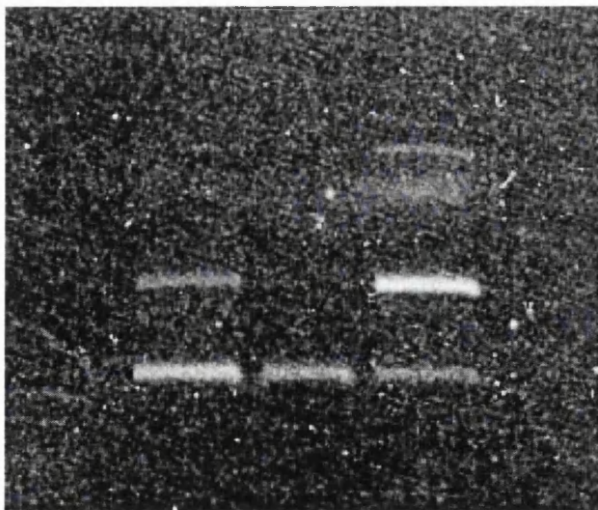


Figure 4.1 Photograph of agarose gel run to determine integrity of pUC19 plasmid. Lane 1 contains pUC19 + Fe(II)/H₂O₂, Lane 2 contains untreated pUC19, Lane 3 contains pUC19 + Cr(VI) + GSH.

4.7.5 Transformation of Competent Cells

To each sample of purified plasmid, 100 μ l aliquots of thawed E. coli JM105 cells were added and the samples left on ice for 45 min. The cell/plasmid suspension was then heated to 45 °C for 90 s, and returned to ice for a few minutes. 400 μ l of pre-warmed SOC medium was then added and each reaction mixture incubated at 37 °C for one hour with vigorous shaking to allow the cells to recover.

For each set of incubation conditions, ten aliquots of 10 μ l of the cell suspension were plated on LB-medium plates and incubated at 37 °C overnight. Plates were differentially scored for coloured colonies and the transformation efficiencies and mutation frequencies for each sample determined.

The viability of E. coli JM105 was assessed in each experiment by plating on LB medium without ampicillin. Transformation efficiency (XFE) was determined as the total number of colonies obtained per microgram of plasmid used in the transformation;

$$\text{XFE} = \text{total number of colonies}/\mu\text{g}$$

Mutation frequency (MF) is given by the ratio of the number of white colonies ($amp^r lacZ^-$) over the total number of colonies (amp^r);

$$\text{MF} = \text{no. of } amp^r lacZ^- \text{ colonies}/\text{no. of } amp^r \text{ colonies}$$

4.8 Results

It should be stressed that in all these experiments the transformation efficiencies achieved were sufficient to negate any deleterious effects which may have arisen as a result of the “double mutation” of both the *lacZ* and *amp^r* genes (Table 4.1).

In order to determine the “background” or spontaneous mutation frequency present in our experimental system, cells were transformed with untreated plasmid and the resulting mutation frequency shown to average 4.0×10^{-4} (all data shown in Table 4.1). This is in good agreement with other studies where background mutations of the *lacZ'* fragment have been assessed in pUC19 (Kortenkamp *et. al.* 1996), or in studies utilising single stranded M13mp2 DNA (Kunkel 1984, McBride *et. al.* 1991). To gain some information about the effect of oxidative damage on mutation frequency, cells were transformed with pUC19 which had been previously treated with Fe(II)-EDTA/H₂O₂ (25 µM/100 µM). The oxidation of Fe(II) by H₂O₂ is known to generate reactive oxygen species which induce DNA damage including SSB (Imlay and Linn 1988, McBride *et. al.* 1991), AP-sites (Povirk and Steighner 1989) and oxidative modification of DNA bases such as 8-OH deoxyguanosine (Fischer-Nielsen *et. al.* 1992, Aruoma *et. al.* 1989) as well as mutations (McBride *et. al.* 1991, Reid *et. al.* 1994). Treatment of the plasmid with Fe(II)/H₂O₂ resulted in an average mutation frequency of 3.8×10^{-3} . This approximately represents a ten-fold increase relative to untreated plasmid and is in agreement with

other studies carried out in this laboratory where treatment of pUC19 with Fe(II)/H₂O₂ yielded mutation frequencies of 5.9×10^{-3} ; an approximate nine-fold increase over control (Kortenkamp *et. al.* 1996). Similarly, in studies where the influence of Fe(II)/H₂O₂ on mutation frequency was investigated in single stranded M13mp2 DNA an eight-fold increase in mutation frequency was demonstrated compared to untreated plasmid (McBride *et. al.* 1991).

Table 4.1 Mutation Frequency in pUC19 Plasmid DNA after In Vitro Modification with Cr(VI)/GSH

	pUC19 treatment	Transformation efficiency (colonies/ μ g plasmid)	Mutation frequency (Amp ^r lacZ ⁻ colonies/total)	Mean mutation frequency (\pm SD)
1	None	3.3×10^7	3.5×10^{-4} (10/28186)	$4.0 \times 10^{-4} \pm 5.0 \times 10^{-5}$
		1.9×10^7	4.4×10^{-4} (8/18053)	
		-	4.0×10^{-4} (6/15003)	
2	Fe(II)/H ₂ O ₂ (25 μ M/100 μ M)	1.8×10^7	6.3×10^{-3} (120/19028)	$3.8 \times 10^{-3} \pm 2.5 \times 10^{-3}$
		1.0×10^7	1.3×10^{-3} (16/12312)	
		-	3.8×10^{-3} (34/8947)	
3	Cr(VI)/GSH (1.5 mM/5 mM)	2.5×10^7	4.4×10^{-3} (135/30743)	$4.8 \times 10^{-3} \pm 1.9 \times 10^{-3}$
		2.7×10^7	6.9×10^{-3} (224/32256)	
		1.5×10^7	3.1×10^{-3} (51/16587)	
4	Cr(VI)/GSH+ catalase (1.5 mM/5 mM+10 μ g/ml)	1.8×10^7	6.1×10^{-3} (119/19399)	$3.5 \times 10^{-3} \pm 2.3 \times 10^{-3}$
		2.7×10^7	2.5×10^{-3} (83/32971)	
		2.1×10^7	1.8×10^{-3} (46/25054)	
5	Cr(VI)/GSH+ denatured catalase (1.5 mM/5 mM +10 μ g/ml)	1.9×10^7	4.8×10^{-3} (97/20217)	$3.5 \times 10^{-3} \pm 1.6 \times 10^{-3}$
		2.7×10^7	4.1×10^{-3} (133/32213)	
		2.0×10^7	1.7×10^{-3} (36/21092)	
6	Cr(VI)/GSH (1.5 mM/20 mM)	2.1×10^7	1.7×10^{-3} (43/24923)	$3.4 \times 10^{-3} \pm 1.7 \times 10^{-3}$
		2.8×10^7	5.2×10^{-3} (128/23936)	
		3.0×10^7	3.4×10^{-3} (98/28946)	

Cr(VI)/GSH = Chromium(VI)/Glutathione

Attempts were made to analyse aliquots of the treated plasmid for levels of strand breaks (Chapter 2). However, analysis of the gels proved to be technically difficult due to the diffuse appearance of the DNA bands. This was believed to be a result of tertiary complexes being formed between the plasmid and Cr species and would support our earlier findings (Chapter 3) of very high levels of Cr-DNA adduct formation (approximately 2 Cr per base pair at 0.5 mM Cr[VI]/5 mM GSH after 18 h). At high levels of DNA damage, plasmid molecules tend to cluster and in doing so “trap” Cr species within the newly formed DNA complexes.

Non-transformed bacteria were unable to grow on plates containing ampicillin (since they lacked the ampicillin resistance gene), but grew as a “lawn” on LB plates. These negative controls (non-transformed E. coli JM105) were performed for each experiment to ensure that cells were not contaminated (LB-plates containing ampicillin - restrictive conditions) and were still viable (LB-plates - permissive conditions).

When cells were transformed with pUC19 which had been exposed to Cr(VI)/GSH (1.5 mM/5 mM) an average mutation frequency of 4.8×10^{-3} was observed, representing a twelve-fold increase above background. This clearly demonstrates the mutagenic potential of Cr(VI)/GSH systems but does not give any indication as to which forms of DNA damage may be involved. Under such conditions, it has been demonstrated that many types of lesion can be generated,

including SSB, AP-sites and Cr-DNA adducts, and that these lesions are mediated by different mechanistic pathways (chapter 3). However, the same studies have also shown that the removal of active oxygen species from the reaction medium by the addition of catalase can inhibit or “shut off” the generation of SSB and AP-sites. When the treatment of pUC19 was modified in this way, an average mutation frequency of 3.5×10^{-3} was observed. While this appears to be a decrease in the number of mutations, compared with Cr(VI)/GSH treatment in the absence of catalase, it still represents an approximate nine-fold increase above background levels. Indeed, the addition of denatured catalase to the incubation mixture as a control yielded an identical mutation frequency of 3.5×10^{-3} .

At GSH levels where maximum numbers of Cr-DNA adducts are observed (20 mM), formation of oxidative damage such as AP-sites and SSB is inhibited due the ability of GSH to scavenge active oxygen species. When pUC19 was treated with 1.5 mM Cr(VI)/20 mM GSH, transformed cells exhibited an average mutation frequency of 3.4×10^{-3} . Again, this represents an approximate nine-fold increase above background counts and corresponds with the mutation frequencies observed in the presence of both active and denatured catalase.

All these observations have been made upon assumptions where the means of treatment groups have been compared, this being done in

an attempt to compare these results with data communicated by previous authors. However the comparison of means for statistical purposes is only appropriate when the data follows a normal (or *Gaussian*) distribution. When mutation distributions were plotted it became apparent that this is not case in these studies. For these comparisons to be meaningful, a more sophisticated statistical evaluation is required and for this reason data were reanalysed using the non-parametric U-test (or *Mann Whitney U-Test*) (Siegel, 1956). This test compares the medians of two independent samples which need not contain the same number of observations and which may be small in sample size. Similarly, the results previously communicated have been based on the pooling of data from three replicate experiments and do not, therefore, take into account any variation between studies. Figure 4.2 shows frequency distributions of mutation frequencies seen in individual profiles inoculated with aliquots of treated plasmid solution for *each* experimental treatment (1-6) from *each* study performed (A-C).

Key to Figure 4.2

Figures represent mutation frequencies for E. coli JM105 obtained from six different treatments (1-6) per study. Each study was repeated three times (A-C). Each treatment group consisted of a single aliquot of E. coli JM105 cells which was incubated under the required conditions then plated onto ten ampicillin-containing LB-plates. The individual bars of the histograms represent the mutation frequency obtained for a single plate in each treatment group.

Experimental conditions were as follows;

Treatment 1: None (5 mM GSH)

Treatment 2: Fe(II)/H₂O₂ (25 μM/100 μM)

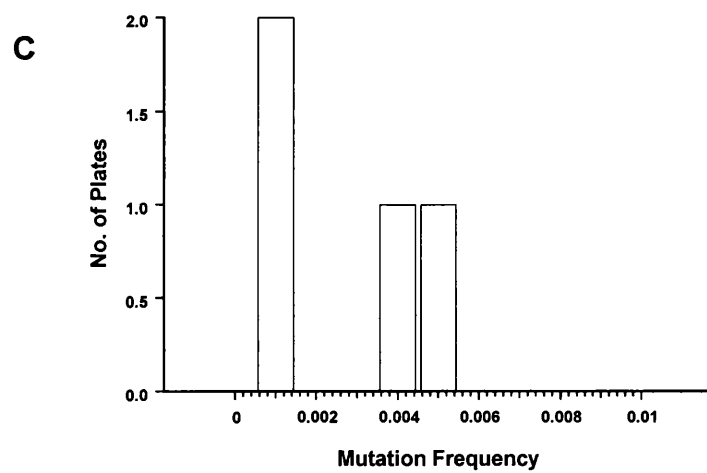
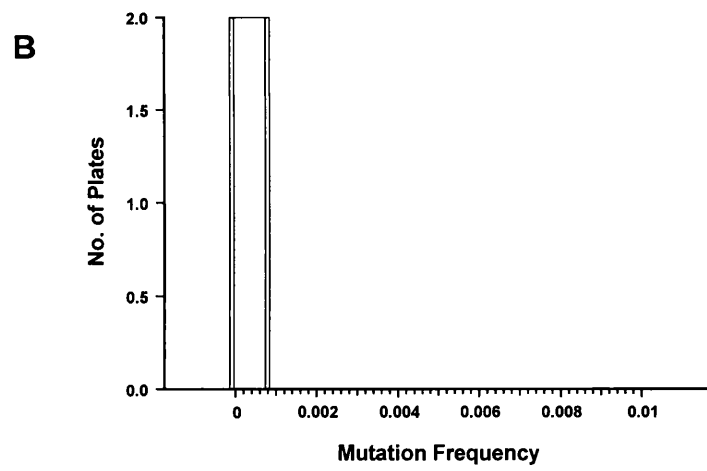
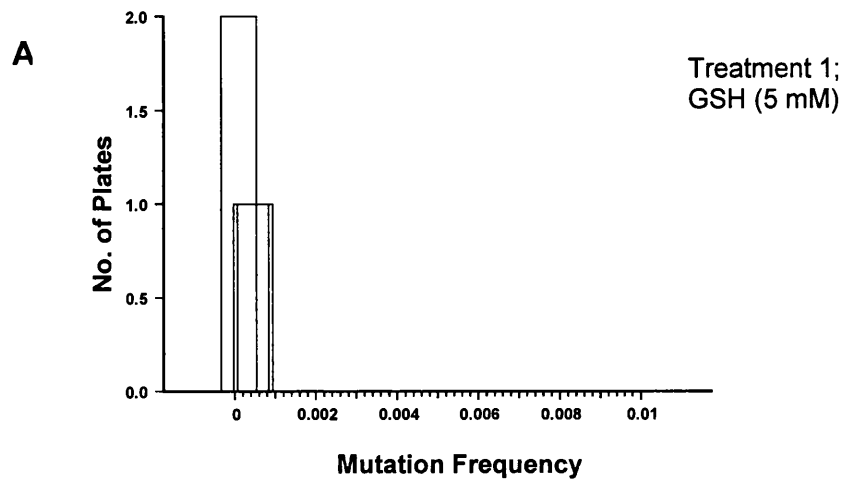
Treatment 3: Cr(VI)/GSH (1.5 mM/5 mM)

Treatment 4: Cr(VI)/GSH + catalase (1.5 mM/5 mM + 10 μg/ml)

Treatment 5: Cr(VI)/GSH + denatured catalase (1.5 mM/5 mM + 10 μg/ml)

Treatment 6: Cr(VI)/GSH (1.5 mM/20 mM)

Figure 4.2 Distribution of mutation frequency for six treatment groups (1-6) as a replicate series of three studies (A-C).



Key to Figure 4.2

Figures represent mutation frequencies for E. coli JM105 obtained from six different treatments (1-6) per study. Each study was repeated three times (A-C). Each treatment group consisted of a single aliquot of E. coli JM105 cells which was incubated under the required conditions then plated onto ten ampicillin-containing LB-plates. The individual bars of the histograms represent the mutation frequency obtained for a single plate in each treatment group.

Experimental conditions were as follows;

Treatment 1: None (5 mM GSH)

Treatment 2: Fe(II)/H₂O₂ (25 μM/100 μM)

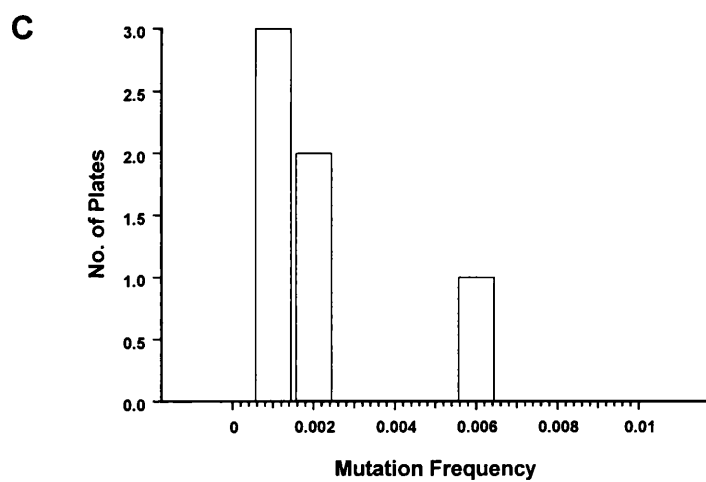
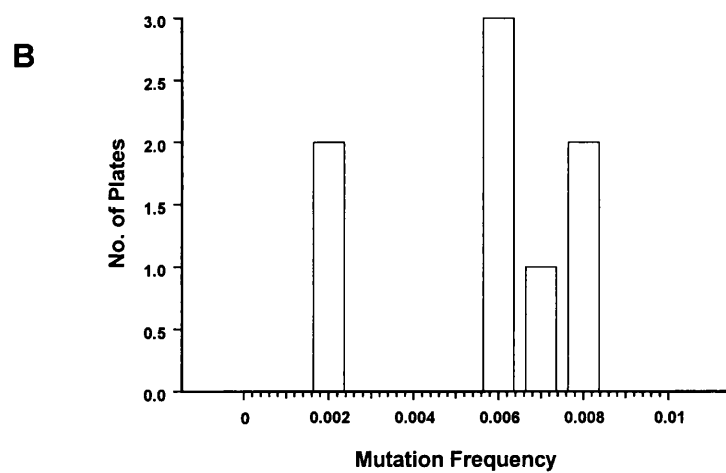
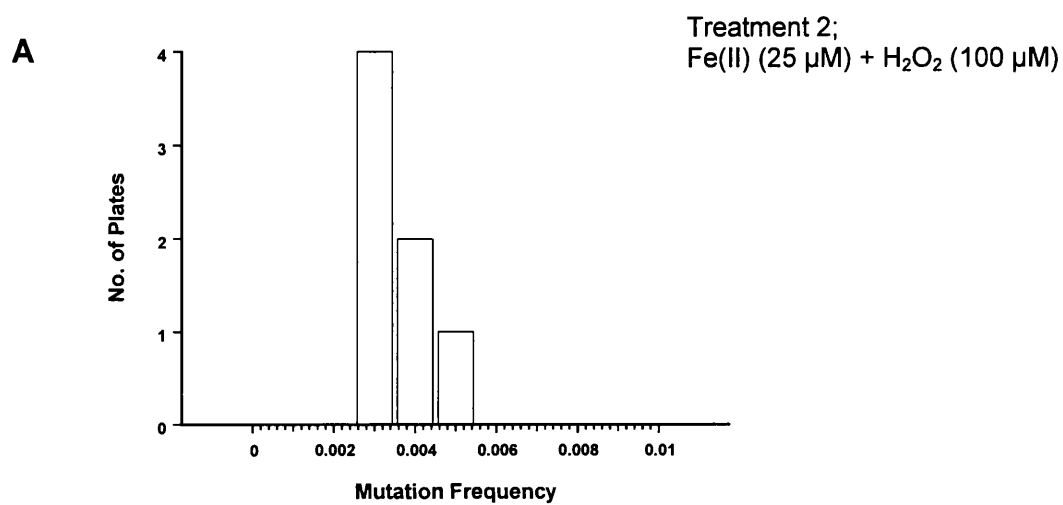
Treatment 3: Cr(VI)/GSH (1.5 mM/5 mM)

Treatment 4: Cr(VI)/GSH + catalase (1.5 mM/5 mM + 10 μg/ml)

Treatment 5: Cr(VI)/GSH + denatured catalase (1.5 mM/5 mM + 10 μg/ml)

Treatment 6: Cr(VI)/GSH (1.5 mM/20 mM)

Figure 4.2 (continued) Distribution of mutation frequency for six treatment groups (1-6) as a replicate series of three studies (A-C).



Key to Figure 4.2

Figures represent mutation frequencies for E. coli JM105 obtained from six different treatments (1-6) per study. Each study was repeated three times (A-C). Each treatment group consisted of a single aliquot of E. coli JM105 cells which was incubated under the required conditions then plated onto ten ampicillin-containing LB-plates. The individual bars of the histograms represent the mutation frequency obtained for a single plate in each treatment group.

Experimental conditions were as follows;

Treatment 1: None (5 mM GSH)

Treatment 2: Fe(II)/H₂O₂ (25 μM/100 μM)

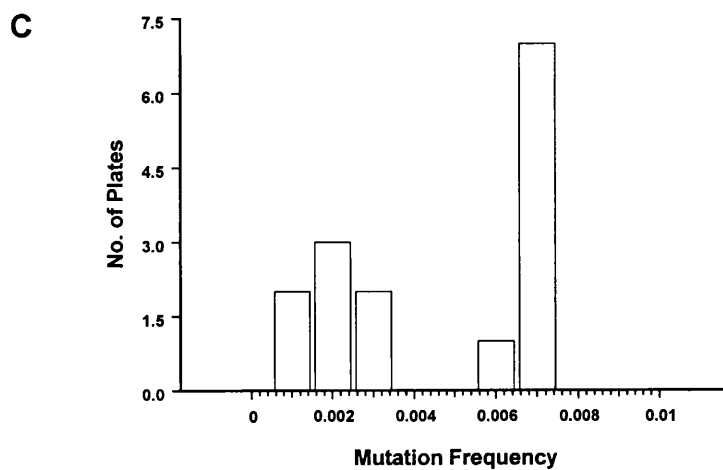
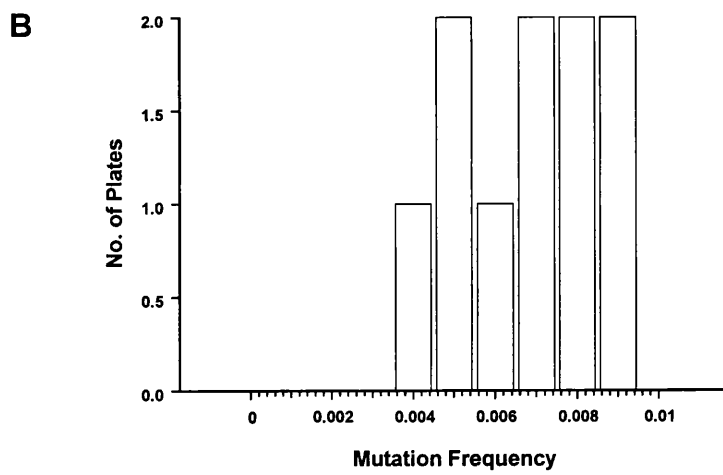
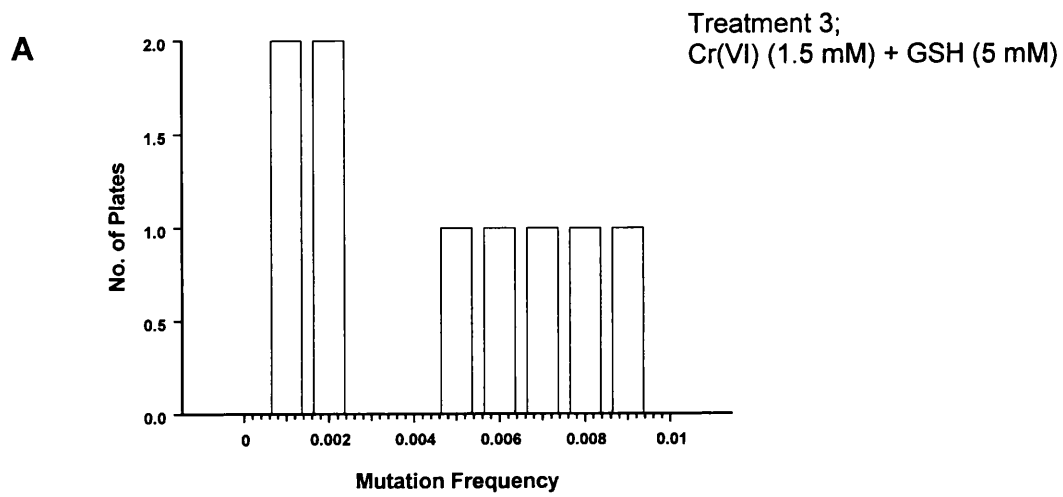
Treatment 3: Cr(VI)/GSH (1.5 mM/5 mM)

Treatment 4: Cr(VI)/GSH + catalase (1.5 mM/5 mM + 10 μg/ml)

Treatment 5: Cr(VI)/GSH + denatured catalase (1.5 mM/5 mM + 10 μg/ml)

Treatment 6: Cr(VI)/GSH (1.5 mM/20 mM)

Figure 4.2 (continued) Distribution of mutation frequency for six treatment groups (1-6) as a replicate series of three studies (A-C).



Key to Figure 4.2

Figures represent mutation frequencies for E. coli JM105 obtained from six different treatments (1-6) per study. Each study was repeated three times (A-C). Each treatment group consisted of a single aliquot of E. coli JM105 cells which was incubated under the required conditions then plated onto ten ampicillin-containing LB-plates. The individual bars of the histograms represent the mutation frequency obtained for a single plate in each treatment group.

Experimental conditions were as follows;

Treatment 1: None (5 mM GSH)

Treatment 2: Fe(II)/H₂O₂ (25 μM/100 μM)

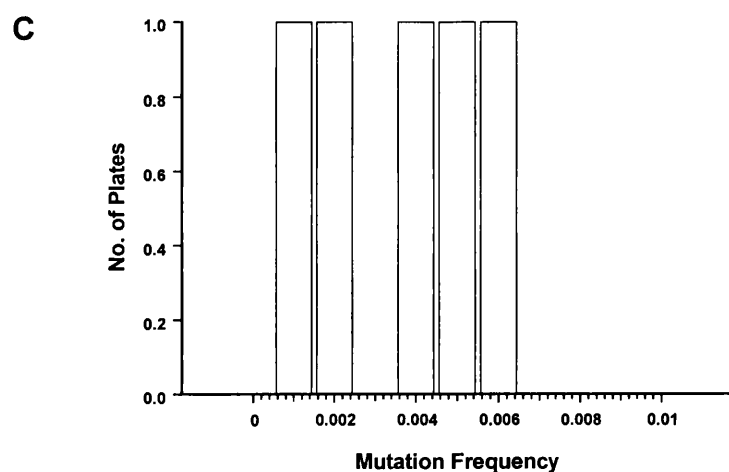
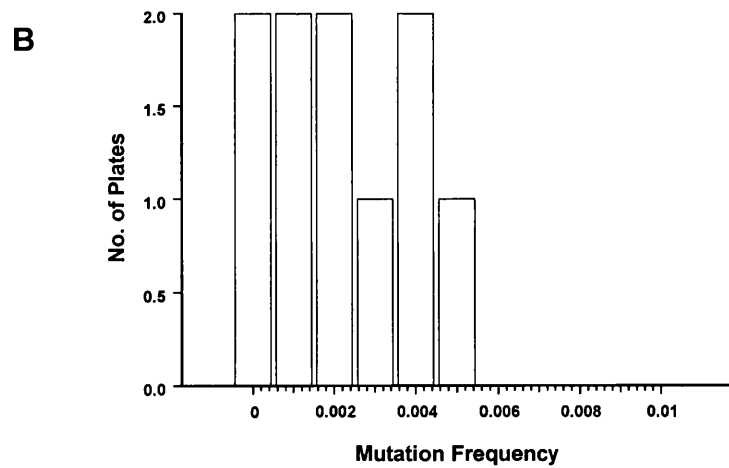
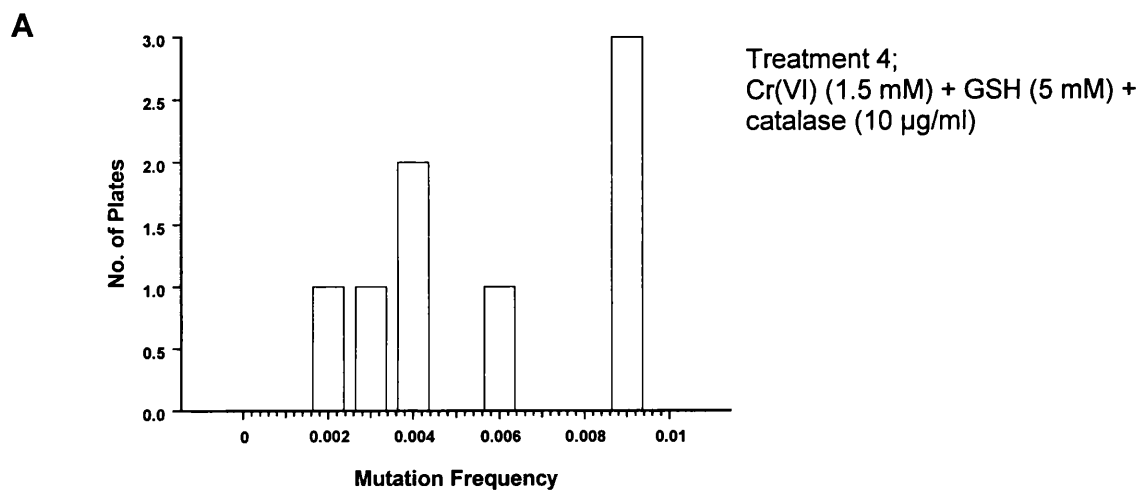
Treatment 3: Cr(VI)/GSH (1.5 mM/5 mM)

Treatment 4: Cr(VI)/GSH + catalase (1.5 mM/5 mM + 10 μg/ml)

Treatment 5: Cr(VI)/GSH + denatured catalase (1.5 mM/5 mM + 10 μg/ml)

Treatment 6: Cr(VI)/GSH (1.5 mM/20 mM)

Figure 4.2 (continued) Distribution of mutation frequency for six treatment groups (1-6) as a replicate series of three studies (A-C).



Key to Figure 4.2

Figures represent mutation frequencies for E. coli JM105 obtained from six different treatments (1-6) per study. Each study was repeated three times (A-C). Each treatment group consisted of a single aliquot of E. coli JM105 cells which was incubated under the required conditions then plated onto ten ampicillin-containing LB-plates. The individual bars of the histograms represent the mutation frequency obtained for a single plate in each treatment group.

Experimental conditions were as follows;

Treatment 1: None (5 mM GSH)

Treatment 2: Fe(II)/H₂O₂ (25 μM/100 μM)

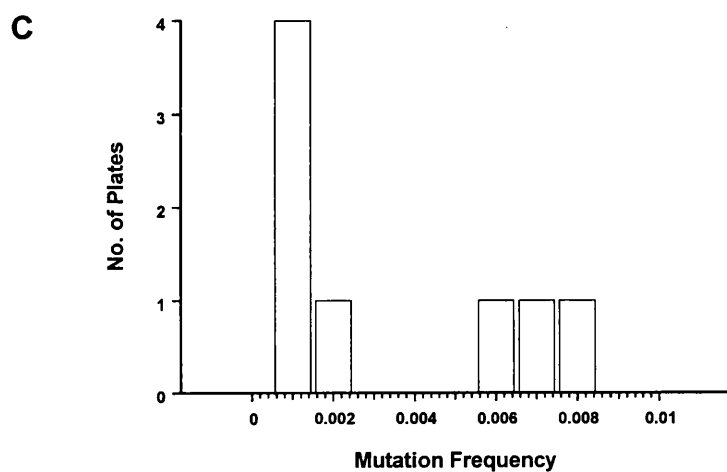
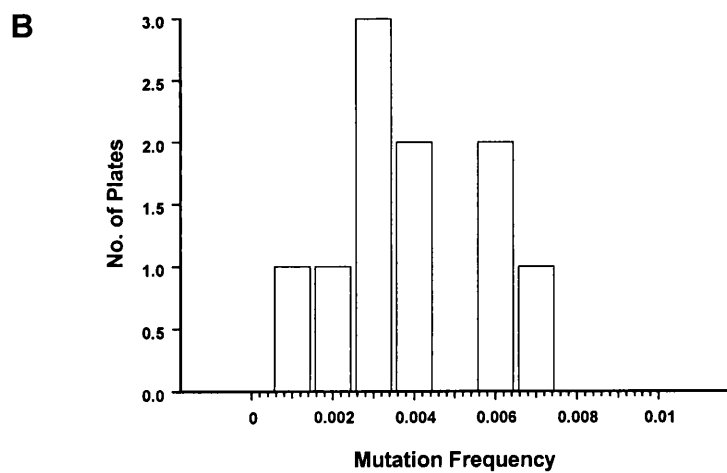
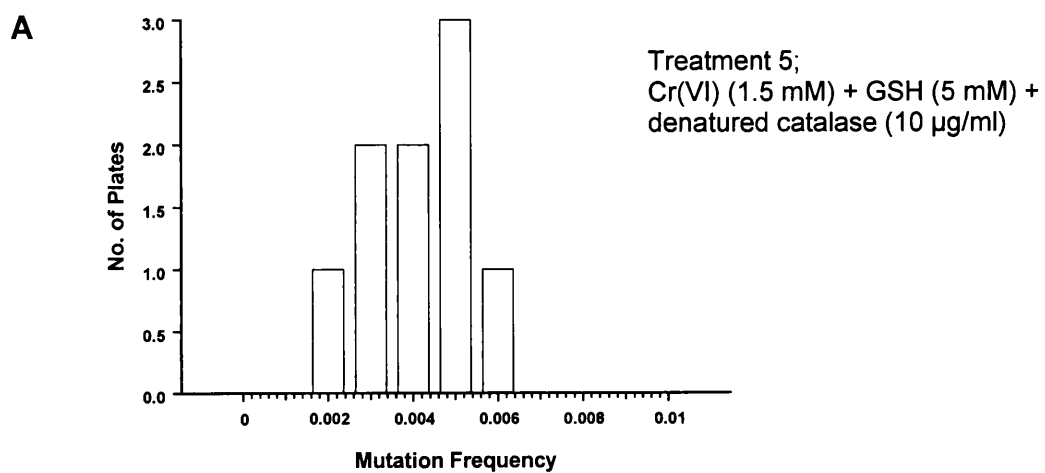
Treatment 3: Cr(VI)/GSH (1.5 mM/5 mM)

Treatment 4: Cr(VI)/GSH + catalase (1.5 mM/5 mM + 10 μg/ml)

Treatment 5: Cr(VI)/GSH + denatured catalase (1.5 mM/5 mM + 10 μg/ml)

Treatment 6: Cr(VI)/GSH (1.5 mM/20 mM)

Figure 4.2 (continued) Distribution of mutation frequency for six treatment groups (1-6) as a replicate series of three studies (A-C).



Key to Figure 4.2

Figures represent mutation frequencies for E. coli JM105 obtained from six different treatments (1-6) per study. Each study was repeated three times (A-C). Each treatment group consisted of a single aliquot of E. coli JM105 cells which was incubated under the required conditions then plated onto ten ampicillin-containing LB-plates. The individual bars of the histograms represent the mutation frequency obtained for a single plate in each treatment group.

Experimental conditions were as follows;

Treatment 1: None (5 mM GSH)

Treatment 2: Fe(II)/H₂O₂ (25 μM/100 μM)

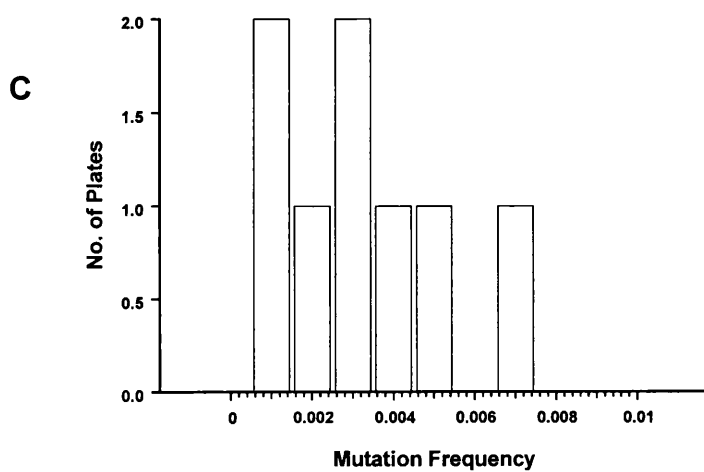
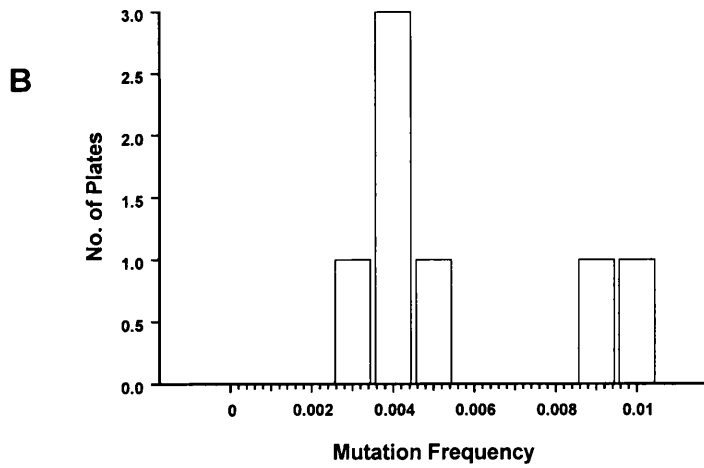
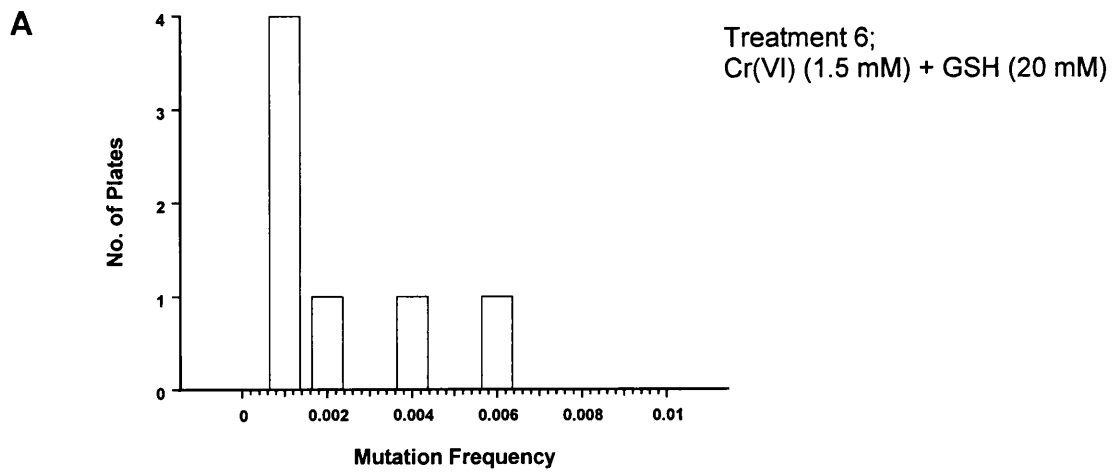
Treatment 3: Cr(VI)/GSH (1.5 mM/5 mM)

Treatment 4: Cr(VI)/GSH + catalase (1.5 mM/5 mM + 10 μg/ml)

Treatment 5: Cr(VI)/GSH + denatured catalase (1.5 mM/5 mM + 10 μg/ml)

Treatment 6: Cr(VI)/GSH (1.5 mM/20 mM)

Figure 4.2 (continued) Distribution of mutation frequency for six treatment groups (1-6) as a replicate series of three studies (A-C).



The distributions shown in Figure 4.2 clearly show a notable shift of frequency distribution towards higher mutation frequency between untreated and treated samples. Furthermore, it becomes apparent that there is no consistent pattern in distribution frequency: some appear normal while others are skewed. This lack of consistency makes statistical analysis very difficult. Another apparent feature of these figures is the variation within sample groups (as well as between them) which becomes more evident when the data are visualised as boxplots (Figure 4.3).

Given the uncertain nature of these findings it becomes necessary to apply a more sophisticated statistical analysis which will prove or disprove the hypothesis drawn from initial observations; that is, that the selection of reaction conditions under which no SSB are observed (inclusion of catalase, GSH>15 mM) has no influence on the level of mutated cells seen when both SSB and Cr-DNA adduct formation are apparent (the “null hypothesis”). Given the non-parametric nature of the data, the Mann-Whitney U-Test was felt to be an appropriate statistical analysis and the following treatment groups were compared for each study (results shown in Table 4.3);

Group 1 (negative control) against Group 3 (Cr(VI) + GSH)

Group 3 (Cr(VI) + GSH) against Group 4 (presence of catalase)

Group 3 (Cr(VI) + GSH) against Group 6 (Cr(VI) + GSH>15 mM)

Figure 4.3 Boxplots showing treatment groups 1-6 for replicate studies A-C. Boxes represent the lowest value, first quartile, median, third quartile and highest value. Means are represented by dots.

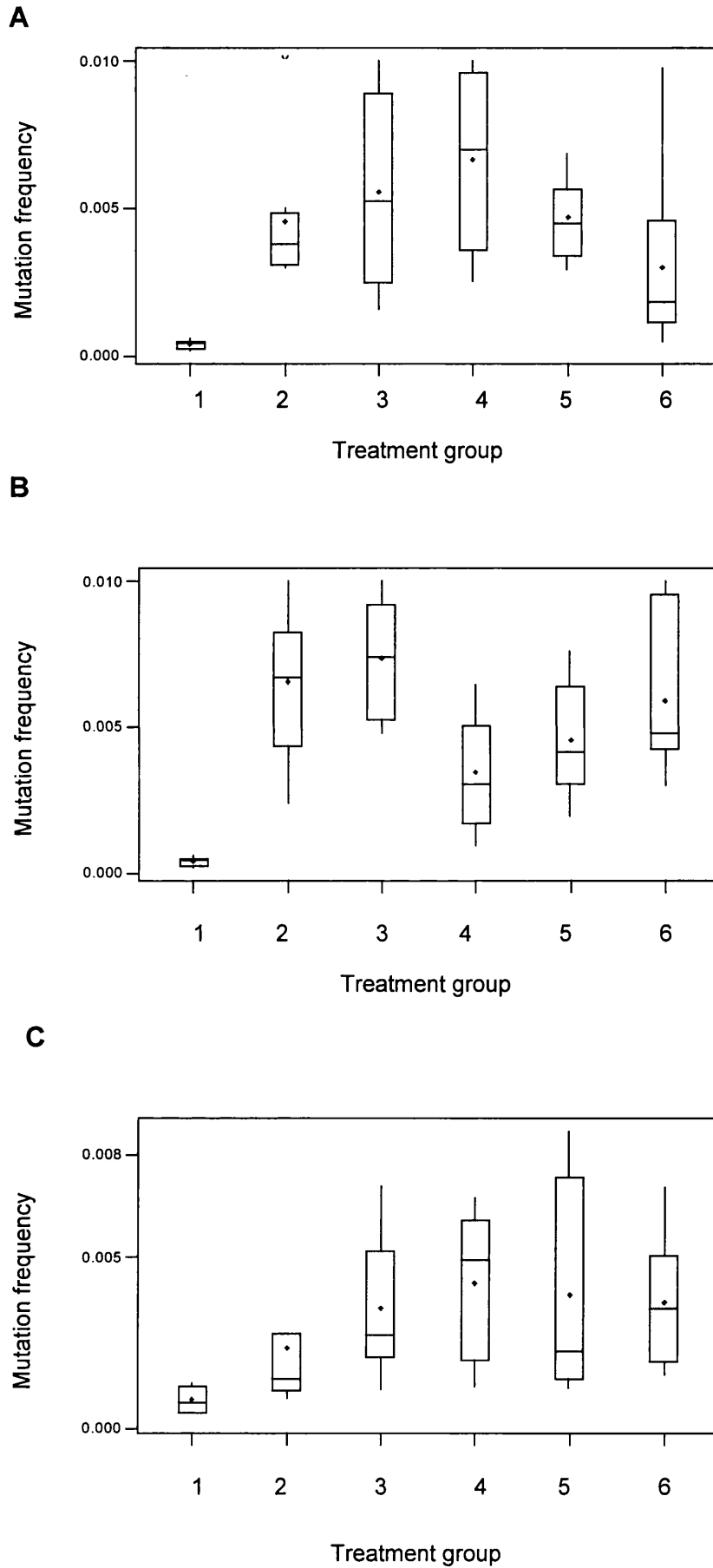


Table 4.2 Results from statistical analysis of mutation frequencies for replicate studies A-C. Data were analysed using the Mann Whitney U-Test. $p < 0.05$.

	A	B	C
Negative control vs. Cr treatment	Significant difference	Significant difference	Significant difference
Cr treatment vs. catalase	No significant difference	Significant difference*	No Significant difference
Cr treatment vs. 20 mM GSH	Significant difference at $p < 0.048^*$	No significant difference	No significant difference

The findings outlined in Table 4.2 clearly show that treatment of pUC19 with GSH and Cr(VI) leads to an increase in mutation frequency of transformed cells. There is also strong evidence to accept the null hypothesis that selection of reaction conditions where SSB are not induced has no effect on mutation frequency. Despite contrary findings in two of the analyses (one of which only demonstrated a marginal difference at $p < 0.048$) these observations strongly rule out any influence of active oxygen species in the mediation of mutagenic lesions during the reduction of Cr(VI) by GSH. They do, however, provide strong evidence for the role of Cr-DNA adducts in Cr-induced mutagenesis.

4.9 Discussion

The experiments described so far clearly demonstrate that the DNA lesions induced *in vitro* during the reductive conversion of Cr(VI) by GSH can be fixed into mutations during DNA replication. A non-lethal DNA lesion carried by pUC19 can be processed by bacterial enzyme systems and either be correctly repaired (see DNA repair mechanisms, this chapter) or converted into a stable mutation. The reductive metabolism of Cr(VI) to Cr(III) can cause several forms of DNA damage, resulting from either DNA adduction by Cr(III) or from oxidative damage by reactive intermediates. Exposure of cells to Cr(VI) results in binding of Cr(III) to DNA yielding binary Cr(III)-DNA adducts as well as various DNA crosslinks (Zhitkovitch *et. al.* 1995, Xu *et. al.* 1996). Several *in vitro* studies have also shown that Cr(VI) reduction can also lead to oxidative DNA lesions such as SSB and AP-sites (da Cruz Fresco and Kortenkamp 1994, Casadevall and Kortenkamp 1995, Sugiyama *et. al.* 1986). It still remains unclear, however, which type of lesion represents a potentially mutagenic form of DNA damage. Previous studies have identified the mutagenicity of oxidative damage such as AP-sites and SSB (Loeb *et. al.* 1986, Schaaper *et. al.* 1983, Kunkel *et. al.* 1981). Indeed, Kunkel (1984) demonstrated an approximate seven-fold increase in mutation frequency after transformation of *E. coli* with depurinated (acid-heat treated) single stranded M13mp2 viral DNA after induction of SOS repair by UV irradiation of cells. Furthermore, studies carried out in this laboratory (Kortenkamp *et. al.* 1996) have demonstrated an

increase in mutation frequency in E. Coli TGI after *in vitro* modification of pUC19 plasmid DNA with Cr(VI)/AsA; conditions well documented as causing SSB and AP-sites.

While the mutagenicity of oxidative forms of DNA damage has been established (Cabral-Neto *et. al.* 1994, Dar and Jorgensen 1995, Liu and Dixon 1996), the mutagenic potential of Cr(III)-mediated DNA adducts remains unclear. Comparison of mutational spectra induced by Cr(VI), hydrogen peroxide and X-rays in exon 3 of the hprt gene from human lymphoblastoid TK6 cells revealed little similarity between Cr(VI) and the oxygen radical-producing agents, pointing to the potential significance of non-oxidative mechanisms in Cr mutagenicity. Further evidence for the role of non-oxidative damage in Cr mutagenicity comes from studies where Zhitkovitch *et. al.* (1995) demonstrated the generation of stable amino acid/GSH complexes with DNA. After treatment of Chinese hamster ovary (CHO) cells with Cr(VI), amino acid/GSH-Cr(III)-DNA crosslinks were formed with the site of adduction being on the phosphate backbone of DNA. It was here for the first time that the mutagenicity of Cr-DNA adducts was reported. These ternary complexes have since been shown to be mutagenic with the Cr(III)-GSH adduct being the most potent (Zhitkovitch *et. al.* 1998). The results obtained using our Cr(VI)/GSH model would strongly suggest an influence of Cr-DNA adduct formation on Cr mediated mutagenesis since, even when experimental conditions were employed under which no oxidative

damage (AP-sites, SSB) was apparent, no significant change in mutation frequency was observed. In all samples, the elevated numbers of mutated cells ($Amp^r lacZ^-$) were similar to those seen when samples were treated with Fe(II)/ H_2O_2 .

Sources of variation in these results would stem mainly from the practical execution of the assay. The dilution of the cell suspension, inoculation and spreading of plates, and interpretation of subsequent colonies are all subject to human error. However, variations in the bacterial population (stage of growth phase, susceptibility to antibiotic treatment, ability to take up and incorporate the plasmid) may also contribute to experimental discrepancy.

CHAPTER 5

Cr Biomonitoring - A Review

5.1 Introduction

It has already been stressed that, with Cr compounds having been identified as hazardous in the workplace, one major research concern is currently to establish the relationship between exposure and cancer risk. Only then, and with a comprehensive knowledge of the mechanisms involved in Cr carcinogenicity, can safe levels of exposure be defined on a sound toxicological basis. This chapter presents a review of biomonitoring techniques which have been employed with such an aim in mind. Previous findings are discussed, and the suitability of various biomonitoring methods assessed in terms of their relevance and efficiency.

At this point it would be worthwhile to define some commonly used terms relevant to the monitoring of Cr exposure. That exposure to a carcinogen and/or its metabolites has occurred can be demonstrated by analysing its presence in body fluids. Such an approach will give a measure of the internalised carcinogen dose (*internal dose*) but provide no information about the potential cancer risk involved. For this reason it is more helpful to look at the levels of DNA damage in easily accessible tissues. The presence of damage such as SSB or DNA-adducts will give an indication of the *biologically effective dose* of a carcinogen. Similarly, detection of *early biological effects* such as

SCE's and gene mutations at known exposure levels will give a more relevant indication of likely cancer risks. Such markers are usually monitored in easily accessible nucleated cells such as lymphocytes. It should be stressed, however, that the evaluation of such genetic changes in these "surrogate" cells relies on the assumption that they accurately reflect the processes occurring in the target organ (in the case of Cr: the lung). Given the complex nature of the multi-stage model of carcinogenesis, whereby the mutational profile of cells may be dramatically altered by repair mechanisms and other subsequent genetic changes, it seems unlikely that this is the case. Indeed, many cell types show DNA damage and even cytogenetic effects as a result of interactions with carcinogenic chemicals yet never transform to cancer cells. Even greater difficulty is encountered when trying to monitor the processes giving rise to the proliferation and clonal expansion of initiated cells in specific tissues. In contrast, the genetic changes which have occurred in tumour cells are amenable to monitoring and are relatively well studied.

5.2 Monitoring Internal Exposure: Cr in Body Fluids

When attempting to demonstrate that Cr exposure has occurred, three methods are generally employed, namely the determination of Cr in red blood cells (erythrocytes), plasma, or urine. Erythrocytes provide a useful model since presence of Cr within the cytoplasm is diagnostic of exposure to Cr(VI). This is explained by the fact that Cr(III) compounds are unable to cross the cell membrane. Despite this selectivity, determination of Cr exposure by the monitoring of erythrocytes is not a particularly sensitive method. Indeed, Angerer *et al.* (1987) demonstrated that airborne levels of Cr(VI) of around 100 $\mu\text{g}/\text{m}^3$ remained undetected in up to 50 % of the steel workers examined (detection limit using atomic absorption spectroscopy was 0.6 $\mu\text{g Cr}/\text{l}$ hemolysate).

Far greater sensitivity is obtained when screening for Cr in plasma, with airborne levels of Cr(VI) at 100 $\mu\text{g}/\text{m}^3$ giving plasma concentrations of around 10 $\mu\text{g}/\text{l}$ (Angerer *et al.* 1987). Such sensitivity means that measurement of Cr in plasma is much more suitable to cover a wider range of exposure levels likely to be encountered occupational settings.

Similar sensitivity was achieved when Cr was investigated in urine, with airborne levels of 100 $\mu\text{g}/\text{m}^3$ Cr(VI) giving rise to urine levels of 40 $\mu\text{g}/\text{l}$. Indeed, the correlation between urinary and plasma Cr is good enough that one technique can be substituted for the other

(Angerer *et. al.* 1987, Strindsklev *et. al.* 1993). This, plus the fact that urine analysis is non-invasive explains why this is the most popular technique for the determination of internal exposure to Cr. Urine sampling is, however, susceptible to changes in renal function but these variations can be corrected for by relating urinary Cr concentrations to the amount of creatinine present in the urine (Araki and Aono 1989). Several authors have demonstrated the influence of other external factors on urinary Cr. Notably, Cr levels were seen to be two to three times higher in smokers than in non-smokers (Kalliomaki *et. al.* 1981, Strindsklev *et. al.* 1993). Similarly, lack of exercise, beer drinking and diabetes have all been shown to contribute to elevated urinary Cr levels (Bukowski *et. al.* 1991).

It is therefore apparent that urinary Cr is a reliable marker of internal Cr exposure, allowing detection at exposure levels well below the occupational limits in a number of industrialised countries. Table 5.1 summarises the urinary Cr levels observed in selected studies of occupationally exposed and non-exposed individuals.

Table 5.1 Urinary Cr levels among occupationally exposed and non-exposed individuals.

Mean airborne Cr(VI) ($\mu\text{g}/\text{m}^3$)	Group	Mean urinary Cr ($\mu\text{g}/\text{g}$ creatinine)	Reference
13.8	SS, smokers	14.2	Strindsklev (1993)
13.5	SS, non-smokers	5.3	
na	SS, smokers	16.0	Kalliomaki (1981)
na	SS, non-smokers	8.7	
1-55	Cr(VI) production	6.0	Gao (1994)
0	Non-exposed	0.76	
0	Diabetics	1.38	Bukowski (1991)
	Referents	0.58	
0	Beer drinkers	0.67	
	Referents	0.49	

na: not analysed, SS: stainless steel welders (MMA)

5.3 Effect Monitoring: Cytogenetic Surveillance Studies in Lymphocytes

A number of studies have demonstrated increased frequencies of chromosome aberrations and SCE's in the lymphocytes of workers involved in Cr(VI) production or Cr plating (Bigaliev *et. al.* 1977, Stella *et. al.* 1982). Unfortunately, such studies did not provide any information concerning the levels of internal or external exposure to Cr. However, more recent studies have taken such parameters into account, thereby allowing the evaluation of the relative sensitivity of markers of early biological effects and of markers of internal exposure in a variety of occupational settings.

Cr Platers and Ferrochromium Steel Production Workers

During both these industrial processes, workers are exposed to Cr(VI) trioxide either in the form of mists generated during the plating process, or as fumes released during the electrothermal reduction of chromite ore. Studies aiming to demonstrate elevated levels of chromosome aberrations and SCE's in workers from these two groups have been inconclusive, although exposure to Cr was readily detected as elevated urinary Cr. Sarto *et. al.* (1982) have shown increased frequency of SCE's in hard platers but these changes only remained apparent in younger workers with high internal exposure to Cr when the data were analysed by age. A significant increase in the number of chromosome aberrations was also seen but this correlated poorly with urinary Cr levels. Elevated SCE frequencies were also demonstrated in Cr surface treatment workers (Choi *et. al.* 1987) however, the same level of observed SCE in exposed workers has frequently been quoted for unexposed controls in other studies. For example, Ashby and Richardson (1985) give a mean value of SCE's in control populations of 47 cytogenetic studies as 8.12 ± 1.82 per cell. This is clearly well above the 6.9 ± 1.8 observed among platers in Choi's study, or 3.6 ± 1.5 among controls. Table 5.2 shows the findings from a series of cytogenetic studies. In most cases urinary Cr was chosen as the marker of internal exposure despite there being no standardisation of Cr levels in the literature. Cr is expressed in relation to urinary Cr/l urine assuming a 1.5 mg creatinine/l urine conversion where necessary.

Study population	Level and duration of exposure	Chromosome aberrations			SCE±sd/ cell	Internal exposure (urinary Cr µg/g creatinine)	Study conclusion	Reference
		Group	N	Ab+gaps (%)				
Platers (hard)	Na, 6 yrs	Exp	21	2.8	8.1±2.7 6.6±0.8	7-11 2	positive	Sarto, 1982
		EC	35	1.7				
Platers	Na, 0.5-3 yrs	Exp	24	Na	9.0±1.0 8.9±1.2	8.7±11.1	negative	Nagaya, 1986
		MC	24	Na				
Platers	27 µg/m ³ 8 µg/m ³ 0 µg/m ³	Exp 1	7	Na	6.9±1.8 5.4±2.1 3.6±1.5	16.0±5.2 10.1±5.9 Na	positive	Choi, 1987
		Exp 2	25	Na				
		MC	15	Na				
Ferro- chromium	Na	Exp MC	14 14	4.29 2.81	Na	Na	negative	Sbrana, 1990
Platers (hard)	Na	Exp	12	4.29	7.8±1.4	17.9±12.6	negative	Nagaya, 1991

Abbreviations: N, number of subjects; Ab, aberrations; Na, not analysed; sd, standard deviation; Exp, exposed; EC, external controls; MC, matched controls

Table 5.2 Cytogenetic surveillance studies among Cr platers and ferroCr workers

Stainless Steel Welders Using the Manual Metal Arc Method

Three methods of stainless steel welding are generally used industrially. Metal Inert Gas (MIG) and Tungsten Inert Gas (TIG) welding, as their names suggest, involve the use of inert gases to prevent metallic Cr being oxidised to Cr(VI) in the vicinity of the electrodes. During Manual Metal Arc (MMA) welding, however, this oxidation does occur and is rapidly followed by reaction of Cr(VI) with alkali oxides from the electrode coating giving rise to the formation of sparingly or readily water soluble alkali chromates including potassium chromate and calcium chromate. Consequently MMA welding produces fumes containing the highest levels of Cr with the total fume concentration in the breathing zone being as high as 100 mg/m^3 , with Cr(VI) contributing up to 4 mg/m^3 in extreme cases (Kalliomaki *et. al.* 1981).

Table 5.3 highlights some of the results from cytogenetic studies among MMA welders. As with studies performed in Cr platers, urinary Cr levels proved to be a reliable marker of internal exposure to Cr(VI) even at relatively low airborne levels. However, the frequency of SCE's was apparently insensitive to Cr exposure with elevated levels only being seen by Koshi *et. al.* (1984) and even then the results obtained were from the pooling of data from three separate studies. Conversely, all the studies carried out after 1990 showed SCE's to be slightly lower in MMA welders, an observation which is apparently masked by smoking (Husgafvel-Purisainen *et. al.* 1982) but is marked

Study population	Level and duration of exposure	Chromosome aberrations			SCE±sd/ ceii	Internal exposure (urinary Cr µg/g creatinine)	Study conclusion	Reference
		Group	N	Ab+gaps (%)				
SS, MMA	55 µg/m ³ , 19 yrs	Exp	24	4.1	11.0	20.8	negative	Littorin, 1983
		EC	24	4.6	12.0			
SS, MMA	Na	Exp, s	9	3.1	10.8±0.6	6.7-51	negative	Husgafvel, 1982
		MC, s	10	1.9	10.5±0.3	Na		
		Exp, ns	12	1.7	8.2±0.2	6.7-51		
		MC, ns	9	2.4	8.9±0.4	Na		
SS, MMA and MIG	Na	Exp	97	4.7*	8.8±1.61*	6.5±6.1	positive	Koshi, 1984
	Na	IC	33	3.2	8.11±1.08	2.73±0.8		

Abbreviations: N, number of subjects; Ab, aberrations; Na, not analysed; sd, standard deviation; Exp, exposed; EC, external controls; MC, matched controls; IC, internal controls; SS, stainless steel welders; MMA, manual metal arc method; MIG, metal inert gas method; s, smokers; ns, non-smokers; * statistically significant differences.

Table 5.3 Cytogenetic surveillance studies among stainless steel welders using the manual metal arc method

Study population	Level and duration of exposure	Chromosome aberrations			SCE±sd/ ceil	Internal exposure (urinary Cr µg/g creatinine)	Study conclusion	Reference
		Group	N	Ab+gaps (%)				
SS, MMA and MIG	Na, 8 yrs	Exp, s	17	Na	6.61±1.46	18.9±13.2	Negative	Popp, 1991
		IC, s	7	Na	7.34±1.53			
		Exp, ns	22	Na	5.93±0.83	18.9±13.2		
		IC, ns	11	Na	6.57±0.81	Na		
SS, MMA and TIG	4.9±11.8 µg/m ³	Exp, s	32	2.25±1.75	7.7±1.1	2.08±2.1	Positive for Ab in ns, negative for SCE	Knudsen, 1992
		MC, s	50	1.85±1.43	8.1±1.4	0.35±0.35		
		Exp, ns	28	2.38±2.18*	6.7±1.0	2.08±2.1		
		MC, ns	25	1.10±1.25	7.4±1.0	0.35±0.35		

Abbreviations: N, number of subjects; Ab, aberrations; Na, not analysed; sd, standard deviation; Exp, exposed; EC, external controls; MC, matched controls; IC, internal controls; SS, stainless steel welders; MMA, manual metal arc method; MIG, metal inert gas method; s, smokers; ns, non-smokers; * statistically significant differences.

Table 5.3 (continued) Cytogenetic surveillance studies among stainless steel welders using the manual metal arc method

Study population	Level and duration of exposure	Chromosome aberrations			SCE±sd/ cell	internal exposure (urinary Cr µg/g creatinine)	Study conclusion	Reference
		Group	N	CB (%)				
SS, MMA	34.7 µg/m ³ , range 0.6- 252 µg/m ³ , 0-20 yrs	Exp, s	22	1.4	6.4	11.1	Positive for chromatid breaks in ns, negative for SCE	Jelmert, 1994
		MC, s	20	1.1	6.6	Na		
		EC, s	46	0.9	6.9	Na		
		Exp, ns	20	1.5*	5.8	11.1		
		MC, ns	20	0.7	5.5	Na		
		EC, ns	48	0.7	5.7	Na		

Abbreviations: N, number of subjects; Ab, aberrations; Na, not analysed; sd, standard deviation; Exp, exposed; EC, external controls; MC, matched controls; IC, internal controls; SS, stainless steel welders; MMA, manual metal arc method; MIG, metal inert gas method; s, smokers; ns, non-smokers; CB, chromatid break; * statistically significant differences.

Table 5.3 (continued) Cytogenetic surveillance studies among stainless steel welders using the manual metal arc method

in non-smokers. A similar study by Popp *et. al.* (1991) confirms this effect even in smokers.

In studies concerned with the influence of Cr exposure on levels of chromosome aberrations, elevated frequencies of these types of damage were observed in three independent studies (Koshi *et. al.* 1984, Knudsen *et. al.* 1992, Jelmert *et. al.* 1994). Studies by Husgafvel-Purisainen *et. al.* (1982) and Littorin *et. al.* (1983) failed to demonstrate such an influence but this is probably due to the relatively small population studied, since small differences in effect require larger sample sizes to demonstrate statistical significance. Rare aberrations such as dicentric chromosomes, translocations, minutes and rings were seen to be increased in two studies (Koshi *et. al.* 1984, Knudsen *et. al.* 1992). In the study by Knudsen these changes were seen only in non-smokers, a trend which was repeated in the study by Jelmert *et. al.* (1994) who showed an increase in chromatid breaks in non-smokers. Clearly, these effects would have been masked had the studies not been stratified according to smoking status.

While these studies provide apparent evidence for genotoxic effects in stainless steel welders using MMA, it should be noted that the frequencies of aberrations in these populations are similar to those of unexposed controls in other studies. For example, Ashby and Richardson (1985) quote a mean value of $1.42 \pm 0.96\%$ for the

percentage of aberrant cells excluding gaps, across the control groups from 60 studies. Given the strong genotoxicity of Cr(VI) compounds, it is surprising that cytogenetic surveillance studies do not demonstrate more pronounced results. It is possible that the effects seen at such exposure levels are too slight to be apparent in small sample groups (less than 60) or that, as a surrogate tissue for the monitoring of such effects, lymphocytes do not represent an appropriate model.

5.4 Monitoring Early Biological Effects: DNA Damage in Lymphocytes

As previous studies have demonstrated, cytogenetic markers such as SCE's or chromosome aberrations respond weakly to Cr(VI) exposure. Therefore it becomes necessary to analyse the effects of such exposure at a molecular level; in other words, levels of DNA damage need to be assessed. Table 5.4 summarises the results of such studies in workers from the stainless steel welding, Cr plating, and Cr(VI) production industries. As part of a study to investigate cytogenetic markers after Cr(VI) exposure, Popp *et. al.* (1991) also analysed DNA from stainless steel welders using filter elution techniques. Samples of DNA from exposed subjects were shown to have reduced elution rates compared with non-exposed; an effect that was felt to be due to the formation of DNA-protein crosslinks (DPC), since this type of DNA damage is known to occur *in vitro* (Zhitkovitch *et. al.* 1996).

Study population	Level and duration of exposure	DNA damage				Internal exposure	Study conclusion	Reference
		Group	N	Type of damage	Level of damage			
SS, MMA And MIG	Na, 8 y	Exp	39	DPC	0.78*	U 18.9±13.2 µg/g crea Na	Positive	Popp, 1991
		IC	18	DPC	0.89*			
Cr(VI) production workers	1-55 µg/m ³ 15 y	Exp	10	SSB 8-OHdG	59% breaks 0.037 8-OhdG/dG	U 5.97 µg/g crea P 2.8 µg/l WB 5.5 µg/l L 1.01 µg/10 ¹⁰ cells	negative	Gao, 1994
		IC	10	SSB 8-OHdG	50% breaks 0.041 8-OhdG/dG			

Abbreviations: N, number of subjects; Na, not analysed. Exp, exposed; IC, internal controls; EC, external controls; DPC, DNA-protein cross-links; U, urinary Cr; P, plasma Cr; WB, Cr in whole blood; L, Cr in lymphocytes; crea, creatinine; SSB, DNA single strand breaks; 8-OhdG, 8-hydroxydeoxyguanosine; dG, deoxyguanosine; * flow rates of DNA through membrane filters – low rate indicative of DPC.

Table 5.4 DNA damage in blood lymphocytes of Cr-exposed workers

Chromium carcinogenesis: Mechanisms and biomonitoring

Study population	Level and duration of exposure	DNA damage				Internal exposure	Study conclusion	Reference
		Group	N	Type of damage	Level of damage			
Platers	0.5-130 µg/m ³	Exp	14	DPC (%)	1.53±0.33	U 9 µg/g crea Ery 22.8 µg/l L 1.16 µg/10 ¹⁰ cells	negative	Zhitkovitch, 1996
				8-OHdG	1.45±0.43	U 1.0 µg/g crea Ery 2.5 µg/l L 0.64 µg/10 ¹⁰ cells		

Abbreviations: N, number of subjects; Na, not analysed. Exp, exposed; IC, internal controls; EC, external controls; DPC, DNA-protein cross-links; U, urinary Cr; P, plasma Cr; WB, Cr in whole blood; L, Cr in lymphocytes; Ery, Cr in erythrocytes; crea, creatinine; SSB, DNA single strand breaks; 8-OHdG, 8-hydroxydeoxyguanosine; dG, deoxyguanosine.

Table 5.4 (continued) DNA damage in blood lymphocytes of Cr-exposed workers

Use of a more sophisticated potassium-SDS precipitation assay has provided more direct evidence for the existence of DPC, and has also enabled the quantification of this type of DNA damage in *ex vivo* isolated DNA (Zhitkovitch *et. al.* 1996). In a study on Bulgarian Cr platers however, Zhitkovitch failed to observe any significant increase in DPC in the DNA of blood lymphocytes, compared to controls, despite elevated Cr levels in erythrocytes and urine. Similarly, studies by Gao *et. al.* (1994), in which DNA damage was assessed in terms of SSB and modified bases such as 8-OH deoxyguanosine, were unable to demonstrate increased levels of oxidative damage in Cr(VI) production workers. In both studies, such findings were based on the levels of Cr in lymphocytes, despite there being very little difference in these levels between exposed and control subjects compared to all other markers of exposure. It is perhaps striking that in one group of exposed individuals, lymphocyte Cr levels were approximately double that of unexposed samples, yet erythrocyte levels of Cr in the same group were 7-9 times higher than control. However, when considered in terms of amount of Cr per cell, lymphocytes contained levels of Cr approximately two orders of magnitude higher than erythrocytes in both exposed and control groups. (1.01 $\mu\text{g}/10^{10}$ lymphocytes vs. 0.01 $\mu\text{g}/10^{10}$ erythrocytes in exposed, 0.76 $\mu\text{g}/10^{10}$ lymphocytes vs. 0.002 $\mu\text{g}/10^{10}$ erythrocytes in unexposed).

It could be argued that these differences in cellular Cr levels are due to a more efficient uptake system for Cr(VI) in lymphocytes. Indeed,

Coogan *et. al.* (1991) have demonstrated that human leucocytes can take up Cr(VI) at a rate approximately three times that of erythrocytes *in vitro*. While this does not account for a one hundred-fold difference in cellular Cr levels it should be pointed out that such experiments were carried out using a single, relatively high concentration of 50 μM Cr(VI) and that it is quite conceivable for uptake rates to change at different Cr(VI) concentrations. Such variation in uptake rates has been demonstrated in erythrocytes (Buttner and Beyersmann, 1985) where low uptake rates were seen at concentrations of 1-10 μM Cr(VI) and higher rates in the range of 50-100 μM Cr(VI). Higher levels of Cr(VI) may also be due to the age of the cells in question; lymphocytes have a lifespan in the body of years compared to only months for erythrocytes. However, these factors still do not explain the apparent similarity between Cr levels in exposed and control groups in the studies by Gao and Zhitkovitch. For this reason, lymphocytes may not be an appropriate surrogate tissue for the effect monitoring of exposed individuals.

5.5 Cr levels in the lung

Upon inhalation, Cr particles remain in the lung for very long periods of time with only a small fraction of the total ingested dose being distributed throughout the body. Even long after the cessation of exposure, most of the Cr is found in the respiratory tract (Hyodo *et. al.* 1980, Tsuneta *et. al.* 1980). Post-mortem analysis of tissues obtained from cancer patients with a history of employment in Cr(VI) production show the amounts of Cr in the lung to be approximately 30-70 mg compared to 0.08-1.2 mg in subjects with no history of Cr(VI) exposure. However, amounts of Cr in the livers of the same subjects were found to be 3.8 mg (compared with 0.3 mg in control) whilst kidney amounts of Cr in exposed samples were 0.8 mg (as opposed to 0.07 mg in unexposed) (Kishi *et. al.* 1987). Similarly, the lungs of stainless steel welders were shown to contain up to 30 times more Cr than those of unexposed individuals (Raithel *et. al.* 1993), data which agree well with the studies by Kishi (1987). These and other findings are summarised in Table 5.5. When obtaining samples of lung for analysis it should be remembered that the distribution of Cr varies throughout the organ, with highest levels of particulate being found in the upper respiratory tract.

Table 5.5 Cr levels in the lungs of occupationally exposed and non-exposed individuals

Study population	Cr in lungs ($\mu\text{g/g}$ dry weight)	Reference
Cr(VI) production: Case 1	397	Kishi, 1987
Case 2	1467	
SS welders	30-86	Raithel, 1993
Referents	0.31	Kishi, 1987
Referents	1.37	Raithel, 1993
Referents, smokers	4.3	Pääkö, 1989
Referents, ex-smokers	4.8	
Referents, non-smokers	1.3	

Other factors have been demonstrated as influencing Cr levels in unexposed individuals. Kollmeier *et. al.* (1990) observed an age-dependent increase in lung Cr levels and found that men, on average, showed levels twice as high as women. Differences were also demonstrable as a result of environment; for example, lung Cr levels of individuals living in a heavily industrialised area (Ruhr region, Germany) were significantly higher than those people living in a city dominated by trade and commerce (Münster). Such slight variations are, as yet, undetectable using any of the currently employed markers of internal Cr dose. Direct monitoring of the lungs would be the most ideal solution, however, lung tissue is not readily available for biomonitoring.

Since the subsequent toxicokinetics of Cr after deposition in the lung apparently compromise the usefulness of lymphocytes as a surrogate tissue, the question arises as to just how and where lymphocytes come into contact with Cr. Two possibilities can be envisaged; firstly, lymphocytes, while travelling through the blood, take up Cr(VI) that has leached from the lungs. Alternatively, lymphocytes homing to the lungs come into contact with Cr particles in the respiratory tract and then migrate back to the systemic circulation.

5.6 Lymphocytes and Cr Uptake

Lymphocytes continuously enter and leave lymphoid and non-lymphoid tissue via the blood. At any given time approximately 2% of the total lymphocyte pool will be present in the systemic circulation where they will remain for approximately 30 minutes. It is estimated that within a 24 hour period 5×10^{11} lymphocytes travel through the blood, a number equivalent to the total lymphocyte population (Westermann and Pabst 1990). It is unlikely, therefore, that the small compartment of systemic lymphocytes at any given time are representative of the total population. Lymphocytes are produced in a variety of organs and are constantly released to the blood. They can migrate through many of the organs of the body and are then able to return to the blood. One established pathway of recirculation from organs to the blood is via the lymph nodes and thoracic duct,

accounting for approximately 5 - 10% of the lymphocyte population which returns to the blood each day (Westermann and Pabst 1990). The spleen is by far the most important organ in lymphocyte recirculation, with 50% of all recirculated lymphocytes being released by this organ (Westermann and Pabst 1990). In comparison, the number of lymphocytes that migrate from the lungs back to the blood is negligible.

With this in mind, only a small fraction of lymphocytes in the systemic circulation will have had the opportunity to take up Cr(VI) while travelling through the lung. The vast majority of these cells will have come into contact with Cr(VI) during their migration through the blood. This short transit time through the systemic circulation is likely to be a complicating factor in the uptake of Cr(VI) by lymphocytes (as opposed to erythrocytes) and may help explain the observations concerning lymphocyte Cr levels discussed previously (Gao *et. al.* 1994, Zhitkovitch *et. al.* 1996).

5.7 Summary

In studies where the lymphocytes of exposed workers were investigated for early biological effects, the results were somewhat inconclusive (Popp *et. al.* 1991, Gao *et. al.* 1994, Zhitkovitch *et. al.* 1996), a surprising observation considering the enormous genotoxic potential of Cr(VI). However, this may be explained by the relatively small differences in Cr concentration between the lymphocytes of exposed and control groups. The toxicokinetics of inhaled Cr(VI) and the dynamics of lymphocyte traffic further complicate matters. After ingestion, only a small fraction of the total inhaled dose is distributed in the body, while the bulk remains in the lung for very long periods of time. Given that the daily recirculation of lymphocytes from the lungs back to the blood is negligible compared to recirculation from such organs as the spleen, it seems more likely that circulating lymphocytes (those under investigation for biological effects) are exposed to Cr from the blood and therefore do not reflect processes occurring in the lung. This would explain the similarities in lymphocyte Cr concentration seen in exposed and control subjects. These findings, taken on their own, would suggest that lymphocytes do not represent an appropriate model for the biomonitoring of exposed individuals. However, it should be stated that in all these studies, workers were exposed to Cr levels below $50 \mu\text{m}^3$, the current exposure limit in many industrialised countries. Whilst at higher exposure levels, lymphocytes may well

provide a useful model for the effect monitoring of Cr exposure, the need for alternative techniques is still apparent. Ideally, a non-invasive method enabling the direct examination of Cr in the lung should be developed, and to this end the application of magnetic resonance imaging (MRI) is suggested and explored.

CHAPTER 6

Magnetic Resonance Imaging (MRI) as a Technique for Cr Biomonitoring

6.1 Nuclear Magnetic Resonance (NMR)

As its name suggests, the fundamental phenomenon of nuclear magnetic resonance arises from the spin of those atomic *nuclei* which possess it (all those containing uneven numbers of protons and/or neutrons), the *magnetic* properties inherent in such nuclei as a result of their spin and positive charge, and the *resonant* frequencies which can be detected when such nuclei are excited and allowed to relax. NMR was first demonstrated independently by Bloch (1946), and Purcell *et. al.* (1946) who were concerned with the existence of magnetic resonance and relaxation phenomena. The first uses of *Electron Spin Resonance (ESR)* and NMR to investigate cellular systems took place in the 1950's, whilst by the 1970's applications of NMR to animal organs yielded important advances in our knowledge of biochemical and physiological processes as they occur in intact tissues (Moon and Richards 1973, Ackerman *et. al.* 1980).

The two major applications of nuclear magnetic resonance phenomena are *Nuclear Magnetic Resonance Spectroscopy (NMRS)* which allows the non-invasive chemical analysis of tissues, notably in assessing the condition of the brain. A second important technique which is directly

relevant to this thesis is *Nuclear Magnetic Resonance Imaging (NMRI)* which enables high quality images of sections in any area of the body to be produced. It is worth noting that, for historical and clinical purposes, use of the word "nuclear" is generally avoided and as such *NMRS* and *NMRI* will be referred to simply as *Magnetic Resonance Spectroscopy (MRS)* and *Magnetic Resonance Imaging (MRI)* throughout this thesis.

The ability to produce tomographic (that is, a picture or drawing of a slice) images using MRI has only been available for a relatively short time. It was not until the late seventies that the first images of the human brain were produced (Moore and Holland 1980) whilst images of the human thorax and abdomen were not generated until 1981 (Edelstein *et al.* 1981). Since such times, advances in understanding of the technique, and in the technology made available, have meant that MRI has forged for itself a position as a new imaging technique as opposed to merely being an adjunct for other more established methods such as X-ray imaging, and has applications in all regions of the body.

6.2 Principle of MRS and MRI

The basic principle of MRS relies on the interaction of certain nuclei with a pulse of radiofrequency within a strong magnetic field. Electrons, protons and certain nuclei (e.g. ^{31}P) possess the property of spin and all charged particles with spin possess a magnetic moment. If the particle is

placed in an external magnetic field it will act like a bar magnet and align itself with that external field. Normally the bar magnet will align itself so that its north pole faces the south pole of the external magnet - a low energy state. However, it is possible to place the bar magnet so that its north pole faces the north pole of the external magnet - a high energy state. In this state there is no lateral force so it cannot move out of this alignment. Given the smallest perturbation, however, it will flip round to the north-south orientation and it would be possible to recover energy from the system during this flip. North-north is, therefore, a high energy state similar to the excited state in MRS. In most forms of absorption spectroscopy the sample is directly responsive to the absorption of the incident energy but in MRS an artificial state has to be produced before a split in energy levels can be observed and into which energy can be absorbed. In a sample which is not exposed to an external magnetic field the magnetic moments of the nuclei will be randomly oriented (Figure 6.1). It is only when an external field is applied that they orient themselves into specific directions and hence into different populations with different energy levels. As would be expected, the majority of nuclei will enter the low energy state whilst a minority will orient themselves in a high energy state. The proportion of nuclei in each state will be influenced by the temperature of the sample and the energy difference between states.

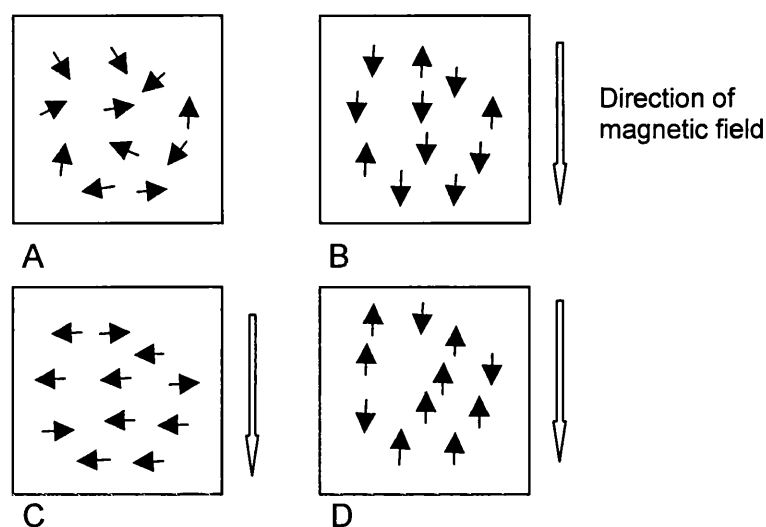


Figure 6.1. Orientation of nuclei during MRS
 A - Nuclei randomly orientated
 B - Nuclei align under influence of magnetic field
 C - 90° pulse at Larmor frequency
 D - 180° pulse; Larmor frequency at 2x duration/amplitude

To induce a change in the orientation of the magnetic moment of the spin system after application of the external magnetic field it is necessary to either donate (low to high energy transition) or remove (high to low energy transition) energy via an electromagnetic (EM) pulse of a particular frequency. This *frequency of precession* or *Larmor frequency* is dependent on both the value of the magnetic moment of the spin particle and the strength of the applied magnetic field. Application of such a pulse will cause the nuclei to reorient themselves within the external magnetic field at 90° or 180° (pulse of twice the duration or amplitude) to their original position. On cessation of EM irradiation the spin population relaxes back to ground state by a combination of two processes; loss of

energy as heat into the immediate environment (spin-lattice relaxation) and a loss of spin orientation with respect to the direction of the applied magnetic field (spin-spin relaxation). If the spin system is considered in three dimensions with z being the axis of the main field and x and y the orthogonal axes then it becomes clear that in the absence of applied EM radiation there is no net magnetic moment (M) in the x and y directions ($M_x = M_y = 0$). The difference between high energy and low energy state nuclei gives a net magnetic moment in the z direction (M_z); the equilibrium state. If EM radiation is then applied at the Larmor frequency, the spin populations begin to angle out from the z axis until they align with the x and y axes (i.e. at 90°) to their original position. As this occurs, $M_{x,y}$ increases as M_z decreases to zero ($M_{x,y} = M_z$). If the EM pulse is maintained (to 180°), the spin population is sent into complete reversal from the equilibrium state i.e. $M_{x,y} = 0$ and M_z has the same value but with a reversed sign. As the EM pulse decays, the spins can relax directly along the z axis, giving no increase in $M_{x,y}$. This longitudinal relaxation process involves a direct loss of energy from the spin system to the surrounding molecular structure i.e. spin-lattice relaxation. Such decay follows exponential kinetics, the time constant of which is referred to as T_1 .

Relaxation after applying a 90° pulse is more complex because it involves not only a transverse relaxation associated with spin-lattice

relaxation but also a loss of energy directly from the $M_{x,y}$ component. As the spin population orients itself along x,y as a result of EM radiation there is randomisation of the spin orientation with respect to the external magnetic field. Interaction between the spins at this stage may result in the loss of energy as spin-spin relaxation and the generation of an electromagnetic force (EMF) which can be detected in a localised coil (the *resonance signal or resonance spectrum*). This signal is a sine-wave and its decay constant is referred to as T_2 . Since T_1 is also associated with energy loss from the spin system via spin-lattice relaxation, and can therefore indirectly influence the T_2 signal, then both T_1 and T_2 are inherent constants of a spin system and are responsible for the resonance spectra recorded during MRS. Figure 6.2 shows a coil into which the sample is placed before being introduced into the superconducting magnet (Figure 6.3) required to generate a sufficient external field.

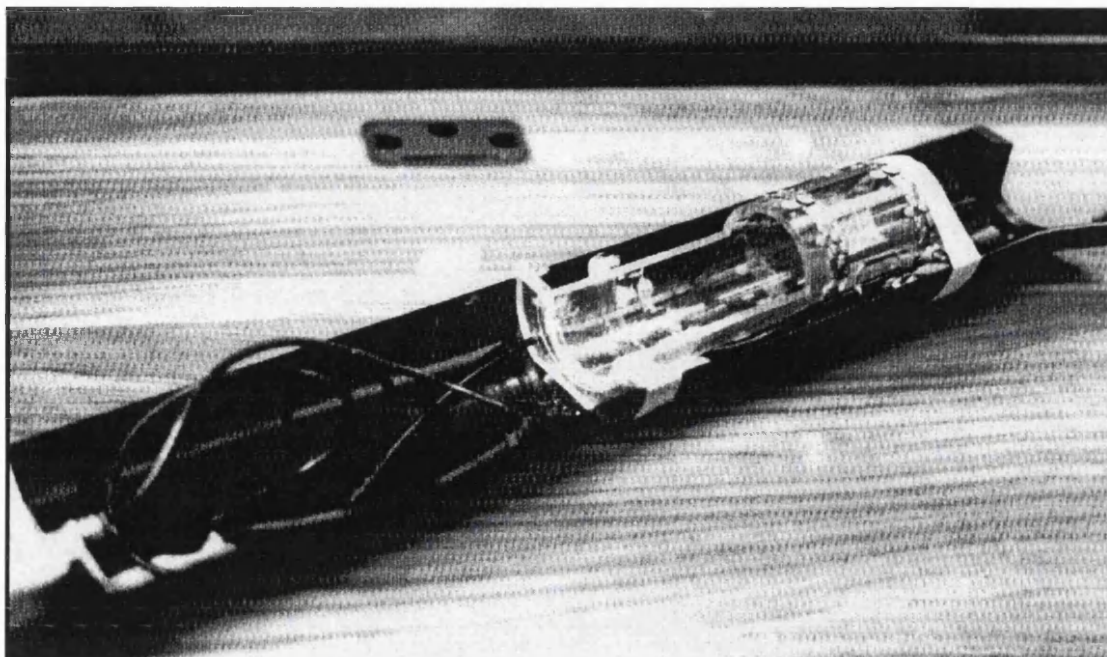


Figure 6.2. "Birdcage" coil into which sample is placed

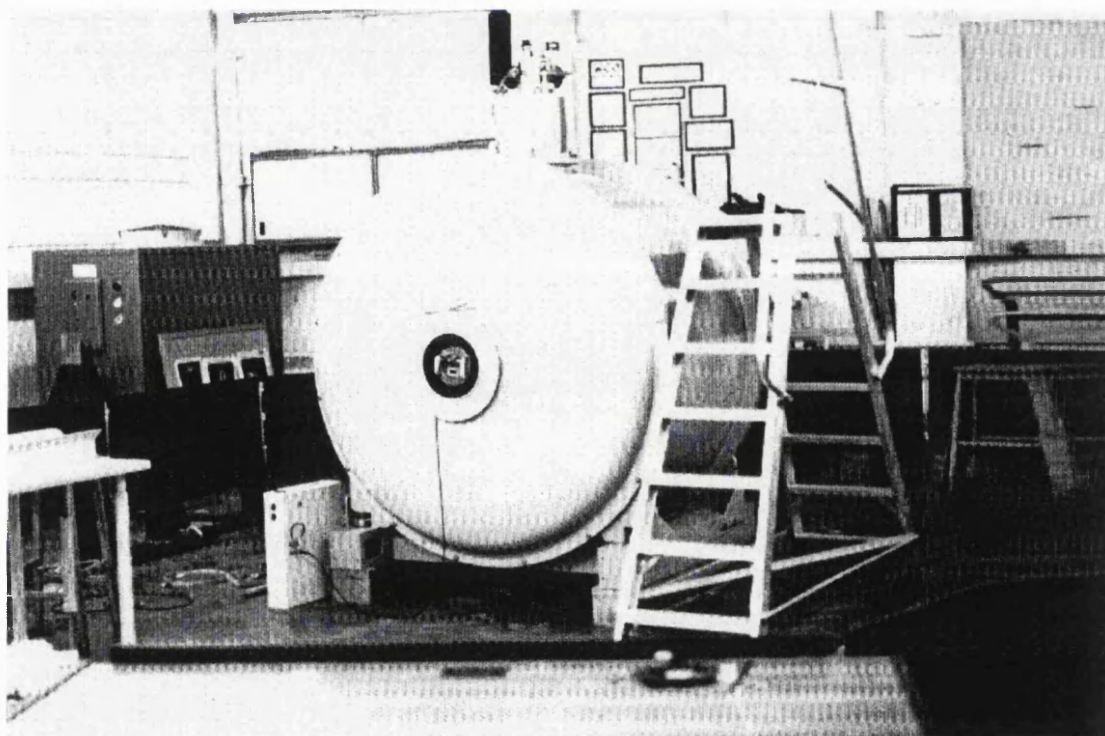


Figure 6.3. Superconducting magnet

It should be noted that during MRS, these phenomena take place in an external magnetic field of constant gradient. Under such conditions, the resonance signal obtained for a particular nucleus is uniquely determined by the nature of the nucleus under investigation and its chemical environment. The situation with MRI is slightly different since resonance spectra are generated in the presence of two or more magnetic gradients. In this instance the signal obtained for a particular nucleus is dependent not only on the nucleus in question and its chemical environment, but on the spatial position of the spins. This enables a two-dimensional image of a "slice" (tomograph) through a tissue to be generated.

6.3 Reproducibility of Magnetic Resonance Images

6.3.1 Magnetic Field Homogeneity

Many internal and external factors can influence the quality and reproducibility of the images generated during MRI. For example, the resolution of the resulting image is greatly dependent on the homogeneity of the magnetic field in the region under investigation (the *sensitive region*). Even small variations in the field strength in this region will yield broad lines in the resulting spectra which can distort fine structures in the final image. Since, under experimentally ideal conditions, the region of magnetic homogeneity should be quite small,

with the field strength falling rapidly in the surrounding regions, positioning of the sample within the instrument is crucial if experiments are to be reproducible. Similarly, and more importantly for our purposes, investigation of the lung can be hampered by the presence of gas-tissue interfaces which generate spectral line broadening and image distortion. Techniques which have previously been employed to overcome this involve degassing the lung either by vacuum or by ventilation with 100% oxygen and allowing the circulation to remove the alveolar gas (Pillai *et al.* 1986).

6.3.2 Water Content of Tissue

Relaxation times of protons in water will be influenced by juxta-position of magnetic nuclei and their rate of movement - that is, the amount of "structure" that is present in a sample. In pure water, for example, compared with water in a dilute solution or within a cell, there is very little association of the individual molecules such that loss of energy via spin-lattice relaxation is comparatively slow. Resultant T_1 times are therefore increased and have been quoted as being approximately 3 seconds. However, if such a sample contains even low levels of air in solution, T_1 is greatly reduced due to the influence of paramagnetic molecular oxygen (see 6.3.3) (Chiarotti *et al.* 1955).

In dilute solutions, a proportion of the water molecules present will be associated with solute molecules as a "hydration sheath" which may consist of several layers of tightly packed water molecules in a state of dynamic orientation. Such structuring allows the rapid loss of energy via spin-lattice relaxation and therefore results in reduced T_1 values. Matters are further complicated by the presence of proteins in solution since the tightly packed water molecules which constitute the hydration shell will be influenced by a variety of different chemical environments arising from amino acid side groups e.g. attraction to polar groups or repulsion from hydrophobic side chains (Koenig *et. al.* 1978). The influence of proteins and other solutes within the cytosol is further compounded by the fact that water within the cytoplasm behaves as a two-phase system. If we assume that the hydration shell associated with cellular macromolecules will only have an influence over a finite distance i.e. a certain number of water molecules from the protein or lipid molecule, for example, then water molecules beyond this range will behave as though in bulk and therefore exhibit very different values for T_1 (Packer 1977, Clegg 1979). Clearly then, since water content within the tissue, and its association with other cellular constituents can vary dramatically, such factors should be a major consideration when attempting to reproduce MRI procedures experimentally.

6.3.3 Influence of Paramagnetic Nuclei

A paramagnetic nucleus may be defined as one which has unpaired spins (e.g. an uneven number of electrons) and which has lower energy when placed in a magnetic field. The magnetic moment of an unpaired electron in a paramagnetic ion is approximately 10^3 times greater than the nuclear magnetic moment and the unpaired electron, therefore, generates a much stronger local magnetic field which, if fluctuating at the appropriate frequency, will induce relaxation in the nuclear resonance. The presence of a paramagnetic substance can therefore induce a more rapid relaxation of the excited NMR nucleus, causing broadening of spectral line profiles (Cohn and Hughes 1962). Many tissues contain fairly high concentrations of paramagnetic metal ions such as copper, iron and manganese, but at insufficient levels to significantly bring about a reduction in T_1 or T_2 .

Cr compounds lend themselves particularly well to investigation by MRI due to their unique chemistry within the cell. Once Cr(VI) compounds have entered the cell and undergone reductive conversion, the resulting Cr(III) complexes are not only extremely stable but, having an uneven number of outer shell electrons, are also paramagnetic. Consequently, the modification of T_1 and T_2 means that by selecting appropriate parameters during an MRI scan, regions of tissue containing Cr(III) can be visualised as areas of intense brightness.

This study aims to demonstrate the potential usefulness of MRI in the detection and quantification of Cr(III) compounds in lung tissue. Using both *in vitro* and whole animal *in vivo* models it is hoped that the suitability and sensitivity of this technique can be assessed with a view to applying similar experimental procedures in Cr-exposed human subjects. Ultimately, application of MRI will allow levels of Cr(III)-containing particles in the lung to be quantified and correlated with Cr levels in body fluids and/or lymphocyte populations in the same subject. From what is already known about Cr exposure and potential cancer risks, further information about the distribution and deposition of Cr-containing particles in the lung will allow a clearer model to be developed of the role of Cr(VI) in carcinogenesis. It is hoped that MRI will eventually serve a role as a screening technique, providing early information about potential cancer risks as a result of pulmonary exposure to Cr(VI).

6.4 Materials and Methods

6.4.1 Materials

Potassium chromate was purchased from BDH Ltd. (Poole, Dorset, UK) and glutathione from Sigma (Poole, Dorset, UK). Saggital was from Centaur Services Ltd. (Somerset, UK) Male Wistar rats were obtained from Charles River (Margate, Kent).

6.4.2 Experimental procedures

Glass vials containing Cr(VI) solutions (potassium chromate, 0.05-0.5 mM) in the presence of 5 mM GSH in phosphate buffer ($\text{Na}_2\text{HPO}_4 \cdot 2\text{H}_2\text{O}/\text{NaH}_2\text{PO}_4 \cdot \text{H}_2\text{O}$, 0.1 M, pH 7.0) were scanned on a VARIAN/Siemens SISCO-200 Imaging Spectrometer equipped with an Oxford Instruments 4.7 Tesla, 33 cm horizontal bore superconducting magnet using the following parameters (table 6.1). The software employed for scanning and image analysis was *VARIAN VNMR*.

Table 6.1. Parameters used during MRI scans

Echo time	10 ms
Slice thickness	0.5 mm
In plane spatial resolution	0.625 mm x 0.625 mm
t_r , acquisition time	2 ms
Number of points (real and imaginary)	256
Number of phase encoding steps	128
90° pulse	2 ms gauss
180° pulse	2 ms gauss
G_{read}	20 mTm^{-1}
Maximum G_{phase}	17.92 mTm^{-1}
G_{slice}	36.2 mTm^{-1}
Number of slices	12
t_r , repetition time	0.5 s
Number of repetitions	4
Total imaging time	4 min 26 s

A vial containing phosphate buffer was included as a negative control, that is, a sample known to be free of any potentially paramagnetic Cr, whilst a 0.5 mM Cr(III) solution (prepared by incubating 0.5 mM potassium chromate with 1 mM AsA in phosphate buffer for 1 h) provided a known concentration of such species.

Two male Wistar rats (approx. 250 g) were killed with an overdose of Saggital (approximately 0.6 ml per animal) and the thoracic cavity exposed by cutting through the ribs on either side of the sternum, before removing the lungs. One pair of lungs was flooded with 0.5 mM Cr(III) (prepared as above) whilst the second pair were filled with buffer only. The tissues were then scanned using the same instrumental parameters as described.

In a whole animal, freshly killed with an overdose of Saggital (0.6 ml) a cannula was introduced into the trachea. Briefly, the neck of a male Wistar rat (approx. 250 g) was dissected open and the trachea exposed. A small incision was made midway along the trachea, taking care not to sever it completely (Figure 6.4), and a short cannula (approx. 3 cm length, 1.5 mm diam) was inserted into the airway until contact was made with the primary bifurcation of the bronchi. The cannula was then withdrawn a few millimetres and secured by tying around the trachea with suture thread (Figure 6.5). A length of plastic tubing was attached to

the cannula and the animal placed within the instrument (Figures 6.6 and 6.7). By means of a 10 ml syringe the lungs were fully inflated and the animal scanned to establish a control image before the introduction of any test solutions. Incremental doses of Cr(III) (0-15 µg as 2.5 µg/100 µl aliquots) were injected and the lungs scanned as before. Alternatively a single dose of 100 µg Cr(VI) in a volume of 100 µl phosphate buffer was introduced and the lungs scanned over a period of time. Using the same whole animal model, several animals (165 - 340 g) were screened before dosing then subsequent single doses of 5 µg Cr(III), 10 µg Cr(III) and 30 µg Cr(III), in volumes of 100 µl, 200 µl and 600 µl of phosphate buffer, respectively, were introduced before repeat screening. Image analysis was performed on all scans to determine the relative intensity of the signal generated as a result of Cr(III)-induced proton relaxation. Briefly, a region of interest was isolated (either a defined region within the image or the whole lung area) and the change in average signal intensity within this region monitored with time or dose, enabling plots to be generated to illustrate the qualitative changes taking place in the dosed tissue.

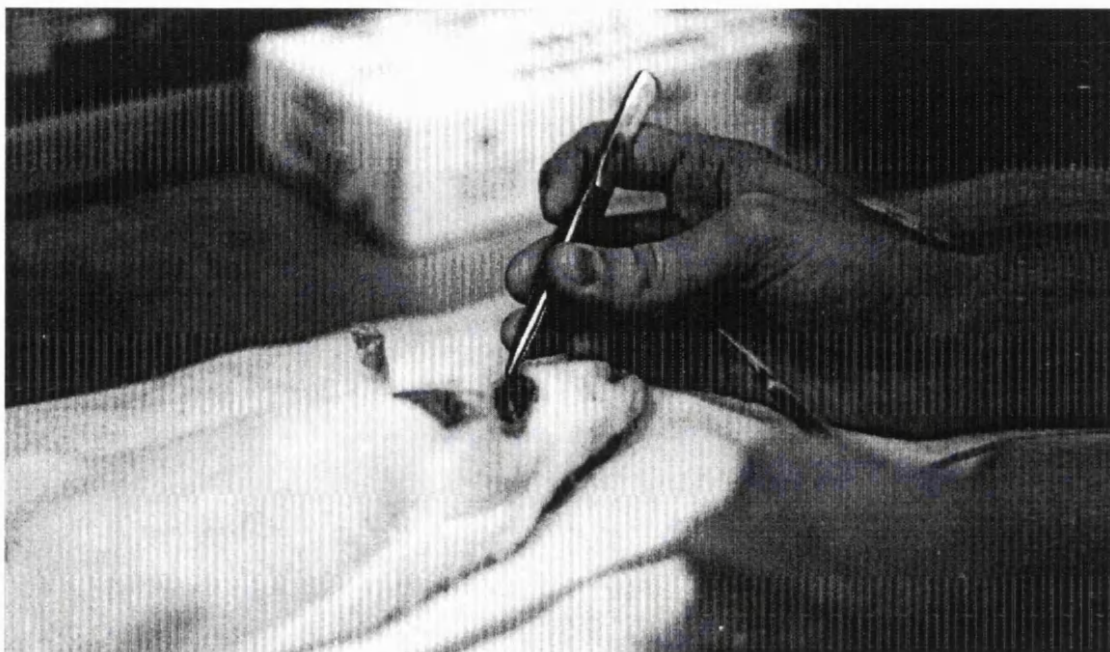


Figure 6.4. Dissection of rat trachea

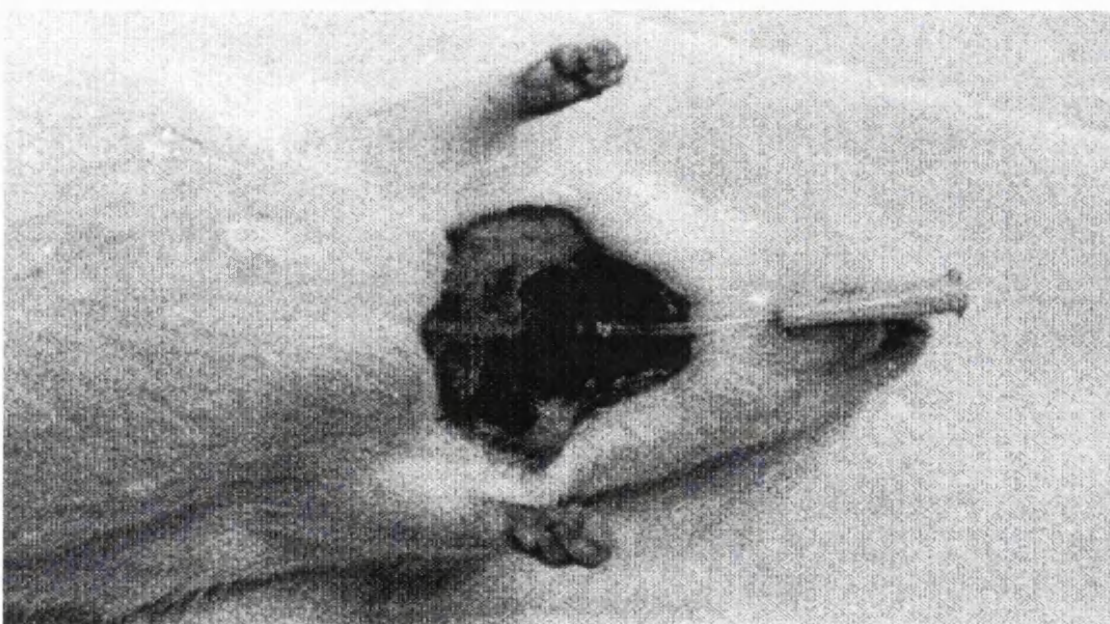


Figure 6.5. Insertion of cannula into rat trachea

Figure 6.6 Assembly of sample in coil

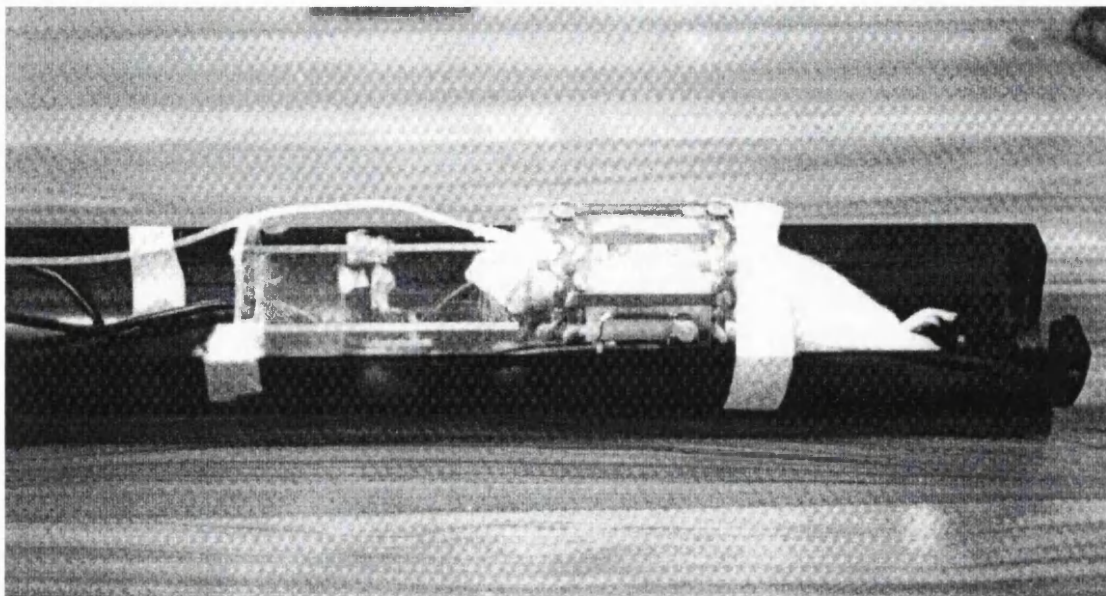


Figure 6.7 Placement of coil in magnet

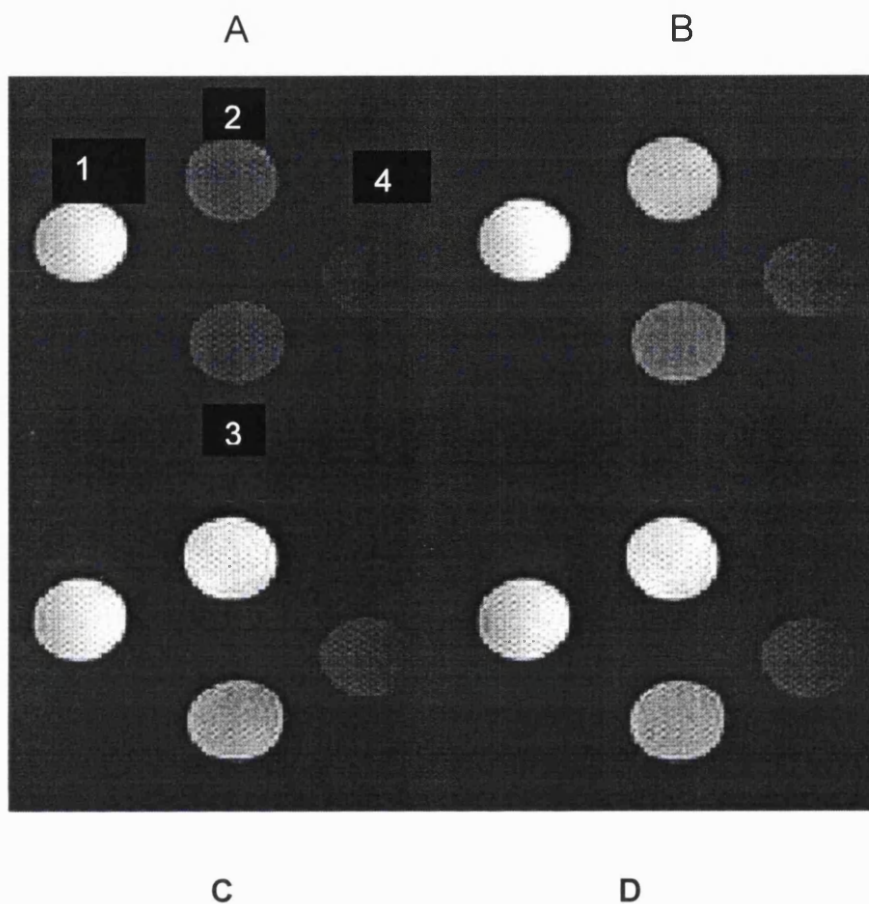


6.5 Results

6.5.1 *In vitro* modelling

Preliminary studies were designed to establish whether MRI can be applied to distinguish between Cr(III) and Cr(VI) in aqueous solution. To this end, glass vials containing various concentrations of Cr(VI) (0.05-0.5 mM) in the presence of 5 mM GSH in phosphate buffer were scanned over a period of time as described. Phosphate buffer was also included as a negative control whilst 0.5 mM Cr(III) was used to provide a positive control. Figure 6.8a shows the resultant MRI scan and illustrates the proportional increases in signal intensity, with time, of the samples containing Cr(VI)/GSH. Densitometry was performed on these images and any changes in signal intensity plotted as arbitrary units. Figure 6.8b shows the conversion of Cr(VI) to Cr(III) with time in the various samples. Baseline levels of intensity (around 50 units) were obtained throughout the experiment for the samples containing phosphate buffer and Cr(VI), whilst samples containing Cr(VI) in the presence of GSH rapidly reached maximum intensity within approximately 2 hours. The level of intensity achieved in the samples was proportional to the initial concentration of Cr(VI), with the brightest images (approximately 800 units of intensity) being seen at 0.5 mM Cr(VI). Such levels correspond to the values obtained for 0.5 mM Cr(III) (also approximately 800 units), indicating the

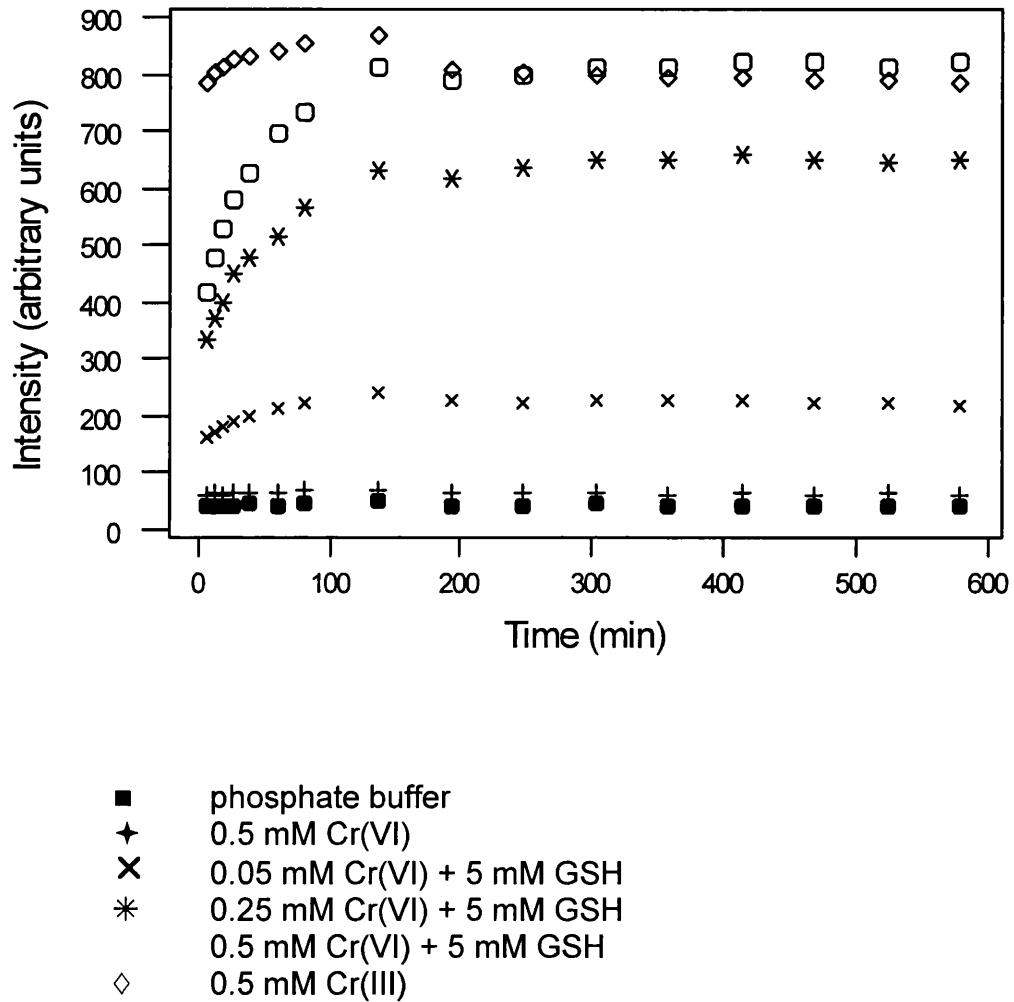
complete conversion of Cr(VI) to Cr(III) in the most concentrated samples.



1. 0.5 mM Cr(III)	A. 25 min after solutions were mixed
2. 0.5 mM Cr(VI) + 5 mM GSH	B. 80 min " " " "
3. 0.25 mM Cr(VI) + 5 mM GSH	C. 321 min " " " "
4. 0.05 mM Cr(VI) + 5 mM GSH	D. 596 min " " " "

Figure 6.8a. MRI scan to show the conversion of Cr(VI) to Cr(III) in the presence of GSH

Figure 6.8b. Reduction of Cr(VI) to Cr(III) by GSH as a function of time



6.5.2 In vivo modelling

Detection of Cr(III) in biological tissue

Preliminary studies demonstrated the potential use of MRI for the detection of Cr(III) in a non-biological system we became interested in exploring the application of this method to animal tissue. Briefly, the lungs were removed from two male Wistar rats (250 g) and one pair was perfused with a Cr(III) solution (0.5 mM, approximately 5 mls) whilst the other was filled with the same volume of phosphate buffer.

The samples were then scanned using the same experimental parameters as before. Figure 6.9 shows the images obtained from this experiment. Clearly, there is a striking difference between the two sets of lungs, the brighter image on the right being the tissue containing Cr(III). Whilst the two samples are from different animals, and a certain amount of inter-animal variation cannot be ruled out, these findings strongly suggest that MRI may be applicable as a technique for the detection of Cr(III) in biological tissue.

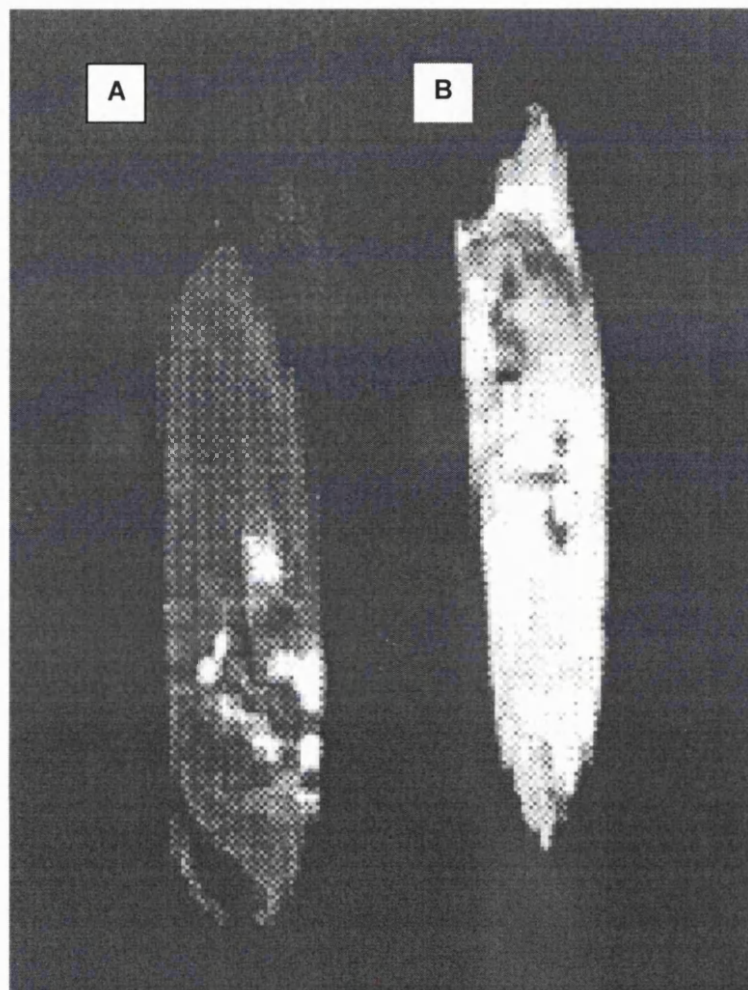


Figure 6.9. MRI scan to show comparison between lungs perfused with phosphate buffer (A) and 0.5 mM Cr(III) (B)

Sensitivity of MRI to detect Cr(III)

To establish the sensitivity of this technique and to try and eliminate the potential variation between animal subjects, a whole animal model was developed. Briefly, a cannula was introduced into the trachea of a freshly killed male Wistar rat and the animal placed into the instrument.

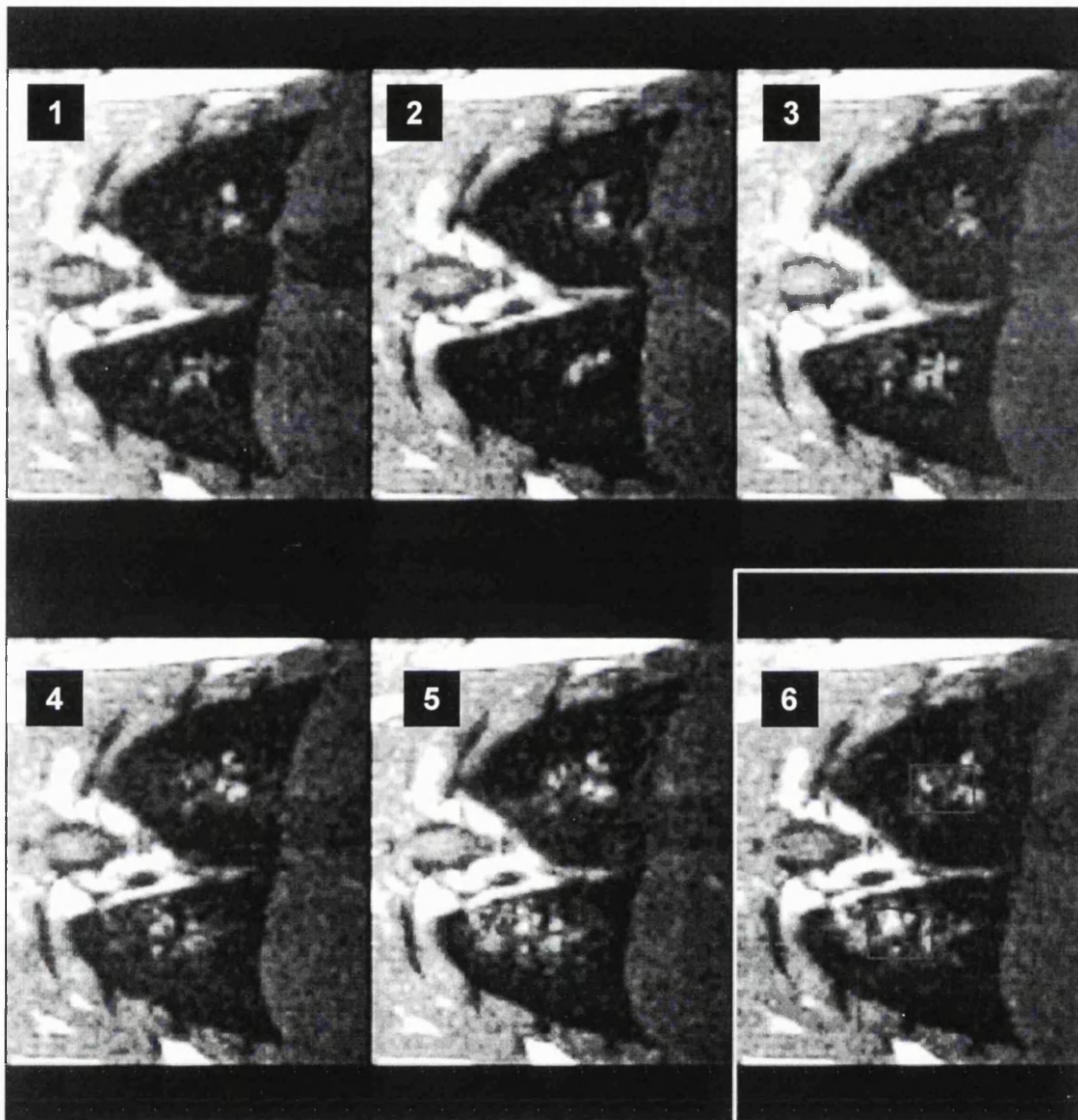
Incremental doses of Cr(III) were then administered to the animal's lungs (0-15 µg as 2.5 µg aliquots) and scans taken at each dose point.

Densitometry was carried out on selected regions of the resulting images and a plot constructed of the total intensity of both lungs (arbitrary units) vs. Cr(III) "load". The results of these scans were corrected for background "noise" i.e. values for the intensity of the control image were subtracted from subsequent images.

Figure 6.10a shows the "slices" generated over the range of Cr(III) dosing (0-15 µg) where the highlighted boxes represent the regions of interest within which densitometry was performed. Clearly there is an increase in the intensity of the selected areas in each lung with rising Cr concentration. These changes are illustrated in Figure 6.10b which shows the linear increase in intensity with rising Cr(III) levels. Whilst intensity levels of up to 50 units were seen at the highest dose of 15 µg Cr(III), changes were detectable at doses between 2.5 and 5.0 µg - a value which could be considered to be the lower limit of sensitivity for this model. It should be stressed that the only variable in this model is the the

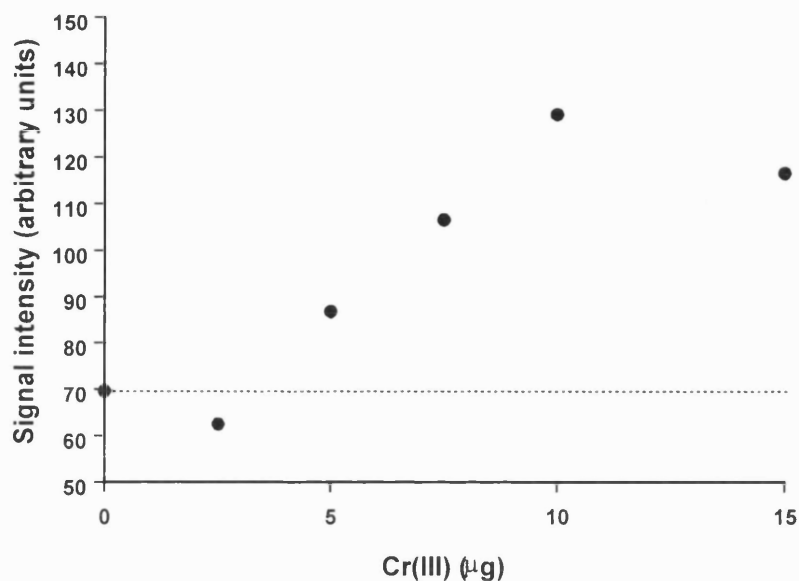
amount of Cr(III) being introduced into the lungs, therefore the animal is acting as its own control. It was felt that this is a reliable model since, in a similar experiment, a second animal was dosed with identical volumes of phosphate buffer and scanned over the same time period to assess the influence of any post-mortem changes. Degradation of tissue and/or accumulation of fluid in the lungs might be expected to considerably affect the images generated, however, no such changes were observed even several hours after death (data not shown). The fact that in all cases animals were scanned within 15 minutes of death and that single experiments take no longer than 30 minutes means that we can ignore post-mortem changes as a variable likely to influence our findings.

Figure 6.10a. MRI scan to illustrate changes in signal intensity with increasing dose of Cr(III)



1. Control
2. 2.5 μg Cr(III)
3. 5.0 μg Cr(III)
4. 7.5 μg Cr(III)
5. 10.0 μg Cr(III)
6. 15.0 μg Cr(III)

Figure 6.10b. Graph to show increase in signal intensity with increasing dose of Cr(III)



Monitoring the conversion of Cr(VI) to Cr(III) in situ

Having established a sensitivity range for this technique, we became interested in whether MRI can be used to detect the internal conversion of Cr(VI) to Cr(III) as a result of the reducing capacity of the lungs. The definition of a relationship between the two Cr species would be invaluable since it is exposure to Cr(VI) which carries the greater carcinogenic potential. The same whole animal model was used with the exception that a single dose of 100 μg Cr(VI) as potassium chromate was introduced into the right lung of a freshly killed male Wistar rat (250 g), and the animal scanned at regular time intervals (0-30 min). The left lung was untreated to provide an internal control. The lungs of a second animal were treated with phosphate buffer and scanned for the same

period of time to determine any post-mortem changes that may have affected signal intensity. As in previous studies, no such changes were apparent. Densitometry was performed on selected regions of both lungs and the data plotted as arbitrary units of intensity vs. time. Figure 6.11a shows the increase in signal intensity after densitometry had been performed on these images whilst Figure 6.11b represents four "slices" generated over our chosen time points. Clearly, the change in intensity of the right lung demonstrates the ability of MRI to monitor the reduction of Cr(VI) to Cr(III) despite post-mortem conditions. The profile of the curve closely mirrors the reduction kinetics seen in previous experiments in our *in vitro* model (Figure 6.8b). The maximum Cr(III) signal is seen after approximately 30 min and corresponds to 80 intensity units. Conversely, in the untreated right lung baseline values of around 20 intensity units are seen over the total time period. Again, it should be stressed that the only variable parameter in these experiments was time since the animal was acting as its own control.

Figure 6.11a. Graph to demonstrate conversion of Cr(VI) to Cr(III) in post-mortem rat lung after single installation of 100 μg Cr(VI)

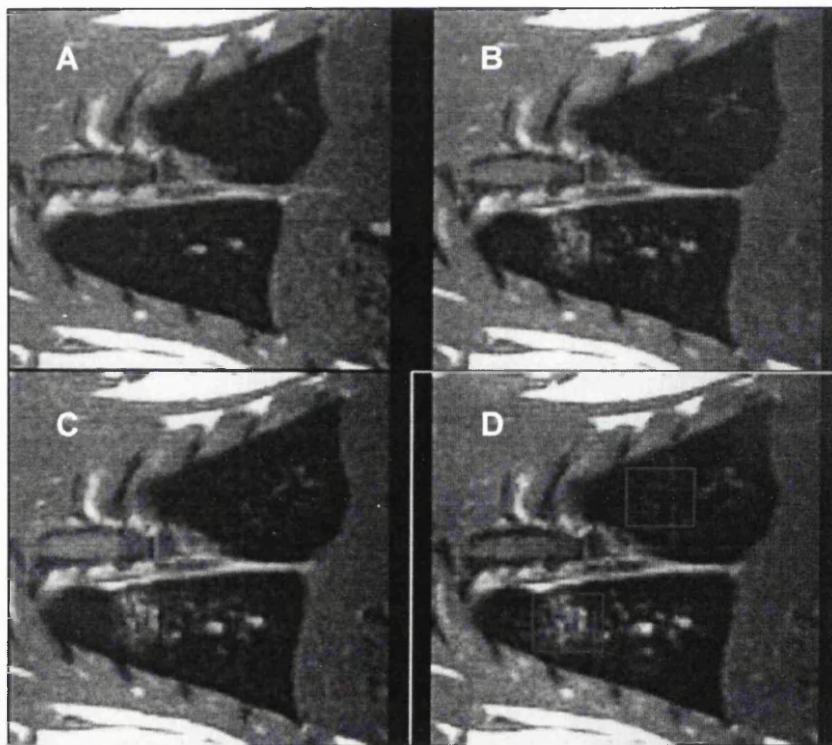
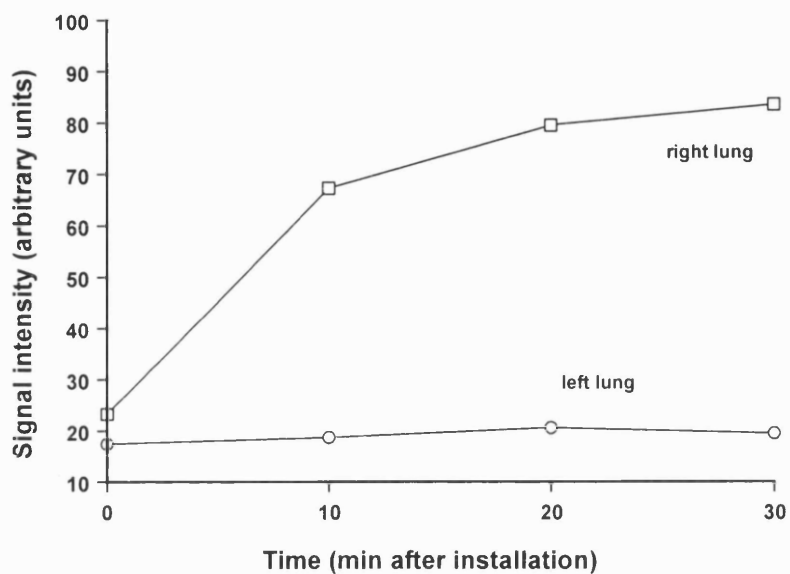


Figure 6.11b Time course scans after single injection of 100 μg Cr(VI)

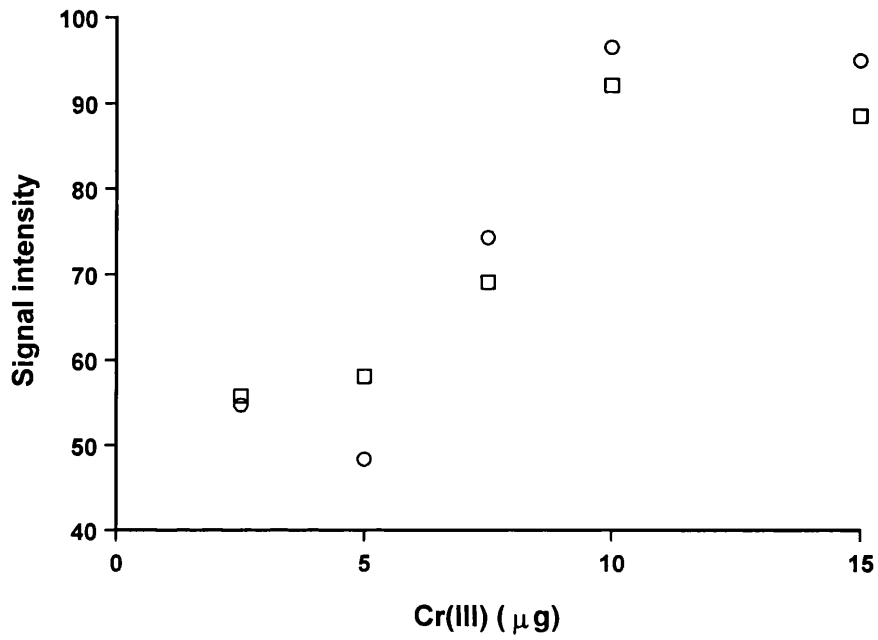
A - 0 min
B - 10 min after injection

C - 20 min after injection
D - 30 min after injection

6.5.3 Image analysis and the "region of interest"

It should be pointed out at this stage that, when performing densitometry on resultant MRI scans, the intensity of the Cr(III) signal has been determined in a focussed region of interest since any changes have been observed in a well defined area of the lung (see figs 6.10a and 6.11a). In later experiments, changes in signal intensity were seen to be dispersed throughout the whole lung region and it was felt that the whole lung should now represent our "region of interest". However, the nature of the software used to analyse these changes means that it is the *average* intensity over a defined region which is determined. In order to rule out any unwanted variation as a result of altering our technique of analysis, images from previous experiments (Figure 6.10a) were reanalysed for signal intensity using the whole lung as the region of interest. Apparent signal intensity in these images was found to be unaffected by the method of analysis (Figure 6.12) and it was felt that use of the whole lung area for intensity determination in subsequent studies would be experimentally valid.

Figure 6.12. Comparison of signal intensity as determined by densitometry using a defined region of interest or the whole lung area



○ - whole lung, □ - isolated region

6.5.4 Quantification of the Cr(III) MRI signal

Whilst initial investigations into the detection of Cr(III) in biological tissue by MRI have provided a great deal of information regarding the suitability and sensitivity of this technique, all our previous conclusions have been drawn on the basis of qualitative data. If MRI is to be of any use as a biomonitoring tool attempts should be made to quantify the information it provides, thereby allowing scans between individuals to be interpreted in the same way and be meaningful. Given the number of parameters which may influence the intensity of the Cr(III) MRI signal this can only be achieved by controlling experimental conditions such as the positioning of the animal within the coil, the size of animals within the same dose group and the degree of inflation of the lungs as stringently as possible. In an attempt to determine a consistent relationship between Cr(III) dose and MRI signal in different experimental subjects three groups of animals of the same weight were scanned to obtain control images and then dosed with various amounts of Cr(III). For both control and dosed subjects, twelve "slices" were scanned through the lungs of each animal and the signal intensity of each slice was determined by densitometry. Thus, the "total" signal intensity for each pair of lungs was calculated and the results of Cr(III)-dosed subjects compared with controls (Table 6.2). At the lower dose group of 5 µg Cr(III) per whole lung it was very difficult to determine whether or not a change in signal intensity had taken place, with image analysis demonstrating a *decrease*

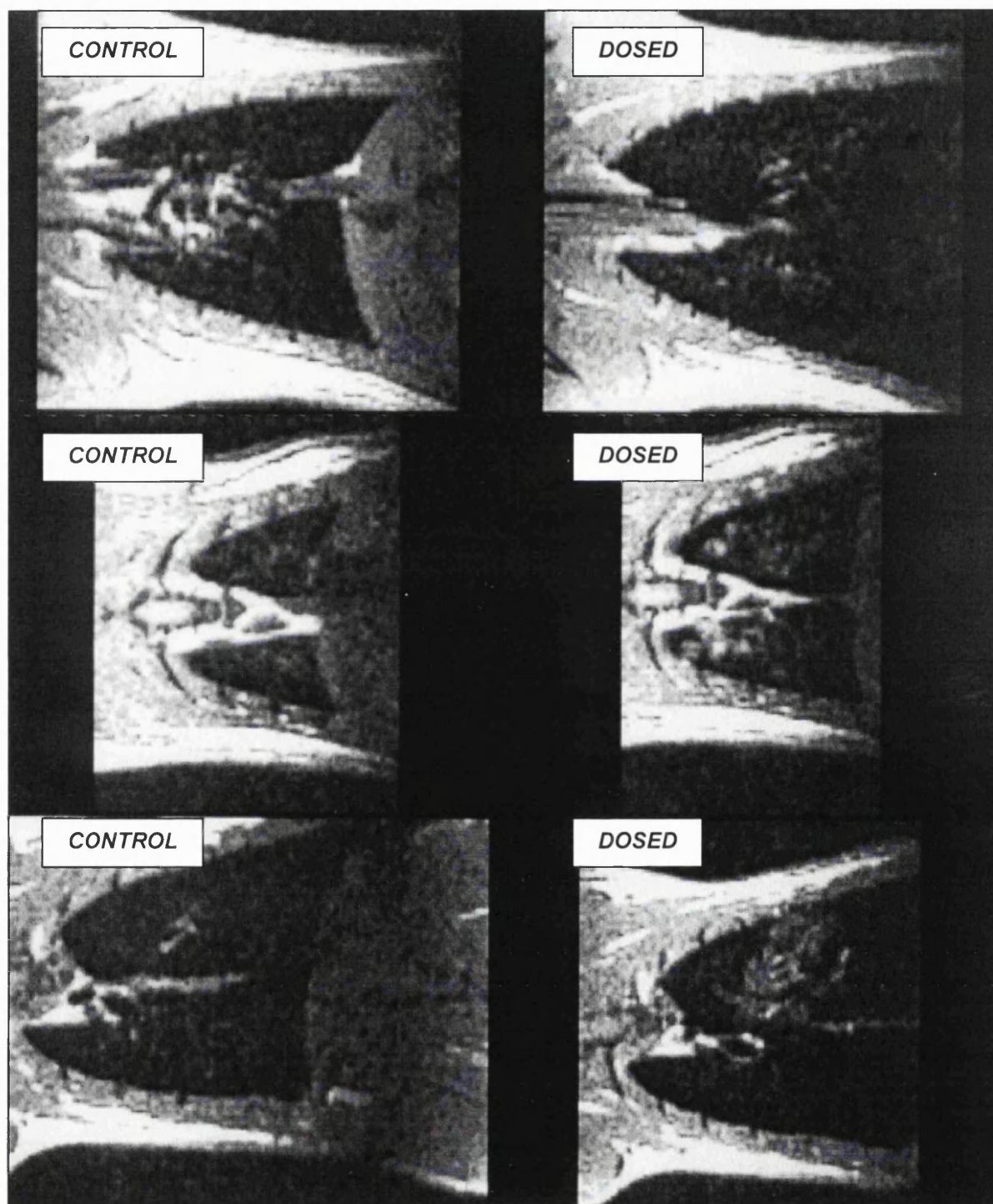
in signal. Similarly, at 10 μg Cr(III) per whole lung it was difficult to detect any change with the naked eye, yet image analysis highlighted a decrease in intensity. At the maximum dose of 30 μg Cr(III) per whole lung it was visually apparent that many of the images showed an increase in Cr(III) signal but again, image analysis revealed a decrease in intensity for most of the subjects under investigation. Only two animals demonstrated an increase in signal despite there being definite regions of brightness obvious to the naked eye. Figure 6.13 illustrates examples of scanned slices from animals before and after dosing with 30 μg Cr(III).

Table 6.2. Results from experiments designed to quantify inter-animal variation Cr(III) MRI signal

Animal Number	Weigh t (g)	Dose ($\mu\text{g Cr(III)}$)	No. of "slices" scanned	Total intensity (dosed)	Total intensity (control)	Net increase in intensity
1	180	5	12	461.1	561.8	-100.7
2	170	5	9	256.3	507.5	-251.2
3	175	5	10	224.3	404.7	-180.4
4	265	5	12	2471.1	-	-
5	265	5	12	682.4	-	-
6	235	5	12	563.5	-	-
7	175	10	12	228.0	327.5	-99.5
8	165	10	12	231.0	255.2	-24.2
9	165	10	8	194.0	339.8	-145.8
10	275	10	12	325.6	-	-
11	265	10	12	684.8	-	-
12	270	10	12	545.6	-	-
13	320	30	12	349.9	525.4	-175.5
14	340	30	12	282.7	335.9	-53.2
15	320	30	10	467.9	385.1	82.8*
16	320	30	9	281.9	410.5	-128.6
17	320	30	12	284.1	284.4	-0.3
18	290	30	12 (left lung only)	192.8	138.4	54.4*

Note; "Intensity" is stated in arbitrary units

Figure 6.13. Comparison of signal intensity after single dose of 30 μg Cr(III)



6.6 Discussion

The finding that lymphocytes do not represent an appropriate tissue for the biomonitoring of Cr-exposed individuals has prompted the search for alternative methods of cytogenic surveillance. The application of MRI for this purpose was investigated and the technique assessed in terms of its suitability, sensitivity and reproducibility.

Initial studies were designed to determine whether or not Cr(III) could be distinguished from Cr(VI) in aqueous solution. By monitoring the conversion of Cr(VI) to Cr(III) by GSH with time it was demonstrated that MRI is indeed sensitive to the paramagnetic Cr species *in vitro*, prompting investigation of this species in biological tissue. Again, the ability of MRI to detect Cr(III) in isolated lung led us to probe the sensitivity of the technique by employing a whole animal model. Analysis of lungs exposed to incremental doses of Cr(III) compounds demonstrated that MRI is able to detect levels of Cr(III) between 2.5 and 5.0 ug per whole lung. Using the same whole animal model we were also able to detect the conversion of Cr(VI) to Cr(III) as a result of the residual reducing capacity of the lungs, despite post-mortem conditions. This represents an interesting finding since it confirms that we can monitor exposure to Cr(VI), which has been shown to be the primary damaging species in Cr-induced carcinogenesis, as opposed to Cr(III) which is relatively unreactive to DNA. However, whilst these initial results are very

promising, for MRI to be useful as a biomonitoring tool it is necessary to be able to quantify such findings and determine a relationship between Cr(III) dose and signal intensity. In other words, any information generated from MRI needs to be "standardised" such that the technique can be applied to different subjects (as would be the case in a "real" screening situation) and the information obtained still be meaningful. Given the number of parameters which can influence the intensity of the Cr(III) MRI signal the amount of variation between subjects may be too great for such extrapolation to be possible. In an attempt to determine an approximate relationship between Cr(III) dose and signal, animals were administered a single dose of Cr(III) known to be detectable by MRI and the "total" intensity obtained compared with control images. The results from such studies were somewhat surprising since, although increases in intensity were apparent to the naked eye in many cases, image analysis data demonstrated an apparent reduction in the Cr(III) signal. Such apparently contradictory findings can be explained in terms of the experimental model employed. Since the very nature of introducing solutions into the lungs of the test animal requires that a significant volume of air also be introduced as the vehicle, there will inevitably be some expansion of the lungs each time an animal is dosed. Since the software used to analyse changes in the MRI signal monitors variation in *average* signal intensity over a selected region, and since our selected region in each case is the whole lung area, any increase in the size of

this region i.e. inflation as a result of dosing, will result in an apparent decrease in signal strength.

Whilst every attempt is made to compensate for this by previous inflation of the lungs before control scans are taken, such precautions were not in this case sufficient. It should be stressed that the failure of these studies to determine a quantifiable relationship between Cr(III) dose and signal intensity is due to the limitations of the chosen model; the limits of which have clearly been reached. This does not mean that such a relationship cannot be defined.

Chapter 7

Summary

The initial aims of this thesis were to further investigate the interaction of Cr(VI) compounds with isolated DNA *in vitro*, and to determine the identity of a potentially pre-mutagenic species arising from the reduction of Cr(VI) by GSH. In addition, techniques previously used for the biomonitoring of Cr-exposed workers were assessed in terms of their suitability and reproducibility. A novel technique utilising MRI was explored with a view to subsequently developing a more complete pharmacokinetic model of Cr(VI) inhalation, deposition and distribution, and subsequent carcinogenic potential.

Studies into the interaction of Cr(VI) with isolated DNA in the presence of GSH were principally concerned with identifying the existence (or absence) of a mutual mechanistic pathway for the mediation of more than one type of prevalent DNA lesion, and the involvement of particular Cr species in the generation of such types of DNA damage. In addition, the role of reactive oxygen species in the mediation of Cr(VI)-induced DNA damage was considered with particular emphasis on specific types of damage such as SSB and AP-sites. Interest was also focussed on the potential sites of interaction of damaging species with the DNA macromolecule. The studies outlined in chapters 2 and 3, along with

previous findings from this laboratory have enabled us draw several conclusions concerning these important considerations;

- Molecular oxygen is required for SSB and AP-sites to be formed (Casadevall and Kortenkamp 1995) but Cr(V) species, in the absence of oxygen, are unreactive (Kortenkamp *et. al.* 1996) as are Cr(III) complexes.
- SSB and AP-sites are formed with equal probability, indicating that the site of attack are carbon atoms of the DNA sugar moiety (Casadevall and Kortenkamp 1995).
- Hydroxyl radicals are unlikely to be the oxidising species leading to SSB and AP-sites (Kortenkamp *et. al.* 1996).
- Cr-DNA adducts can be formed independently of the reaction pathways giving rise to SSB and AP-sites.
- Cr(V), and possibly Cr(IV) species, as well as hydrolysing Cr(III)/GSH complexes are responsible for the formation of Cr-DNA adducts.
- DNA-phosphate groups are the binding site of Cr-DNA adducts.

With these observations in mind, a model for the role of Cr(VI) in oxidative DNA damage is proposed involving the initial binding of a hypervalent Cr species (oxidation state IV or V) to the phosphate groups of DNA, yielding a 1:1 Cr-GSH DNA adduct. If the partly reduced metal centre then encounters reactive oxygen species (for example from the reaction of molecular oxygen from GSH), highly oxidising intermediates may be produced leading to oxidation of carbon atoms of the DNA sugar moiety. Such interactions are thought to give rise to SSB or AP-sites, leaving a Cr(III) residue attached to the site of reaction. Alternatively,

SSB and AP-sites may be generated by highly oxidising species, involving partly reduced Cr, being formed free in solution and diffusing to the surface of DNA. The nature of the oxidising species arising from hypervalent Cr and reactive oxygen species is unclear but a possibility first suggested by Lefebvre and Pezerat (1992) involving Cr(V) superoxo- or peroxy- complexes is currently favoured. In the absence of any interactions between Cr(V) or (IV) and reactive oxygen species (ROS), Cr-DNA adducts are likely to form. Even in the presence of oxygen, high levels of antioxidants such as GSH will favour this reaction pathway by both scavenging radicals and by promoting the formation of Cr(III). As they accumulate, slowly hydrolysing Cr(III)/GSH complexes are likely to contribute more and more to the formation of Cr-DNA adducts.

If we have in any way been able to clarify the processes leading to the induction of DNA damage during the *in vitro* reduction of Cr(VI) by GSH this still does not provide any indication about the potential mutagenicity of the various lesions generated. While evidence has been put forward for the mutagenic potential of oxidative damage such as SSB and AP-sites in various *in vitro* systems (Loeb *et. al.* 1986, Schaaper *et. al.* 1983, Kunkel *et. al.* 1981, Schaaper and Loeb 1981, Kortenkamp *et. al.* 1996), the role of these types of damage is unclear. Indeed, studies which have directly compared the mutagenic potential of DNA damage induced by Cr(VI) and known oxygen radical producing agents such as hydrogen peroxide and X-rays, have shown considerable differences in the subsequent mutational spectra produced by such treatments (Cabral-Neto *et. al.* 1994, Dar and Jorgensen 1995, Liu and Dixon 1996). Zhitkovitch *et. al.* (1995) have even proposed a positive role for the

mutagenicity of GSH-Cr(III)-DNA adducts in Chinese Hamster Ovary cells treated with Cr(VI). These observations support findings in our Cr(VI)/GSH model that, even under conditions where no oxidative damage is seen (presence of catalase), mutation frequencies in E. coli JM105 remained consistent with levels seen in populations treated with Fe(II)/H₂O₂ (treatment known to be consistent with both oxidative and non-oxidative types of DNA damage). It is clear then, that DNA lesions induced during the *in vitro* conversion of Cr(VI) by GSH can be fixed into mutations during replication and passed on to progeny cell lines, and that there is an apparent role for non-oxidative damage in this process. We therefore propose that Cr-DNA adducts represent a potentially mutagenic lesion and that, since evidence is apparent for the role of Cr(III) complexes in the formation of this type of lesion, Cr(III) represents a species with the potential capacity to cause fixed mutations in cell lines.

Turning our attention away from the molecular mechanisms of Cr carcinogenicity we became concerned with how these interactions may provide markers for, or be indicative of potential cancer risks.

Biomonitoring studies involving the determination of early biological effects in lymphocytes have proved inconclusive in this respect, and have raised questions about the relevance of employing such cells in the prediction of the potential carcinogenic effects of Cr compounds (Popp *et. al.* 1991, Gao *et. al.* 1994, Zhitkovitch *et. al.* 1996). For this reason, alternative methods of surveillance need to be developed and the application of MRI for this purpose was investigated, an exercise which

necessitated the development of a novel whole animal model. Having demonstrated that MRI can be used to detect Cr(III) species both *in vitro* and in whole animal models (indeed, the sensitivity of this technique enabled the detection of levels of Cr[III] between 2.5 and 5.0 µg per whole lung) we became concerned with applying this method to monitor the conversion of Cr(VI) to Cr(III) *in situ*. Despite the post-mortem conditions enforced by our model we were still able to detect the reduction of Cr(VI) with time. This represents an important finding since it not only demonstrates the powerful reductive capacity of the lung but also allows us to detect exposure to Cr(VI), significant in that Cr(VI) has been shown to be the primary damaging species in Cr-induced carcinogenesis. However, for MRI to provide a practical biomonitoring tool we need to be able to quantify our observations and determine a reproducible relationship between Cr(III) dose and MRI signal intensity. The number of parameters which influence the intensity of the Cr(III) MRI signal are vast and include subtle factors such as the exact positioning of the animal within the coil, and the degree of inflation of the lungs (a crucial consideration since ultimately these scans are to be performed on live subjects). In addition, inherent factors such as the fluid content of the tissue under investigation and the presence of other paramagnetic species will modify the MRI spectra produced and may generate inconsistencies between individual subjects. While every effort was made to minimise these variables in our investigations, it was

almost impossible to reproduce comparable MRI images in different subjects treated with the same dose of Cr(III). It should be stressed however, that the failure of these studies to determine a quantifiable relationship between Cr(III) dose and signal intensity was due to the employment of an inappropriate model. That such a relationship cannot be demonstrated in our studies by no means proves that it is an impossible task. Therefore, we would stress the need for further work to develop suitable models since the advantages of MRI (its sensitivity, ease of execution, and its non-invasive nature) make it an ideal candidate for the biomonitoring of Cr-exposed individuals.

References

Aiyar, J., Borges, K. M., Floyd, R. A. and Wetterhahn, K. E. (1989) Role of chromium(V), glutathionyl and hydroxyl radical intermediates in chromium(VI)-induced DNA damage, *Toxicol. Environ. Chem.* **22**, 135-148.

Aiyar, J., Berkovits, H. J., Floyd, R. A. and Wetterhahn, K. E. (1991) Reaction of chromium(VI) with glutathione or with hydrogen peroxide: Identification of reactive intermediates and their role in chromium(VI)-induced damage, *Environ. Health. Perspect.* **92**, 53-62.

Ackerman, J. J. H., Grove, T. H., Wong, G. G., *et. al.* (1980) Mapping of metabolites in whole animals by ³¹P NMR using surface coils, *Nature* **283**, 167-170.

Angerer, J., Amin, W., Heinrich-Ramm, R., Szadowski, D., and Lehnert, G. (1987) Occupational chronic exposure to metals, I. Chromium exposure of stainless steel welders - biological monitoring, *Int. Arch. Occup. Environ. Health* **59**, 503-512.

Araki, S. and Aono, H. (1989) Effects of water restriction and water loading on daily urinary excretion of heavy metals and organic substances in metal workers *J. Ind. Med.* **46**, 389-392.

Aruoma, O. I., Halliwell, B., Gajewski, E. and Dizdaroglu, M. (1989) Damage to the bases in DNA induced by hydrogen peroxide and ferric ion chelates, *J. Biol. Chem.*, **264**(34), 20509-20512.

Ashby, J., and Richardson, C. R. (1985) Tabulation and assessment of 113 human surveillance cytogenetic studies conducted between 1965

and 1984, *Mutat. Res.* **154**, 111-133.

Bellomo, G., Vairetti, M., Stivala, L., Mirabelli, F., Richelmi, P. and Orrenius, S. (1992) Demonstration of nuclear compartmentalisation of glutathione in hepatocytes, *Proc. Natl. Acad. Sci. USA*, **89**(10), 4412-4416.

Bianchi, V. and Levis, A. G. (1985) Mechanisms of chromium genotoxicity, in: *Carcinogenic and mutagenic metal compounds*, vol. 8, pp. 269-293, Eds. E. Merian, R. W. Frei, W. Hardi and C. Schlatter, Gordon & Breach.

Bianchi, V. and Levis, A. G. (1987) Recent advances in chromium toxicity, *Toxicol. Environ. Chem.* **15**, 1-24.

Bigaliev, A. B., Elemesova, M. S., and Turebaev, M. N. (1977) Evaluation of the mutagenic activity of chromium compounds, *Gig. Tr. Prof. Zabol.* **6**, 37-40.

Bloch, F. (1946) Nuclear Induction, *Phys. Rev.* **70**, 460 – 474.

Borges, K. M. and Wetterhahn, K. E. (1989) Chromium cross-links glutathione and cysteine to DNA, *Carcinogenesis* **10**, 2165-2168.

Borges, K. M., Boswell, J. S., Liebross, R. H. and Wetterhahn, K. E. (1991) Activation of chromium(VI) by thiols results in chromium(V) formation, chromium binding to DNA and altered DNA conformation, *Carcinogenesis* **12**, 551-561.

Bose, R. N., Moghaddas, S. and Gelerinter, E. (1992) Long-lived chromium(IV) and chromium(V) metabolites in the chromium(VI)-

glutathione reaction: NMR, ESR, HPLC, and kinetic characterisation, *Inorg. Chem.*, **31**, 1987-1994.

Bridgewater, L. C., Manning, F. C. R. and Patierno, S. R. (1994) Base-specific arrest of *in vitro* DNA replication by carcinogenic chromium: relationship to DNA interstrand crosslinking, *Carcinogenesis* **15**, 2421-2427.

Bukowski, J. A., Goldstein, M. D., Korn, L. R., and Johnson, B. B. (1991) Biological markers in chromium exposure assessment: confounding variables, *Arch. Environ. Health* **46**, 230-236.

Buettner, G. R. (1988) In the absence of catalytic metals ascorbate does not autoxidise at pH 7: ascorbate as a test for catalytic metals, *J. Biochem. Biophys. Methods*, **16**, 27-40.

Buttner, B. and Beyersmann, D. (1985) Modification of the erythrocyte anion carrier by chromate, *Xenobiotica* **15**, 735-741.

Cabral Neto, J. B., Cabral, R. E., Margot, A., Le Page, F., Sarasin, A. and Gentil, A. (1994) Coding properties of a unique apurinic/aprimidinic site replicated in mammalian cells, *J. Mol. Biol.*, **240**(5), 416-420.

Cantoni, O. and Costa, M. (1984) Analysis of the induction of alkali sensitive sites in DNA by chromate and other agents that induce single strand breaks, *Carcinogenesis* **5**, 1207-1209.

Casadevall, M. and Kortenkamp, A. (1995) The formation of both apurinic/aprimidinic sites and single strand breaks by chromate and glutathione arises from attack by the same single reactive species and is dependent on molecular oxygen, *Carcinogenesis*, **16**(4), 805-809.

Chen, J. and Thilly, W. G. (1994) Mutational spectrum of chromium(VI) in human cells, *Mutat. Res.* **323**, 21-27.

Chiarotti, G., Cristiani, G. and Giulotto, L. (1955) Proton relaxation in pure liquids and in liquids containing paramagnetic gases in solution, *Nuovo Cimento* **1**, 863-873.

Choi, Y. J., Kim, Y. W., and Cha, C. W. (1987) A study on sister chromatid exchanges in lymphocytes in some metal plating workers, *Korea Univ. Med. J.* **24**, 249-257.

Christie, N. T., Cantoni, O., Evans, R. M., Meyn, R. E. and Costa, M. (1984) Use of mammalian DNA repair-deficient mutants to assess the effects of toxic metal compounds on DNA, *Biochem. Pharmacol.*, **33**, 1661-1670.

Clegg, J. S. (1979) Metabolism and the intracellular environment: The vicinal water network model. In *Cell-Associated Water*, W. Drost-Hansen and J. S. Clegg (eds.) Academic Press, New York, pp. 363-413.

Cohen, M. D., Kargacin, B., Klein, C. B. and Costa, M. (1993) Mechanisms of chromium carcinogenicity and toxicity, *Crit. Rev. Toxicol.* **23**, 255-281.

Cohn, M. and Hughes, T. R. (1962) Nuclear magnetic resonance spectra of adenosine di- and triphosphate. Effect of complexing with divalent metal ions, *J. Biol. Chem.* **237**, 176-181.

Connett, P. H. and Wetterhahn, K. E. (1983) Metabolism of the carcinogen chromate by cellular constituents, *Struct. Bonding*. **54**, 93-124.

Connett, P. H. and Wetterhahn, K. E. (1985) *In vitro* reaction of the carcinogen chromate with cellular thiols and carboxylic acids, *J. Am. Chem. Soc.* **107**, 4282-4288.

Coogan, T., Squibb, K., Motz, J., Kinney, P. and Costa, M. (1991) Distribution of chromium within cells of the blood, *Tox. Appl. Pharmacol.* **108**, 157-166.

Costa, M. (1990) Analysis of DNA-protein complexes induced by chemical carcinogens, *J. Biol. Chem.*, **44**, 127-135.

Costa, M. (1991) DNA-protein complexes induced by chromate and other carcinogens, *Environ. Health. Perspect.* **92**, 45-52.

Cupo, D. Y. and Wetterhahn, K. E. (1984) Repair of chromate-induced DNA damage in chick embryo hepatocytes, *Carcinogenesis* **5**, 1705-1708.

da Cruz Fresco, P. and Kortenamp, A. (1994) The formation of DNA cleaving species during the reduction of chromate by ascorbate, *Carcinogenesis*, **15**(9), 1773-1778.

da Cruz Fresco, P., Shacker, F. and Kortenamp, A. (1995) The reductive conversion of chromium(VI) by ascorbate gives rise to apurinic/apyrimidinic sites in isolated DNA, *Chem. Res. Toxicol.* **8**, 884-890.

Dar, M. E. and Jorgensen, T. J. (1995) Deletions at short direct repeats and base substitutions are characteristic mutations for bleomycin-induced double- and single-strand breaks, respectively, in a human shuttle vector system, *Nucleic Acids Res.*, **23**(16), 3224-3230.

Drinkwater, N. R., Miller, E. C. and Miller, J. A. (1980) Estimation of apurinic/aprimidinic sites and phosphotriesters in deoxyribonucleic acid treated with electrophilic carcinogens and mutagens, *Biochemistry* **19**, 5087-5092.

Edelstein, W. A., Hutchinson, J. M. S., Smith, F. W., Mallard, J. R., Johnson, G. and Redpath, T. W. (1981) Human whole body NMR tomographic imaging: Normal sections, *Br. J. Radiol.* **54**, 149-151.

Farrell, R. P., Judd, R. J., Lay, P. A., Dixon, N. E., Baker, R. S. U. and Bonin, A. M. (1989) Chromium(V)-induced cleavage of DNA: are chromium(V) complexes the active carcinogens in chromium(VI)-induced cancers? *Chem. Res. Toxicol.* **2**, 227-229.

Fischer-Nielsen, A., Poulson, H. E. and Loft, S. (1992) 8-Hydroxydeoxyguanosine in vitro: effects of glutathione, ascorbate and 5-aminosalicylic acid, *Free Radic. Biol. Med.*, **13**(2), 121-126.

Gamper, H. B., Bartholomew, J. C. and Calvin, M. (1980) Mechanism of benzo(a)pyrene diol epoxide induced deoxyribonucleic acid strand incision, *Biochemistry*, **19**(17), 3948-3946.

Gao, M., Levy, L. S., Faux, S. P., Aw, T. C., Braithwaite, R. A. and Brown, S. S. (1994) Use of molecular epidemiology techniques in a pilot study on workers exposed to chromium, *Occup. Environ. Med.*, **51**(10), 663-668.

Gochfeld, M. and Witmer, C. (1991) A research agenda for environmental health aspects of chromium, *Environ. Health. Perspect.* **92**, 141-144.

Goodgame, D. M. and Joy, A. M. (1986) Relatively long-lived chromium(V) species are produced by the action of glutathione on carcinogenic chromium(VI), *J. Inorg. Biochem.*, **26**(3), 219-224.

Hamilton, J. W. and Wetterhahn, K. E. (1986) Chromium(VI)-induced DNA damage in chick embryo liver and blood cells *in vivo*, *Carcinogenesis* **7**, 2085-2088.

Hneihen, A., Standeven, A. M. and Wetterhahn, K. E. (1993) Differential binding of chromium(VI) and chromium(III) complexes to salmon sperm nuclei and nuclear DNA, and isolated calf-thymus DNA, *Carcinogenesis* **14**, 1795-1803.

Husgafvel-Purisainen, K., Kalliomaki, P. L. and Sorsa, M. (1982) A chromosome study among stainless steel welders, *J. Occup. Med.* **24**, 762-766.

Hyodo, K., Suzuki, S., Furuya, N. and Meshizuka, K. (1980) An analysis of chromium, copper and zinc in organs of a chromate worker, *Int. Arch. Occup. Environ. Health* **46**, 141-150.

IARC (1990) Monographs on the evaluation of the carcinogenic risk of chemicals to humans, vol. 49, chromium, nickel and welding. International Agency on the Research of Cancer, Lyon.

Imlay, J. A. and Linn, S. (1988) DNA damage and oxygen radical toxicity, *Science*, **240**(4857), 1302-1309.

Jelmert, O., Hansteen, I. L., and Langard, S. (1994) Chromosome damage in lymphocytes of stainless steel welders related to past and current exposure to manual metal arc welding fumes, *Mutat. Res.* **320**, 223-233.

Jennette, K. W. (1979) Chromate metabolism in liver microsomes, *Biol. Trace. Elem. Res.*, **1**, 55-62.

Jones, P., Kortenkamp, A., O'Brien, P., Wang, G. and Yang, G. (1991) Evidence for the generation of hydroxyl radicals from a chromium(V) intermediate isolated from the reaction of chromate with glutathione, *Arch. Biochem. Biophys.*, **286**, 652-655.

Kalliomaki, P. L., Rahkonen, E., Vaaranen, V., Kalliomaki, K., and Aittoniemi, K. (1981) Lung-retained contaminants, urinary chromium and nickel among stainless steel welders, *Int. Arch. Occup. Environ. Health* **49**, 67-75.

Kawanishi, S., Inoue, S. and Sano, S. (1986) Mechanism of DNA cleavage induced by sodium chromate(VI) in the presence of peroxide, *J. Biol. Chem.*, **261**(13), 5952-5958.

Kishi, R., Tarumi, T., Uchino, E., and Mijake, H. (1987) Chromium content of organs of chromate workers with lung cancer, *Am. J. Ind. Med.* **11**, 67-74.

Kitagawa, S., Seki, H., Kametani, F. and Sakurai, H. (1988) EPR study on the interaction of hexavalent chromium with glutathione or cysteine: Production of pentavalent chromium and its stability, *Inorganica Chimica Acta*, **152**, 251-255.

Knudsen, L. E., Boisen, T., Christensen, J. M., Jelnes, J. E., Jensen, J. C., Lundgren, K., Lundsteen, C., Pedersen, B., Wassermann, K., Wilhardt, P., Wulf, H. C., and Zebitz, U. (1992) Biomonitoring of genotoxic exposure among stainless steel welders, *Mutat. Res.* **279**, 129-143.

Koenig, S. H., Bryant, R. G., Hallenga, K. and Jacob, G. S. (1978) Magnetic cross-relaxation among protons in protein solutions, *Biochemistry* **17**, 4348-4358.

Kollmeier, H., Seemann, J. W., Rothe, G., Muller, K. M. and Wittig, P. (1990) Age, sex, and region adjusted concentrations of chromium and nickel in lung tissue, *Br. J. Ind. Med.* **47**, 682-687.

Kortenkamp, A., Ozolins, Z., Beyersmann, D. and O'Brien, P. (1989) Generation of PM2 DNA breaks in the course of reduction of chromium(VI) by glutathione, *Mutat. Res.* **216**, 19-26.

Kortenkamp, A., Oetken, G. and Beyersmann, D. (1990) The DNA cleavage induced by chromium(V) complex and by chromate and glutathione is mediated by activated oxygen species, *Mutat. Res.*, **232**, 155-161.

Kortenkamp, A. and O'Brien, P. (1991) Studies on the binding of chromium(III) complexes to phosphate groups of adenosine triphosphate, *Carcinogenesis* **12**, 921-926.

Kortenkamp, A., Curran, B. and O'Brien, P. (1992) Defining conditions for the efficient *in vitro* cross-linking of proteins to DNA by chromium(III) compounds, *Carcinogenesis*, **13**(2), 307-308.

Kortenkamp, A. and O'Brien, P. (1994) The generation of DNA single-strand breaks during the reduction of chromate by ascorbic acid and/or glutathione *in vitro*, *Environ. Health. Perspect.* **103**, suppl. 3, 237-241.

Kortenkamp, A., Casadevall, M. Faux, S. P., Jenner, A., Shayer, R. O. J., Woodbridge, N. and O'Brien, P. (1996) Evidence for the activation of molecular oxygen during the reduction of the carcinogen chromium(VI) by glutathione via non-Fenton pathways, *Arch. Biochem. Biophys.* **329**, 199-207.

Kortenkamp, A., Casadevall, M. and da Cruz Fresco, P. (1996) The reductive conversion of the carcinogen chromium(VI) and its role in the formation of DNA lesions, *Anal. Clin. Lab. Sci.* **26**, 160-175.

Koshi, K., Yagami, T. and Nakanishi, Y. (1984) Cytogenetic analysis of peripheral blood lymphocytes from stainless steel workers, *Ind. Health* **22**, 305-318.

Kunkel, G. R., Mehrabian, M. and Martinson, H. G. (1981) Contact-site cross-linking agents, *Mol. Cell. Biochem.* **34**(1), 3-13.

Kunkel, T. A. (1984) Mutational specificity of depurination, *Proc. Natl. Acad. Sci. USA*, **81**(5), 1494-1498.

Larkworthy, L. F., Nolan, K. B. and O'Brien, P. (1988) Chromium. In Wilkinson, G. (ed.), *Comprehensive Coordination Chemistry*. Pergamon Press, New York, Vol. 3, 699-969.

Lees, P. S. J. (1991) Chromium and disease: a review of epidemiologic studies with particular reference to aetiologic information provided by measures of exposure, *Environ. Health. Perspec.*, **92**, 93-104.

Lefebvre, Y. and Pezerat, H. (1992) Production of activated species of oxygen during chromium(VI)-ascorbate reaction: implication in carcinogenesis, *Chem. Res. Toxicol.*, **5**, 461-463.

Levis, A. G. and Bianchi, V. (1982) Mutagenic and cytogenic effects of chromium compounds, *Top. Environ. Health*, **5**, 171-208.

Liebross, R. H. and Wetterhahn, K. E. (1992) *In vivo* formation of chromium(V) in chick embryo liver and red blood cells, *Carcinogenesis* **13**, 2113-2120.

Lindahl, T. and Andersson, A. (1972) Rate of chain breakage at apurinic sites in double-stranded deoxyribonucleic acid, *Biochemistry*, **11**(19), 3618-3623.

Lindahl, T. (1982) DNA repair mechanisms, *Annu. Rev. Biochem.* **51**, 61-87.

Littorin, M., Hoegstedt, B., Stroembaeck, B., Karlsson, A., Welinder, H., Mitelman, F. and Skerving, S. (1983) No cytogenic effects in lymphocytes of stainless steel welders, *Scan. J. Work Environ. Health* **9**, 259-264.

Liu, S. and Dixon, K. (1996) Induction of mutagenic DNA damage by chromium(VI) and glutathione, *Environ. Mol. Mutagen.*, **28**(2), 71-79.

Loeb, L. A., Preston, B. D., Snow, E. T. and Schaaper, R. M. (1986) Apurinic sites as common intermediates in mutagenesis, *Basic Life Sci.*, **38**, 341-347.

Loeb, L. A. and Preston, P. D. (1986) Mutagenesis by apurinic/aprimidinic sites, *Ann. Rev. Genet.* **20**, 201-230.

McBride, T. J., Preston, B. D. and Loeb, L. A. (1991) Mutagenic spectrum resulting from DNA damage by oxygen radicals, *Biochemistry*, **30**(1), 207-213.

Mertz, W. (1975) Effects and metabolism of Glucose Tolerance Factor, *Nutrition reviews*, **33**(5), 129-135.

Misra, M., Alcedo, J. A. and Wetterhahn, K. E. (1994) Two pathways for chromium(VI)-induced DNA damage in 14 day chick embryos: Chromium-DNA binding in liver and 8-oxo-2' deoxyguanosine in red blood cells, *Carcinogenesis* **15**, 2911-2917.

Moon, R. B. and Richards, J. H. (1973) Determination of intracellular pH by ³¹P magnetic resonance, *J. Biol. Chem.* **248**, 7276-7278.

Moore, W. S. and Holland, G. W. (1980) Nuclear magnetic resonance imaging, *Br. Med. Bull.* **36**, 297-299.

Nagaya, T. (1986) No increase in sister-chromatid exchange frequency in lymphocytes of chromium platers, *Mutat. Res.* **170**, 129-132.

Nagaya, T., Ishikawa, N., Hata H. and Otobe, T. (1991) Sister-chromatid exchanges in lymphocytes from 12 chromium platers: a 5-year follow-up study, *Toxicology Letters* **58**, 329-335.

O'Brien, P., Barrett, J. and Swanson, F. J. (1985) Chromium(V) can be generated in the reduction of chromium(VI) by glutathione, *Inorg. Chim. Acta.* **108**, L19-L20.

O'Brien, P. and Wang, G. (1992) Is a one electron path significant in the reduction of chromate by glutathione under physiological conditions? *J. Chem. Soc. Chem. Commun.*, 690-692.

Pääkö, P., Kokkonen, P., Anttila, S., and Kalliomaki, P. L. (1989) Cadmium and chromium as markers of smoking in human lung tissue, *Environ. Res.* **49**, 197-207.

Packer, K. J. (1977) The dynamics of water in heterogenous systems, *Phil. Trans. Roy. Soc. Lond. B.* **278**, 59-87.

Pillai, R. P., Buescher, P. C., Pearse, D. B. *et. al.* (1986) ³¹P NMR spectroscopy of isolated perfused lungs, *Magn. Res. Med.* **3**, 467-472.

Popp, W., Vahrenholz, C., Schmieding, W., Krewet, E. and Norpoth, K. (1991) Investigations of the frequency of DNA strand breakage and cross-linking and of sister-chromatid exchange in the lymphocytes of electric welders exposed to chromium- and nickel-containing fumes, *Int. Arch. Occup. Environ. Health* **63**, 115-120.

Porvirk, L. F. and Steighner, R. J. (1989) Oxidised apurinic/apyrimidinic sites formed in DNA by oxidative mutagens, *Mutat. Res.*, **214**(1), 13-22.

Prakash, A. S. and Gibson, N. W. (1992) Sequence-selective depurination, DNA interstrand cross-linking and DNA strand break formation associated with alkylated DNA, *Carcinogenesis*, **13**(3), 425-431.

Purcell, E. M., Torrey, H. C. and Pound, R. V. (1946) Resonance absorption by nuclear magnetic moments in a solid, *Phys. Rev.* **69**, 37 – 40.

Raithel, H. J., Schaller, K. H., Kraus, T., and Lehnert, G. (1993) Biomonitoring of nickel and chromium in human pulmonary tissue, *Int. Arch. Occup. Environ. Health* **65**, S197-S200.

Reid, T. M., Feig, D. I. and Loeb, L. A. (1994) Mutagenesis by metal-induced oxygen radicals, *Environ. Health Perspect.*, **102**, 57-61.

Sambrook, J. and Pollack, R. (1974) Basic methodology for cell culture – cell transformation, *Methods Enzymol.*, **32**, 583-592.

Sanilkow, K., Zhikovitch, A. and Costa, M. (1992) Analysis of the binding sites of chromium to DNA and protein *in vitro* and intact cells, *Carcinogenesis*, **13**, 2341-2346.

Sarto, F., Cominato, I., Bianchi, V., and Levis, A. G. (1982) Increased incidence of chromosomal aberrations and sister chromatid exchanges in workers exposed to chromic acid in electroplating factories, *Carcinogenesis*, **3**, 1011-1016.

Sbrana, I., Caretto, S., Lascialfari, D., Rossi, G., Marchi, M. and Loprieno, N. (1990) Chromosomal monitoring of chromium-exposed workers, *Mutat. Res.*, **242**, 305-312.

Schaaper, R. M., Kunkel, T. A. and Loeb, L. A. (1983) Depurination of DNA as a possible mutagenic pathway for cells, *Basic Life Sci.*, **20**, 199-211.

Schaaper, R. M. and Loeb, L. A. (1981) Heat mutagenesis of bacteriophage Φ X174 in SOS-induced bacteria, *Mutat. Res.*, **104**, 75-78.

Sehlmeyer, U., Hechtenberg, S., Klyszcz, H. and Beyersmann, D. (1990) Accumulation of chromium in Chinese hamster V-79 cells and nuclei, *Arch. Toxicol.* **64**, 506-508.

Shearman, C. W. and Loeb, L. A. (1977) Depurination decreases fidelity of DNA synthesis *in vitro*, *Nature*, **270**(5637), 537-538.

Shi, X., Mao, Y., Knapton, A. D., Ding, M., Rojanasakul, Y., Gannett, P. M., Dalal, N. and Liu, K. (1994) Reaction of Cr(VI) with ascorbate and hydrogen peroxide generates hydroxyl radicals and causes DNA damage: role of a Cr(IV)-mediated Fenton-like reaction, *Carcinogenesis*, **15**(11): 2475-2478.

Siegel, S. (1956) Nonparametric statistics for the behavioural sciences. *McGraw-Hill, New York and Maidenhead.*

Snow, E. T. (1994) Effects of chromium on DNA replication *in vitro*, *Environ. Health. Perspec.* **103**, suppl. 3, 41-44.

Snyder, R. D. (1988) Role of active oxygen species in metal-induced DNA strand breakage in human diploid fibroblasts, *Mutat. Res.* **193**, 237-246.

Standeven, A. M. and Wetterhahn, K. E. (1991a) Is there a role for reactive oxygen species in the mechanism of chromium(VI) carcinogenesis? *Chem. Res. Toxicol.* **4**, 616-625.

Standeven, A. M. and Wetterhahn, K. E. (1991b) Ascorbate is the principal reductant of chromium(VI) in rat liver and kidney ultrafiltrates, *Carcinogenesis* **12**, 1733-1737.

Stearns, D. M. and Wetterhahn, K. E. (1994) Reaction of chromium(VI) with ascorbate produces chromium(V), chromium(IV), and carbon-based radicals, *Chem. Res. Toxicol.*, **7**, 219-230.

Stearns, D. M., Kennedy, L. J., Courtney, K. D., Giangrande, P. H., Phieffer, L. S. and Wetterhahn, K. E. (1995) Reduction of chromium(VI) by ascorbate leads to chromium-DNA binding and DNA strand breaks *in vitro*, *Biochemistry* **34**, 910-919.

Stella, M., Montaldi, A., Rossi, R., Rossi, G., and Levis, A. G., (1982) Clastogenic effects of chromium on human lymphocytes *in vivo* and *in vitro*, *Mutat. Res.* **101**, 151-164.

Strindsklev, I. C., Hemmingsen, B., Karlsen, J. T., Schaller, K. H., Raithel, H. J., and Langard, S. (1993) Biologic monitoring of chromium and nickel among stainless steel welders using the manual metal arc method, *Int. Arch. Occup. Environ. Health.* **65**, 209-219.

Sugden, K. D., Burris, R. B. and Rogers, S. J. (1990) An oxygen dependence in chromium mutagenesis, *Mutat. Res.* **244**, 239-244.

Sugden, K. D., Geer, R. D. and Rogers, S. J. (1992) Oxygen radical-mediated DNA damage by redox-active Cr(III) complexes, *Biochemistry*, **31**(46), 11626-11631.

Sugiyama, M., Patierno, S. R., Cantoni, O. and Costa, M. (1986) Characterisation of DNA lesions induced by CaCrO₄ in synchronous and asynchronous cultured mammalian cells, *Mol. Pharmacol.* **29**(6), 606-613.

Sugiyama, M., Tsuzuki, K. and Ogura, R. (1991) Effect of ascorbic acid on DNA damage, cytotoxicity, glutathione reductase and formation of paramagnetic chromium in Chinese hamster V-79 cells treated with sodium chromate(VI), *J. Biol. Chem.*, **266**(6), 3383-3386.

Sugiyama, M. and Tsuzuki, K. (1994) Effect of glutathione depletion on formation of paramagnetic chromium in Chinese hamster V-79 cells, *FEBS lett.*, **341**(2-3), 273, 276.

Suzuki, Y. (1990) Synergism of ascorbic acid and glutathione in the reduction of hexavalent chromium *in vitro*, *Ind. Health*, **28**, 9-19.

Suzuki, Y. and Fukuda, K. (1990) Reduction of hexavalent chromium by ascorbic acid and glutathione with special reference to the rat lung, *Arch. Toxicol.*, **64**, 169-176.

Tsapakos, M. J. and Wetterhahn, K. E. (1983) The interaction of chromium with nucleic acids, *Chem. Biol. Interactions*. **46**, 265-277.

Tsuneta, Y., Ohsaki, Y., Kimura, K., Mikami, H., Abe, S. and Murao, M. (1980) Chromium content of lungs of chromate workers with lung cancer, *Thorax* **35**, 294-297.

Westermann, J. and Pabst, R. (1990) Lymphocyte subsets in the blood: A diagnostic window on the lymphoid system? *Immunol. Today*, **11**(11), 406-410.

Wolf, P. L., Horwitz, J. P., Friesler, J. Vazquez, J. and Muehll, E. von der (1968) The indigogenic reaction for histochemical demonstration of β -xylosidase, *Enzymologia*, **34**(1), 20-22.

Xu, J., Manning, F. C. and Patierno, S. (1994) Preferential formation and repair of chromium-induced DNA adducts and DNA-protein cross-links in nuclear matrix DNA, *Carcinogenesis*, **15**, 1443-1450.

Xu, J., Bublely, G. J., Detrick, B., Blankenship, L. J. and Patierno, S. R. (1996) Chromium(VI) treatment of normal human lung cells results in guanine-specific DNA polymerase arrest, DNA-DNA cross-links and S-phase blockade of cell cycle, *Carcinogenesis*, **17**, 1511-1517.

Yang, J. J., Hseih, Y. C., Wu, C. W. and Lee, T. C. (1992) Mutational specificity of chromium(VI) compounds in the hprt locus of chinese hamster ovarian-K1 cells, *Carcinogenesis* **13**, 2053-2057.

Zhitkovitch, A., Voitkun, V. and Costa, M. (1995) Glutathione and free amino acids form stable complexes with DNA following exposure of intact mammalian cells to chromate, *Carcinogenesis* **16**, 907-913.

Zhitkovitch, A., Lukanova, A., Popov, T., Taioli, E., Cohen, H., Costa, M., and Toniolo, P. (1996) DNA-protein crosslinks in peripheral lymphocytes of individuals exposed to hexavalent chromium compounds, *Biomarkers*, **1**, 86-93.

Zhikovitch, A., Voitkun, V., Kluz, T. and Costa, M. (1998) Utilisation of DNA-protein cross-links as a biomarker of chromium exposure, *Environ. Health Perspect.*, **106**, 969-974.